CHARACTERIZATION OF *VITREOSCILLA* HEMOGLOBIN INCLUSION BODIES PRODUCED IN *ESCHERICHIA COLI*

Thesis by

Roger A. Hart

In Partial Fulfillment of the Requirements

for the Degree of

Doctor of Philosophy

California Institute of Technology

Pasadena, California

1991

(Submitted May 23, 1991)

ACKNOWLEDGEMENTS

The work contained in this thesis would not have been possible without the support of my family. I am especially grateful to my parents Edward and Jean for their love and confidence. I am but a reflection of you. Also, thanks to my older brother Robert for having shown me the way and to my younger brother Rodney for having always been there.

To my officemate and hiking buddy Mike Kosinski - Thanks for being such a good friend! I owe much of my insanity to the wild ones among the Bailey group, especially: Todd, Val, Chaitan, Pete, Bernd, Karl, and Uschi. It has been great fun.

My teachers opened my eyes to the world of science. Thanks to Mrs. Hilliard for introducing me to chemistry and to Dr. Richard Mead for challenging me to challenge myself. Special thanks to my thesis advisor Dr. James Bailey for his patience and confidence in my ideas and abilities. Thanks also to Dr. Francis Arnold and Dr. Sunney Chan for their critical evaluation of the contents of this thesis.

ABSTRACT

The process of inclusion body (IB) formation in the gram-negative bacterium *Escherichia coli* (*E. coli*) was investigated. The homodimeric hemeprotein *Vitreoscilla* hemoglobin (VHb) from the gram-negative bacterium *Vitreoscilla* was taken as the model protein.

Expression of VHb under control of its native promoter from a pUC19-derived plasmid in strain JM101 lead to high-level accumulation of VHb in both soluble and insoluble forms. The soluble form was purified by sequential two-phase extraction techniques and used as a basis for analyzing the insoluble form. The amino acid content and N-terminal sequence of purified soluble VHb is consistent with that of VHb purified from *Vitreoscilla*. Soluble and insoluble VHb exhibit identical migration properties during denaturing two-dimensional electrophoresis.

The protein composition of VHb inclusion bodies was analyzed by one-dimensional and two-dimensional electrophoresis techniques. Results indicate the presence of two types of cytoplasmic aggregates of differing morphology in single bacterial cells. These aggregates also differ in their relative content of VHb, pre-β-lactamase, and the cytoplasmic protein elongation factor Tu and are separable by differential centrifugation.

Conformational properties of soluble and insoluble VHb were studied by electron paramagnetic resonance spectroscopy. Purified soluble VHb exhibits three high-spin resonances in the vicinity of g 6 from two heme centers. One center is axial (g 6.00). The other is rhombic (g 5.50 and 6.39). Inclusion body isolates containing insoluble VHb exhibit a single resonance (g 5.98) which is also present in control cell debris. Iron quantitation demonstrates that inclusion body VHb uniformly lacks heme. Titration of IB fractions with monomeric

ferrous heme followed by difference absorption spectroscopy suggests that some inclusion body VHb is competent for heme binding.

A series of perturbation-response experiments was conducted to determine what cellular processes influence VHb IB formation. Results show that VHb inclusion body formation is highly influenced by the expression plasmid construction and the heme biosynthetic capacity. The level of induction and accumulation appear less important than the general metabolic state of the culture. Temperature and chaperone protein levels have little effect. Efforts to reduce inclusion body formation through genetic amplification of ALA synthase and ALA dehydratase levels were unsuccessful, presumably due to regulation. Results suggest a heme biosynthetic limitation is involved in VHb *in vivo* insolubilization.

TABLE OF CONTENTS

CHAPTER 1

Introduction

1.1 Significance of Inclusion Bodies

Through the use of recombinant DNA technology, man can alter cells to synthesize proteins which they do not ordinarily produce. The gram-negative bacterium *Escherichia coli* has been used extensively as a host for producing recombinant proteins because of the efficient expression vectors available for this organism (Pouwels *et al.*, 1985). Protein produced in recombinant *Escherichia coli* using high-level expression vectors can have a variety of fates. It can be degraded, secreted, or accumulated in soluble or insoluble forms. Large intracellular aggregates of cloned protein are called inclusion bodies.

Intracellular aggregation may be desirable during expression of some proteins. In particular, aggregation may prevent some protease-susceptible proteins from being degraded (Hellebust *et al.*, 1989; Cheng *et al.*, 1981). Additionally, aggregation of proteins toxic to the cell may ensure cell viability (Mitraki and King, 1989). The accumulation of recombinant protein in inclusion bodies may also be desirable from a protein recovery point of view (Schoner *et al*, 1985; Marston and Hartley, 1990). This is because the protein is concentrated in a form which is easily recovered by centrifugation following cell lysis. As most cell proteins remain soluble following lysis, aggregate recovery can also constitute a significant initial purification step.

Aggregation of protein in inclusion bodies is only beneficial if the insoluble protein can be subsequently recovered in a soluble and active form. High concentrations of denaturants are commonly used for inclusion body protein solubilization (Marston and Hartley, 1990). With this treatment the protein is recovered in a soluble but denatured form. Consequently, protein refolding

is required to obtain active protein. Some proteins are difficult to refold and may only be recovered in very low yield. Complications in protein refolding may arise from complex structural hierarchy, prevalence of intermolecular and intramolecular disulfide cross-links, a high frequency of proline residues, and a variety of other factors (Jaenicke, 1987). Protein refolding in general must be done in dilute solution to minimize losses from competing aggregation processes (Zettlmeissl *et al.*, 1979).

1.2 Motivation for Characterizing Inclusion Bodies

Critical factors in industrial recombinant protein production are protein integrity and purified protein recovery yield. Given the comments in the previous section, inclusion body formation can clearly affect both these factors. Thus, it is desirable not only to predict when inclusion bodies may form but also to control the processes leading to their formation.

Inclusion body formation is known to be influenced by a number of factors. These factors include cultivation conditions used for cell growth, properties of the recombinant host, and properties of the recombinant protein (Schein, 1989). While correlations between protein properties and insolubilization have been proposed (Wilkinson and Harrison, 1991), it is not yet possible to predict *a priori* whether a given protein expressed in a given host will accumulate in inclusion bodies. This is because the specific mechanisms governing inclusion body formation are poorly understood. Aberrant protein folding is generally believed important in inclusion body formation (Mitraki and King, 1989). This mechanism is quite rational as the aggregated state of the protein and the conditions

required for its solubilization clearly indicate that the protein is non-native.

Inclusion bodies may contain information about their formation mechanism. By characterizing inclusion body protein composition, for example, it may be possible to determine if certain cellular proteins are involved in the insolubilization process. Alternatively, by characterizing inclusion body protein conformation it may be possible to determine the extent of protein folding prior to insolubilization. This in turn may suggest what conformational forms are most susceptible to aggregation. Thus, by characterizing inclusion bodies, information may be obtained which can ultimately be used to predict or control inclusion body formation.

Inclusion body characterization may also provide information which can be used to design suitable recovery strategies. In particular, it is possible that some inclusion body protein possesses conformational attributes worth preserving. If true, then the use of high concentration denaturants for inclusion body dissolution, which destroys these partially folded conformers, may not be an optimum strategy.

Early work aimed at inclusion body characterization focused on the colloidal properties of the aggregates. Properties of interest included aggregate size, density, and morphology (Taylor *et al.*, 1986). Investigations were also conducted to examine the forces involved in inclusion body stabilization. Most work was aimed at determining the importance of intermolecular disulfide bonds (Schoemaker *et al.*, 1985; Tsuji *et al.*, 1987; Langley *et al.*, 1987).

As chaotropic agents can generally solubilize inclusion body protein, hydrophobic interactions are believed important in inclusion body stabilization (Thomson and Bigelow, 1986)

The most potentially useful information which can be derived from inclusion body characterization concerns the conformational state of the insoluble protein. Unfortunately, the protein insolubilized by this process has been subjected to direct conformational analysis on only one occasion. In this case, the protein was shown to be a thermolabile intermediate in the productive folding pathway. (Haase-Pettingell and King, 1988). Absence of work in this area is likely due to the difficulty of analyzing the properties of a single protein in a protein mixture. One approach to analyzing the properties of inclusion body protein not yet exploited involves the use of target-protein-specific probes. With the use of such probes it may be possible to discriminate the properties of the target protein from the properties of contaminants. In this approach, the properties of the target protein are determined by investigating the properties of the probe.

1.3 Scope of Thesis

We have examined the properties of inclusion bodies produced by a model system using a variety of methods. The model system examined is a recombinant strain of *Escherichia coli* (*E. coli*) which overproduces the homodimeric heme protein *Vitreoscilla* hemoglobin (VHb) (Khosla and Bailey, 1988). This protein bears structural and functional similarity to a number of eucaryotic hemoglobins (Wakabayashi *et al.*, 1986). In the system used, VHb is expressed from a high copy number plasmid under the control of its native oxygen-regulated promoter

and accumulates in both soluble and insoluble forms. VHb was chosen as the recombinant protein for this study for two reasons. First, it contains a potential probe, the heme prosthetic group, which can be used to examine the inclusion-body-bound protein. Second, VHb can be considered as a simple example of more complex oligomeric proteins. Inclusion bodies of such proteins have rarely been studied.

To provide a basis for analyzing the insoluble VHb contained in inclusion bodies, it was necessary to purify the active protein. Chapter 2 describes the protocol developed for purifying soluble VHb from recombinant *E. coli*.

As proteins involved in the aggregation of VHb could themselves be insolubilized, the protein composition of VHb inclusion bodies was characterized. Results of this analysis are presented in Chapter 3.

Inclusion body VHb and purified soluble VHb were examined by various spectroscopic techniques to ascertain the similarities and differences between the two forms. Results from this analysis are presented in Chapter 4

Results from Chapter 4 suggest some heme-free VHb contained in inclusion bodies is competent for heme binding. In Chapter 5, experiments are described which were conducted to determine whether active VHb can be recovered from inclusion bodies by dissolution and heme reconstitution without formal refolding.

Results from the studies described in Chapters 4 and 5 suggest heme availability may influence VHb insolubilization. Chapter 6 presents results from investigations conducted to determine the influence of heme biosynthesis on VHb insolubilization *in vivo*.

1.4 References

1. Cheng, Y. E., Kwoh, D. Y., Kwoh, T. J., Soltvedt, B. C., and Zipser, D. (1981) *Gene* **14**, 121 - 130
2. Haase-Pettingell, C. A., and King, J. (1988) *J. Biol. Chem.* **263**, 4977 - 4983
3. Hellebust, H., Murby, M., Abrahmsen, L., Uhlen, M., and Enfors, S. (1989) *Bio/Technology* **7**, 165 - 168
4. Jaenicke, R. (1987) *Prog. Biophys. Molec. Biol.* **49**, 117 - 237
5. Khosla, C., and Bailey, J. E. (1988) *Mol. Gen. Genet.* **214**, 158 - 161
6. Langley, K. E., Berg, T. F., Strickland, T. W., Fenton, D. M., Boone, T. C., and Wypych, J. (1987) *Eur. J. Biochem* **163**, 313 - 321
7. Marston, F. A. O., and Hartley, D. L. (1990) *Meth. Enzym.* **182**, 264 - 277
8. Mitraki, A., and King, J. (1989) *Bio/Technology* **7**, 690 - 697
9. Pouwels, P. H., Enger-Valk, B. E., and Brammar, W. J. (1985) *Cloning Vectors: A Laboratory Manual*, Elsevier, Amsterdam
10. Schein, C. H. (1989) *Bio/Technology* **7**, 1141 - 1149
11. Schoemaker, J. M., Brasnett, A. H., and Marston, F. A. O. (1985) *EMBO Journal* **4**, 775 780
12. Schoner, R. G., Ellis, L. F., and Schoner, B. E. (1985) *Bio/Technology* **3**, 151 - 154

13. Taylor, G., Hoare, M., Gray, D. R., and Marston, F. A. O. (1986) *Bio/Technology* **4**, 553 - 557

14. Thomson, J. A., and Bigelow, C. C. (1986) *Biochem. Cell Biol.* **64**, 993 - 998

15. Tsuji, T., Nakagawa, R., Sugimoto, N., and Fukuhara, K. (1987) *Biochemistry* **26**, 3129 - 3134

16. Wakabayashi, S., Matsubara, H., and Webster, D. A. (1986) *Nature* **322**, 481 - 483

17. Wilkinson, D. L., and Harrison, R. G. (1991) *Bio/Technology* **9**, 443 - 448

18. Zettlmeissl, G., Rudolph, R., and Jaenicke, R. (1979) *Biochemistry* **18**, 5567 - 5575

CHAPTER 2

Purification and Aqueous Two-Phase Partitioning Properties of Recombinant *Vitreoscilla* Hemoglobin

2.1 Summary

Soluble recombinant *Vitreoscilla* hemoglobin was purified from *E. coli* lysate by sequential two-phase extraction techniques. Extraction of lysate containing VHb in PEG / dextran gave a 3.6 fold increase in VHb purity in the PEG-rich phase via a size exclusion mechanism. Further extraction of the recovered PEG phase in PEG / sodium sulfate gave an additional 2.0 fold increase in purity in the PEG-rich phase due to an electrostatic mechanism. Final extraction of the PEG phase in PEG / magnesium sulfate gave an additional 1.3 fold increase in VHb purity in the magnesium sulfate-rich phase. The final yield from the extractive purification was 47% with purity of VHb estimated to be greater than 95%. Yields from the sulfate salt extractions are essentially quantitative due to the extreme partitioning behavior of VHb in these systems. VHb partition coefficients as large as 46 in PEG / sodium sulfate and as small as 0.06 in PEG / magnesium sulfate were observed. Similar small partition coefficients were obtained with PEG / manganese sulfate extractions. This dramatic effect of divalent cation content on the partition coefficient of VHb in PEG / sulfate salt systems was investigated by pH and magnesium ion titration experiments. Results show the effect to be largest and nearly constant for pH values greater than 6.0 and diminished at lower pH values. A model based on magnesium ion binding to negatively charged amino acids is shown to correlate the data well. Based on model formulation and the partitioning behavior of contaminant proteins, the observed effect is expected to be applicable to other proteins.

2.2 Introduction

The strict aerobic bacterium *Vitreoscilla* produces a soluble homodimeric heme protein with considerable amino acid homology[1] and functional similarity[2] to eucaryotic hemoglobins when grown under oxygen-limiting conditions. Intracellular expression of this protein, referred to as *Vitreoscilla* hemoglobin (VHb), has been shown to improve the growth[3] and recombinant protein productivity[4] of *Escherichia coli* under microaerobic conditions. Similar effects have also been seen with *Streptomyces*[5]. The physiological role of this protein is as yet undetermined; presumably it acts to facilitate oxygen transport and/or to alter the intracellular redox state[4]. Identification of the intracellular function of this protein will aid in its utilization to improve bioprocess yield. *In vitro* investigations of the purified proteins ligand and effector binding properties can provide information regarding its physiological function. Investigations of this nature have provided tremendous insight regarding the function of other cytoplasmic hemoglobins[6].

VHb has previously been isolated from its native host *Vitreoscilla* where it is expressed at low levels. Purification from high-level expression recombinant hosts, however, has not been investigated. We have examined a variety of protein purification techniques for isolating VHb from recombinant *E. coli*. Of the procedures investigated, aqueous two-phase extraction techniques were judged most useful based on resolution and yield. This is due in large part to the extreme partitioning behavior of VHb in PEG / sulfate salt two-phase systems. The partitioning properties of VHb in these systems can be effectively modulated by

the divalent cations magnesium and manganese. In this report we examine the mechanisms of partitioning which manifest themselves in the aqueous two-phase purification of recombinant VHb and discuss the advantages of this technique relative to that employed previously for purification from the native host. We also discuss the mechanism by which magnesium and manganese modulate the partitioning of VHb in PEG / sulfate salt systems and its possible application to the extractive purification of other proteins.

2.3 Materials and Methods

Bacterial growth and soluble lysate collection - The recombinant *E. coli* strain JM101:pRED2, which produces both soluble and insoluble forms of VHb, was grown as described previously.[7] Cells were washed with buffer A, consisting of 100 mM Tris-HCl (pH 8.0), 50 mM NaCl, 1 mM EDTA, 1mM dithiothreitol, and 0.1 mM phenylmethylsulfonyl fluoride, concentrated in this buffer to an effective concentration of 100 gdw/l, and lysed by sonication on ice. The resulting cell lysate was fractionated into soluble and insoluble fractions by centrifugation at 26,000 g for 1 hour. SDS-PAGE with Coomassie blue staining indicated that VHb represents approximately 10% of total soluble protein. Visible absorption spectrophotometry demonstrated that the soluble VHb produced is active.

VHb purification - VHb was purified from the soluble lysate fraction of JM101:pRED2. The soluble lysate (L) was extracted in an aqueous two-phase system consisting of 12% (w/w) dextran T-500, 7.7% (w/w) PEG 4000, 20 mM Tris-HCl (pH 8.0), and 10 mM NaCl, and the PEG-rich phase was collected

(E1). The E1 fraction was then extracted in a two-phase system consisting of 12.4% (w/w) Na_2SO_4, 11.8% (w/w) PEG 4000, and 20 mM Tris-HCl, and the PEG-rich phase was collected (E2). The E2 fraction was then extracted in a two-phase system consisting of 9.7% (w/w) $MgSO_4$, 10.8% (w/w) PEG 4000, and 50 mM Tris-HCl, and the $MgSO_4$ fraction was collected (E3). The VHb in fraction E3 was estimated to be greater than 95% pure as judged by SDS-PAGE with Coomassie blue staining. Higher purity preparations of VHb were obtained by subjecting the E3 fraction to metal affinity chromatography (fraction M1; Pharmacia Chelating Sepharose Fast Flow; immobilized Cu^{+2}; 20 mM sodium phosphate (pH 7.5), 0.5 M NaCl, 3.5 mM Nα-acetyl-L-histidine elution) followed by gel permeation chromatography (fraction GPC; Pharmacia Sephadex G-75 Superfine; 50 mM potassium phosphate (pH 7.0), 10 mM NaCl). Resulting preparations were devoid of contaminants as judged by two-dimensional electrophoresis with silver staining. Purified VHb was dialyzed against distilled water, lyophilized, and stored at -70 °C.

Two-phase extractions - Aqueous two-phase systems were prepared on a weight percent basis from common polymer, salt, and buffer stock solutions. In some cases, salt was dissolved directly in a polymer solution to induce phase separation. Glass distilled water was used throughout. Phases were formed in graduated centrifuge tubes and separated by centrifugation. All procedures were carried out at room temperature. Tie line lengths were estimated from published two-phase binodial data. [8] Addition of soluble lysate to the aqueous two-phase systems resulted in an apparent shift in the critical point to lower polymer concentrations, similar to that reported previously.[9] For this reason, in

some cases the value of the tie line length could not be estimated.

Analytical procedures - VHb concentration was determined by difference absorption spectrophotometry (carbon monoxide minus reduced) using the monomer extinction coefficient (ϵ(VHbCO-VHb, 419 nm) - ϵ(VHbCO-VHb, 437 nm)) The value of the extinction coefficient was determined by amino acid analysis to be $1.067x10^5(Mcm)^{-1}$. Total protein was determined by the Bradford dye binding assay[10] with a commercial kit (Bio-Rad, Richmond, CA) using bovine serum albumin (Sigma, St. Louis, MO) as standard. VHb and contaminant protein concentration were also determined in some cases by scanning Coomassie blue stained SDS-PAGE gels.

Electrophoresis - A Pharmacia Phastsystem was used for many of the electrophoretic analyses (Pharmacia, Uppsala, Sweden). SDS-PAGE was done with Phastgel Homogeneous 20 medium (Pharmacia technical bulletin #111). Isoelectric focusing and electrophoretic titration were done with Phastgel IEF 3 - 9 medium (technical bulletin #100). Protein bands were visualized by silver staining (technical bulletin #210). Protein molecular weight or pI calibration standards were used throughout.

Materials - Dextran T-500 (M_r 487,000) was purchased from Sigma Chemical Co (St. Louis, MO). Poly(ethylene glycol) (PEG) 4000 (M_r 3000-3700) was obtained from Serva Chemical Co. (Heidelberg, FRG). PEG 6000 (M_r 6000-7400) was from Fisher Chemical Co. (Fair Lawn, NJ). All other chemicals were analytical grade.

2.4 Results

Aqueous Two-Phase Purification of *Vitreoscilla* Hemoglobin

Isolated *E. coli* soluble lysate containing VHb was initially extracted in PEG / dextran systems. The soluble lysate was extracted in PEG 4000 / dextran T-500 and PEG 6000 / dextran T-500 two-phase systems. This procedure led to substantial purification of VHb in the PEG-rich phase due to the strong partitioning of contaminating proteins to the dextran-rich phase. The results of these extractions, shown in Figure 1, indicate that while VHb partitioning to the PEG-rich phase is largely unaffected by the molecular weight of PEG, the partitioning of contaminating proteins is strongly affected. SDS-PAGE analysis of the resulting fractions (from the extraction designated as E1 in Figure 1) indicates that high molecular weight proteins favor the dextran-rich phase while low molecular weight proteins including VHb dimer (31.5 kDa) favor the PEG-rich phase. This trend becomes more pronounced with increasing tie line length (data not shown). At the critical point the tie line length (L) equals zero and the two phases are indistinguishable; thus, the partition coefficient is expected to approach one. As the tie line length increases, the properties which distinguish the two phases, such as the composition and density, become increasingly different generally leading to a monotonic change in the protein partition coefficient. As these systems have a relatively low ionic strength (10 mM NaCl, 20 mM Tris-HCl (pH 8)) and are composed of ionic species which do not strongly partition, electrostatic effects are likely comparable and small. All results indicate that VHb and contaminant protein partitioning in these systems are dominated by

a size exclusion mechanism.[11]

Extraction of the PEG-rich phase from extraction E1 by the direct addition of anhydrous sodium sulfate in the presence of 20 mM Tris-HCl (pH 8.0) gave the results shown in Figure 2. In this case, VHb is partitioned principally to the PEG-rich phase with the partition coefficient increasing with increasing tie line length and approaching unity near the critical point. Contaminant proteins are also partitioned to the PEG-rich phase but to a much lesser degree. Thus, substantial purification of VHb is obtained by this procedure. Native isoelectric focusing analysis of the PEG-rich phase (from the extraction designated as E2 in Figure 2) indicates that only proteins with a pI less than 6, which are negatively charged under these conditions, are found in the PEG-rich phase. Additionally, anion exchange chromatography of the PEG-rich phase from extraction E1 at pH 8 yields upon sodium chloride elution a VHb-enriched protein solution containing essentially the same contaminants as the PEG-rich phase from extraction E2. Each of these observations is consistent with a partitioning mechanism dominated by electrostatic effects. Electrostatic effects are known to be important in polymer / polymer two-phase systems containing phosphate or sulfate because of the unequal partitioning of these anions between the two polymer phases.[12] The same is expected for polymer / salt two-phase systems. However, thermodynamic analysis in this case is greatly complicated by the presence of concentrated ionic solutions.

Extractions of PEG-rich phases containing VHb with magnesium sulfate showed behavior qualitatively different from extractions with sodium sulfate. Results from extractions of the PEG phase resulting from extraction E2 with

magnesium sulfate are shown in Figure 3. In these experiments, the PEG-rich phase from extraction E2 was diluted with buffer A to yield a solution with approximately the same PEG concentration as that in the PEG-rich phase from extraction E1. Magnesium sulfate was then added directly to induce phase formation. Results show that under these conditions, VHb is strongly partitioned to the magnesium sulfate-rich phase. Contaminant proteins also partition to the magnesium sulfate phase, but, to a lesser degree. The partitioning of VHb in PEG / magnesium sulfate systems is not strongly dependent on the tie line length for large values of the tie line length. The protein composition of the magnesium sulfate-rich phase (from the extraction designated as E3 in Figure 3) is similar to the protein composition of the eluent from anion exchange chromatography of the PEG-rich phase from extraction E2.

The combined effect of the respective successive extractions on the purity of VHb can be seen in Figure 4. These results show that the greatest purification of VHb is achieved by the PEG / dextran and PEG / sodium sulfate extractions. Examination of the E3 fraction by SDS-PAGE with Coomassie blue staining indicates that VHb constitutes greater than 95% of the protein in this fraction (data not shown). Further purification can be achieved by metal affinity chromatography and gel permeation chromatography. To enable visualization of contaminant proteins, the SDS-PAGE gel shown in Figure 4 was over-developed during silver staining. Consequently, it over-represents the relative content of contaminant proteins and cannot be used for quantitative purposes. Examination of the difference absorption spectra of VHb demonstrates that the shape and relative intensity of the Soret, alpha and beta bands are not affected by any

of the purification procedures. Data concerning the purity and yield resulting from preparative application of the procedure are given in Table 1. Quantitative yields were obtained from both the PEG / salt extractions due to the extreme partitioning of VHb in these two-phase systems. Comparison of the achieved purity and yields shows that the most favorable purification step is the PEG / sodium sulfate extraction. This is also true when the preceding PEG / dextran extraction is omitted (data not shown).

Partitioning Mechanism in PEG / $MgSO_4$ Two-Phase Systems

Processing of the VHb-enriched PEG 4000 phase resulting from extraction E1 was hampered by its high viscosity. Consequently, attempts were made to extract VHb into a low viscosity, salt-rich phase by the direct addition of salts. As expected, the addition of salts containing multivalent anions, including sulfates and phosphates, uniformly lead to the formation of two phases[13]. Salts containing a multivalent anion and a monovalent cation, such as potassium phosphate (pH 8), sodium sulfate and ammonium sulfate, yielded extreme partitioning of VHb to the PEG 4000-rich phase. In contrast, salts containing a multivalent anion and a divalent cation, such as magnesium sulfate and manganese sulfate, yielded extreme partitioning of VHb to the salt-rich phase. Other salts, such as zinc sulfate, ferrous sulfate, and cupric sulfate lead to VHb precipitation. Representative partitioning data indicating these findings are given in Table 2.

The presence of a divalent cation in these systems could affect the partitioning of VHb in several ways. Solvent-based effects could arise through a change in dielectric constant or water structure (through formation of aquo ions), and

protein-based effects could arise through structure disruption or cation binding. Given the magnitude of the observed effect, the cation must partition strongly to one phase if a solvent-based effect is responsible. Further, difference absorption spectrophotometry indicates VHb structure is not affected by the presence of either magnesium or manganese (data not shown). Negatively charged acidic residues are known, however, to bind magnesium ion when present in high concentration.[14] Binding of the cation would change the effective protein charge making it more positive than expected and may explain the observed inversion of the partition coefficient.

To test this latter hypothesis, we sought to titrate a PEG / sulfate salt two-phase system with respect to divalent cation and pH while keeping other phase properties constant and examine the effect on the partition coefficient of VHb. Only PEG / magnesium sulfate and PEG / sodium sulfate systems were examined further. All experiments conducted indicate that, for a fixed total system weight percent PEG and weight percent sulfate salt (sodium sulfate plus magnesium sulfate), volume ratio is independent of pH and cation type. This observation suggests that the binodials are not strongly dependent on these variables. The total weight percent PEG and weight percent sulfate salt was kept constant throughout, corresponding to a two-phase system with a tie line length of approximately 32%(w/w). The ratio (R) of weight percent magnesium sulfate to weight percent sulfate salt was varied to modulate cation type. The system pH was varied by addition of either Tris-HCl (points above pH 8) or sodium phosphate (points below pH 8) to a concentration of approximately 50 mM. The difference between the pH of the two phases never exceeded 0.2 pH

units. Purified VHb was used throughout to allow precise partition coefficient determination through total protein measurement. The results of these titration experiments are indicated by the data points in Figure 5a. Results show that the partitioning is not strongly dependent on pH for values greater than 6.0 but is sensitive to pH for lower pH values. Extrapolation of the titration curves suggests convergence near pH 4.8. The curves have dramatically different slopes between pH 4.8 and 6.0, differing not only in magnitude but also in sign. If cation binding to acidic residues is responsible for the partitioning behavior, the effect should be diminished at low pH values where acidic residues are increasingly protonated. The partitioning should also be relatively independent of pH above approximately 6.5 as most acidic residues are fully deprotonated above this pH. Each of these trends are seen in the observed titration results.

To test the consistency of the proposed mechanism with experimental findings, a model was developed to examine the possible effect of magnesium on VHb partitioning properties. For this analysis, VHb charge was predicted from its amino acid content[1] and commonly reported pK values for amino acids in proteins.[15] All amino acids were assumed accessible for titration except for the histidine which presumably occupies the proximal site in heme binding.[1] The predicted charge-titration curve is in qualitative agreement with that determined experimentally, although the predicted isoelectric point of 5.15 differs from the experimental value of approximately 5.0 (data not shown). The magnesium-modulated VHb charge was predicted by simultaneous solution of the equilibrium expressions for the protonation of acidic and basic residues, given by equations (1) and (2), and the equilibrium expression for magnesium binding to

acidic residues, given by equation (3).

$$AH \rightleftharpoons A^- + H^+ \tag{1}$$

$$BH^+ \rightleftharpoons B + H^+ \tag{2}$$

$$AMg^+ \rightleftharpoons A^- + Mg^{+2} \tag{3}$$

The resulting specific protein charge was calculated through the use of equation (4).

$$z = (\frac{1}{[VHb]})(\sum_i [B_i H^+] - \sum_j [A_j^-] + \sum_k [A_k Mg^+]) \tag{4}$$

The calculated specific protein charge was related to the partition coefficient through application of the commonly used theory predicting linearity of the natural logarithm of the partition coefficient with protein charge.[8,13,16]

$$lnK_p = lnK_p{}^0 + \frac{zF}{RT}\Delta\psi \tag{5}$$

The values of all parameters in equations (4) and (5) were determined from the literature with the exception of $K_p{}^0$, $\Delta\psi$ and the acidic residue magnesium binding constant, K_{Mg}. The values of these parameters were determined from the data by a least squares fit with resulting lines as shown in Figure 5.

An estimate of the magnitude of K_{Mg} of $10^{0.51}$ was obtainable from the literature. This is the value of the equilibrium constant for the binding of magnesium ion to acetic, proprionic and butyric acid.[17] Simulations corresponding

to this binding constant are shown in Figures 5a and 5b. The value of the equilibrium constant determined by a least squares fit of the full data set is $10^{0.40}$. Simulations corresponding to this binding constant are shown in Figures 5c and 5d. Examination of these results indicates that the qualitative trends seen in the experimental data above and below pH 6.0 are predicted by the model. The greatest quantitative deviation between model predictions and experimental data occur below pH 6.0. The model fails to predict the sharp convergence of the experimental data near pH 4.8, which is close to the experimentally-determined isoelectric point. As deviation below pH 6.0 may be due to protein precipitation effects, discussed further below, the value of the equilibrium binding constant was also determined by a least squares fit considering only the data above pH 6.0. The value of the binding constant was determined in this case to be $10^{0.18}$. Corresponding simulations are shown in Figures 5e and 5f. A summary of the determined parameters is given in Table 3. The values determined for $\Delta\psi$ are in good agreement with those reported previously for similar PEG / potassium sulfate systems [12].

Titration at low pH values was hampered by a decrease in the solubility of VHb in the two-phase system as shown in Figure 6. The solubility limitation appears to reside in the PEG-rich phase as a decrease in the partition coefficient at a given pH leads to an increase in the total solubility of the protein. The insoluble protein aggregates and is found at the interface between the two phases. The solubility trends seen in the two-phase titration are in agreement with those seen in the electrophoretic titration of purified VHb. Examination of the results indicates two apparent titration curves, one exhibiting a monotonic

increase in negative charge with increasing pH and another showing essentially no charge below pH 6. We interpret these curves to correspond to two species, soluble active VHb whose negative charge increases monotonically with pH and aggregated VHb whose mobility in the gel is hindered by its effective molecular weight. This aggregated species is not removed by high-speed centrifugation (16,000 g for 1 hour) and is most significant below pH 6.5. Visible absorption spectrophotometry indicates a progressive change in the structure of VHb for pH values below 6 indicating that protein denaturation is occurring in this regime (data not shown). VHb also focuses poorly during IEF due to aggregation at low pH caused by protein denaturation. VHb aggregation at low pH values could affect the magnitude of the partition coefficient as well as the solubility in the two-phase system. Aggregation appears maximized in the vicinity of the isoelectric point (data not shown).

2.5 Discussion

Only one other purification procedure has been published for the isolation of *Vitreoscilla* hemoglobin[18]. It involves successive precipitation of VHb with protamine sulfate and ammonium sulfate followed by gel permeation chromatography on Sephadex G-100 and ion exchange chromatography on DEAE-cellulose. This procedure has been applied extensively for purifying VHb from its native organism, *Vitreoscilla.* Its utility for purifying highly expressed VHb from recombinant hosts has not, however, been examined. We investigated the use of this procedure for the purification of VHb from recombinant *E. coli.* Various elements of the procedure were found to perform poorly with the recombinant

system. In particular, optimum conditions for precipitation of lysates using 40% saturated ammonium sulfate gave only a 2.1 fold increase in purity with 80% yield. Serial precipitation with 30% and 50% saturated ammonium sulfate gave only a 1.6 fold increase in purity with 70% yield. Somewhat better performance was reported for purification of VHb from the native host. In that case serial precipitation with 45% and 65% saturated ammonium sulfate gave a 4.6 fold increase in purity with a 65% yield. In all cases with the recombinant system, two-phase extraction with PEG / dextran performed better than ammonium sulfate precipitation. Yields of 70% with 3.0 fold increase in purity were routinely obtained at analytical scale. Two-phase extraction with PEG / sodium sulfate similarly performed better than ion exchange chromatography for purification of VHb from the recombinant system. Quantitative yields were obtained with a 2.0 fold increase in purity with the extractive technique. To obtain similar increases in purity with gradient elution ion exchange chromatography, yields as low as 30% were suffered. Similar performance statistics for ion exchange chromatography were previously reported for purification from *Vitreoscilla.* Part of the loss during ion exchange chromatography is attributed to VHb aggregation in the chromatographic matrix. Similar losses were seen during metal affinity chromatography but not during gel permeation chromatography. Losses generally increased with protein loading and were not affected by mobile phase ionic strength.

Our results indicate that extraction in PEG / magnesium sulfate systems can be an efficient means for the separation of protein and PEG. Additional procedures for the separation of protein and PEG involve ion exchange chro-

matography, electrophoresis and dialysis or ultrafiltration[8]. Each of these latter methods possess certain disadvantages. The high viscosity of PEG-rich phases can make chromatography difficult. Electrophoretic techniques are poorly suited to large-scale separations. Dialysis and ultrafiltration are only useful when the molecular weights of the protein and PEG differ substantially. Two-phase extraction at reduced pH can also be used to separate protein and PEG provided the protein is stable at low pH. In some cases, magnesium titration may be a less denaturing method for modulating protein charge than pH titration. The generality of the mechanism is indicated by the good correlation between model predictions and experimental observations. The described model does not assume specific protein binding sites for magnesium, but rather a general ionic interaction which is expected to be applicable to other proteins. This suggestion is further supported by the observation that contaminant proteins are similarly partitioned to the magnesium sulfate-rich phase during the purification of VHb. This same mechanism may also be responsible for the dramatic reduction in the partition coefficient of β-galactosidase-protein A fusions with the inclusion of magnesium ion in PEG 4000 / potassium phosphate aqueous two-phase systems as reported previously[19].

2.6 Acknowledgements

This research was supported by the National Science Foundation (Grant No. EET-8606179). R. H. was supported in part by a predoctoral training grant in biotechnology from the National Institute of General Medical Sciences (National Research Service Award 1 T32 GM 08346-01, Pharmacology Sciences Program).

2.7 References

1. Wakabayashi, S., Matsubara, H., and Webster, D. A. *Nature* 1986, **322**, 481 - 483

2. Webster, D. A. *Adv. Inorganic Biochem.* 1988, **7**, 245 - 265

3. Khosla, C., and Bailey, J. E. *Nature* 1988, **331**, 633 - 635

4. Khosla, C., Curtis, J. E., DeModena, J., and Bailey, J. E. *Bio/Technology* 1990, **8**, 849 - 853

5. Magnolo, S. K., Leenutaphong, D. L., DeModena, J. A., Curtis, J. E., Bailey, J. E., Galazzo, J. L., and Hughes, D. E. *Bio/Technology* 1991, **9**, 473 - 476

6. Wittenberg, J. B., and Wittenberg, B. A. *Annu. Rev. Biophys. Chem.* 1990, **19**, 217 - 241

7. Hart, R. A., Rinas, U., and Bailey, J. E. *J. Biol. Chem.* 1990, **265**, 12728 - 12733

8. Albertsson, P. A. *Partition of Cell Particles and Macromolecules* Wiley-Interscience, New York, 1971

9. Kohler, K., von Bonsdorff-Lindeberg, L., and Enfors, S. *Enzyme Microb. Technol.* 1989, **11**, 730 - 735

10. Bradford, M. M. *Anal. Biochem.* 1976, **72**, 248 - 254

11. Baskir, J. N., Hatton, T. A., and Suter, U. W. *Biotechnol. Bioeng.* 1989, **34**, 541 - 558

12. Brooks, D. E. et al. *J. Colliod Interface Sci.* 1984, **102**, 1 - 13

13. Kula, M. R., Kroner, K. H., and Hustedt, H. *Adv. Biochem. Engr.* 1982, **24**, 73 -

14. Laurie, S. H. in *Comprehensive Coordination Chemistry* (Wilkinson, G., ed.) 1987, 739 - 776

15. Cantor, C. R., and Schimmel, P. R. *Biophysical Chemistry, Part 1* Freeman, New York, 1980, p. 49

16. King, R. S., Blanch, H. W., and Prausnitz, J. M. *AIChE Journal* 1988, **34**, 1585 - 1594

17. Martell, A. E. *Critical Stability Constants* Plenum, New York, 1977, **3**, 3

18. Webster, D. A., and Liu, C. Y. *J. Biol. Chem.* 1974, **249**, 4257 - 4260

19. Veide, A., Strandberg, L., and Enfors, S. *Enzyme Microb. Technol.* 1987, **9**, 730 - 738

Table 1: VHb purification performance

Sample	Volume (ml)	Protein (mg)[1]	VHb (mg)[2]	P.F.(i)	P.F.(net)	Yield(i)	Yield(net)
Lysate	571	8288	912				
E1	1422	1196	469	3.56	3.56	0.51	0.51
E2	1422	606	465	1.96	6.98	0.99	0.50
E3	994	435	433	1.30	9.07	0.93	0.47

1. Determined by protein dye binding assay

2. Determined by VHb difference absorption spectroscopy

Table 2: Partition coefficients in PEG 4000 / sulfate salt two-phase systems

System (W/W)	V_t/V_b	K_{tp}	K_{VHb}
9.7% $MgSO_4$, 10.8% PEG 4000	0.67	0.09	0.06
12.8% $MnSO_4$, 11.5% PEG 4000	0.67	0.05	0.08
11.7% $(NH_4)_2SO_4$, 11.9% PEG 4000	0.67	1.979	18.32
12.4% Na_2SO_4 , 11.8% PEG 4000	0.43	2.439	45.75

Table 3: Partitioning model parameters

Parameter	Simulation 1	Simulation 2	Simulation 3
K_p^o	1.42	1.34	1.34
$\Delta\Psi$ (mV)	- 2.7	- 2.9	- 3.3
K_{Mg} (M^{-1})	$10^{0.51}$	$10^{0.40}$	$10^{0.18}$

2.9 Figures

Figure 1. Extraction of JM101:pRED2 soluble lysates containing VHb in PEG / dextran two-phase systems. (**A**) Partition coefficient data for VHb (filled) and total protein (open) following extraction in PEG 4000 / dextran T-500 (circle) and PEG 6000 / dextran T-500 (square) as a function of tie line length. The partition coefficient (K) is defined as the ratio of the protein concentration in the top phase to the protein concentration in the bottom phase. The tie line length (L) is defined as the length of a line on a binodial curve connecting the compositions of two coexisting phases. (**B**) SDS-PAGE analysis of extraction E1. Lane 1: soluble lysate; lane 2: PEG 4000-rich phase; lane 3: dextran-rich phase.

Figure 2. Extraction of the PEG 4000-rich top phase from extraction E1 by the addition of Na_2SO_4. (**A**) Partition coefficient data for VHb (filled) and total protein (open) as a function of tie line length. W indicates gm Na_2SO_4 added to 4 gm of PEG 4000-rich phase from extraction E1 containing 13.5% (w/w) PEG 4000. (**B**) Isoelectric focusing of the PEG 4000-rich phase from extraction E2. Lane 1: JM101:pRED2 soluble lysate; lane 2: PEG 4000-rich phase from extraction E2; lane 3: eluent from anion exchange chromatography of the PEG 4000-rich phase from extraction E1 (DEAE-cellulose, pH 8.0, 0.5 M NaCl elution). VHb focuses poorly in IEF due to pH instability properties discussed in the text.

Figure 3. Extraction of the PEG 4000-rich phase from extraction E2 by the addition of $MgSO_4$. (**A**) Partition coefficient data for VHb (filled)

and total protein (open) as a function of tie line length. W indicates gm $MgSO_4$ $7H_2O$ added to 4 gm of diluted PEG4000-rich phase from extraction E2 containing 13.5% (w/w) PEG 4000. (**B**) SDS-PAGE of the $MgSO_4$-rich phase from extraction E3. Lane 1: JM101:pRED2 soluble lysate; lane 2: $MgSO_4$-rich phase from extraction E3; lane 3: eluent from anion exchange chromatography of the PEG 4000-rich phase from extraction E2 (see Figure 2 for conditions).

Figure 4. Results of VHb purification protocol. (**A**) SDS-PAGE analysis of JM101 control soluble lysate (lane 2), JM101:pRED2 soluble lysate (lane 3), E1 (lane 4), E2 (lane 5), E3 (lane 6), M1 (lane 7) and GPC (lane 8) fractions. (**B**) Difference absorption spectra of Soret region of purification fractions. (**C**) Difference absorption spectra of alpha and beta region of purification fractions.

Figure 5. Effect of pH and Mg^{+2} concentration on the partitioning of purified VHb in PEG 4000 / sulfate salt two-phase systems. All systems are composed of 15% (w/w) PEG 4000 and 8% (w/w) sulfate salt. The measure of magnesium content in each system, R, equals 0.0 (□), 0.25 (■), 0.5 (○), 0.75 (●), and 1.0 (△) where,

R = (% (w/w) $MgSO_4$) / (% (w/w) Na_2SO_4 + % (w/w) $MgSO_4$)

The partition coefficient is plotted as a function of pH (**A, C and E**) and magnesium-modulated VHb charge (**B, D and F**). Simulations correspond to magnesium binding constants of $10^{0.51}$ (**A and B**), $10^{0.40}$ (**C and D**) and $10^{0.18}$ (**E and F**).

Figure 6. Solubility of VHb as a function of pH. (**A**) Relative solubility of purified VHb in the PEG 4000 / sulfate salt two-phase systems shown in Figure 5. If all VHb added to the two-phase systems remained soluble, the concentration would equal 100. (**B**) Electrophoretic titration analysis of purified VHb. Arrows indicate soluble VHb (**1**) and aggregated VHb (**2**).

Figure 1.

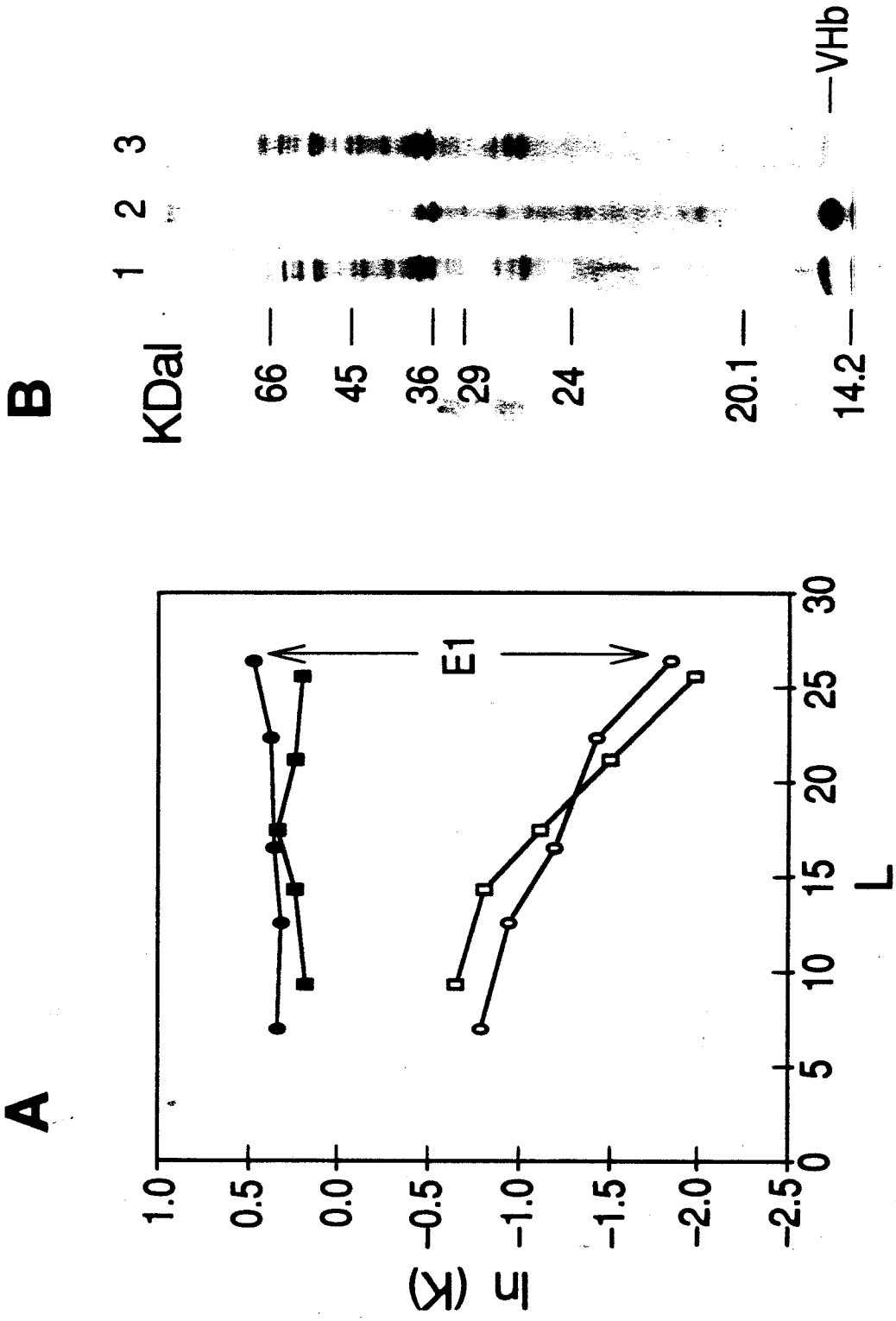
A
B
KDal
66
45
36
29
24
20.1
14.2
1
2
3
—VHb
E1
ln (K)
L
1.0
0.5
0.0
-0.5
-1.0
-1.5
-2.0
-2.5
0
5
10
15
20
25
30

Figure 2.

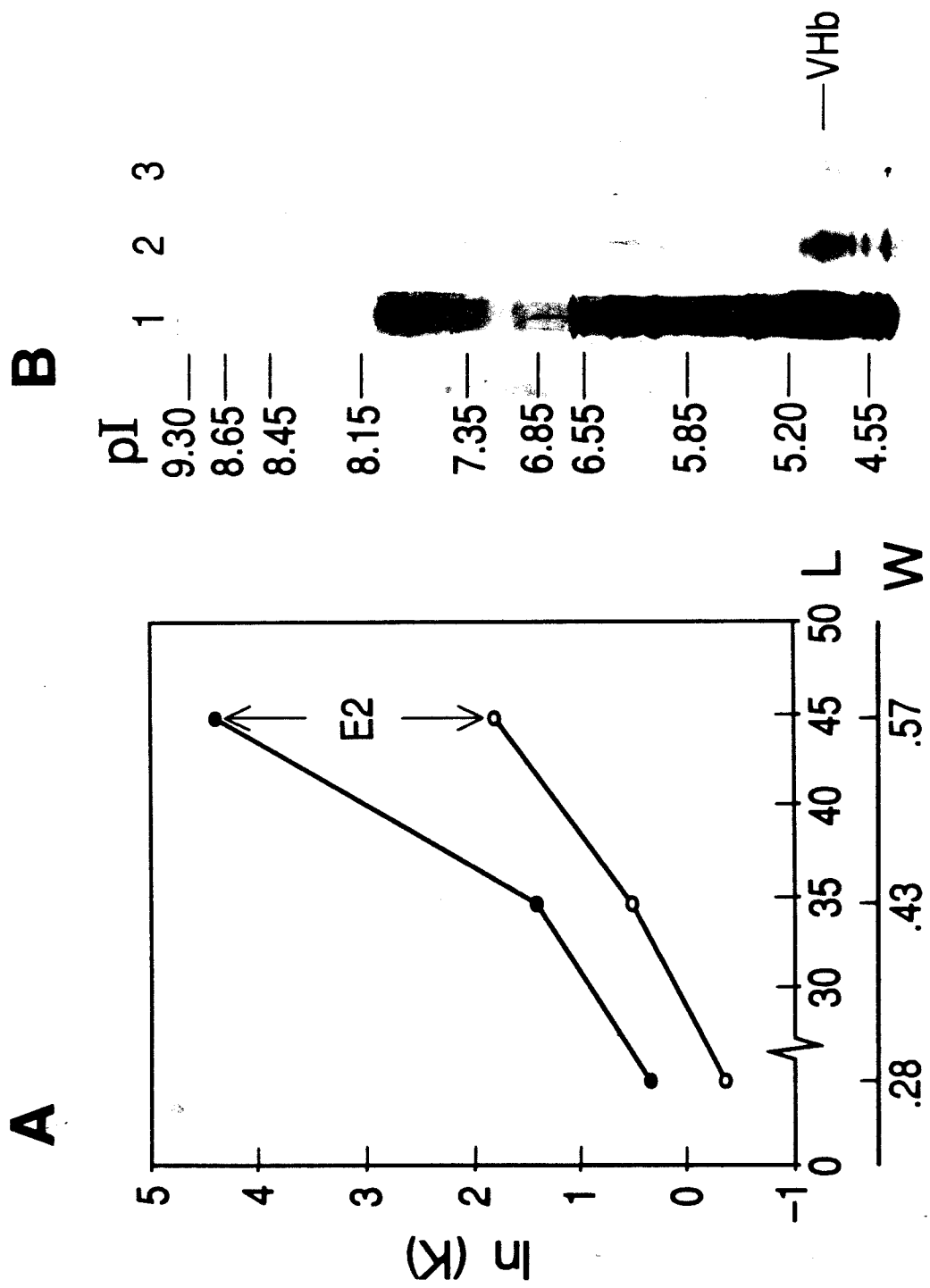
A
B
ln (K)
5
4
3
2
1
0
-1
E2
0
30
35
40
45
50
L
.28
.43
.57
W
pI
9.30
8.65
8.45
8.15
7.35
6.85
6.55
5.85
5.20
4.55
1
2
3
—VHb

Figure 3.

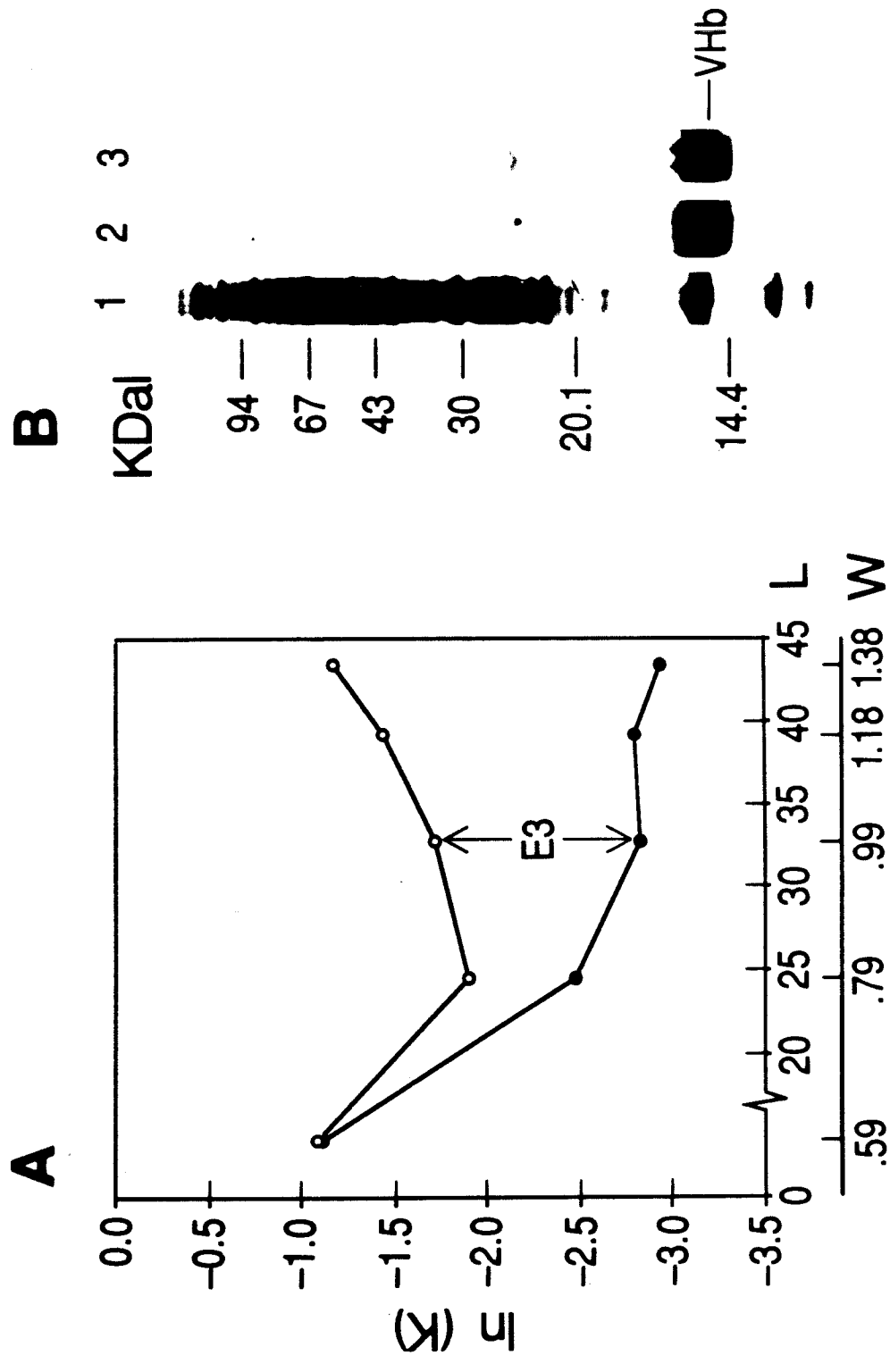
A
B
KDal
1 2 3
94
67
43
30
20.1
14.4
VHb
E3
0.0
-0.5
-1.0
-1.5
-2.0
-2.5
-3.0
-3.5
n (K)
0
20
25
30
35
40
45
L
.59
.79
.99
1.18
1.38
W

Figure 4.

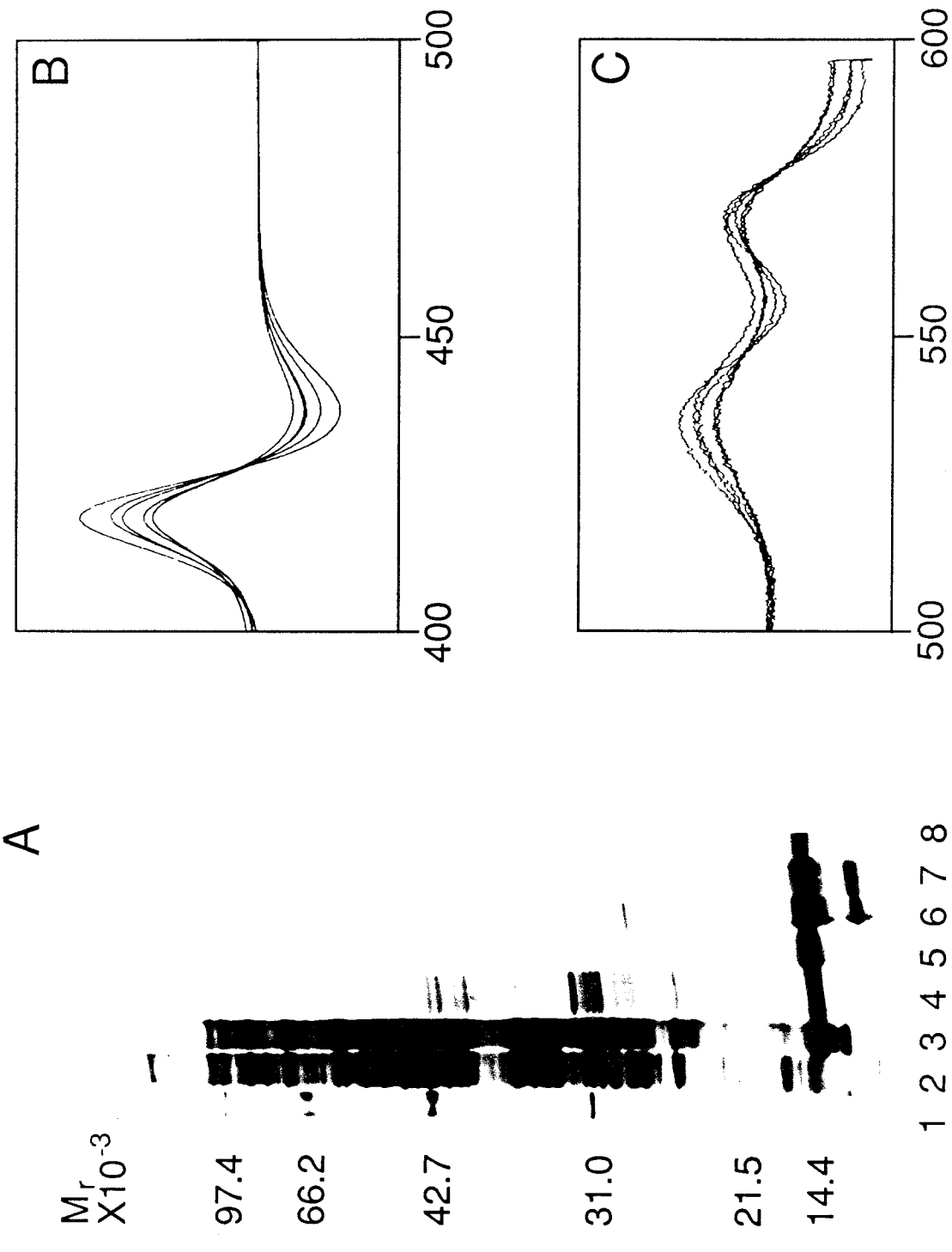
A
B
C
M_r X10^{-3}
97.4
66.2
42.7
31.0
21.5
14.4
1 2 3 4 5 6 7 8
400
450
500
500
550
600

Figure 5.

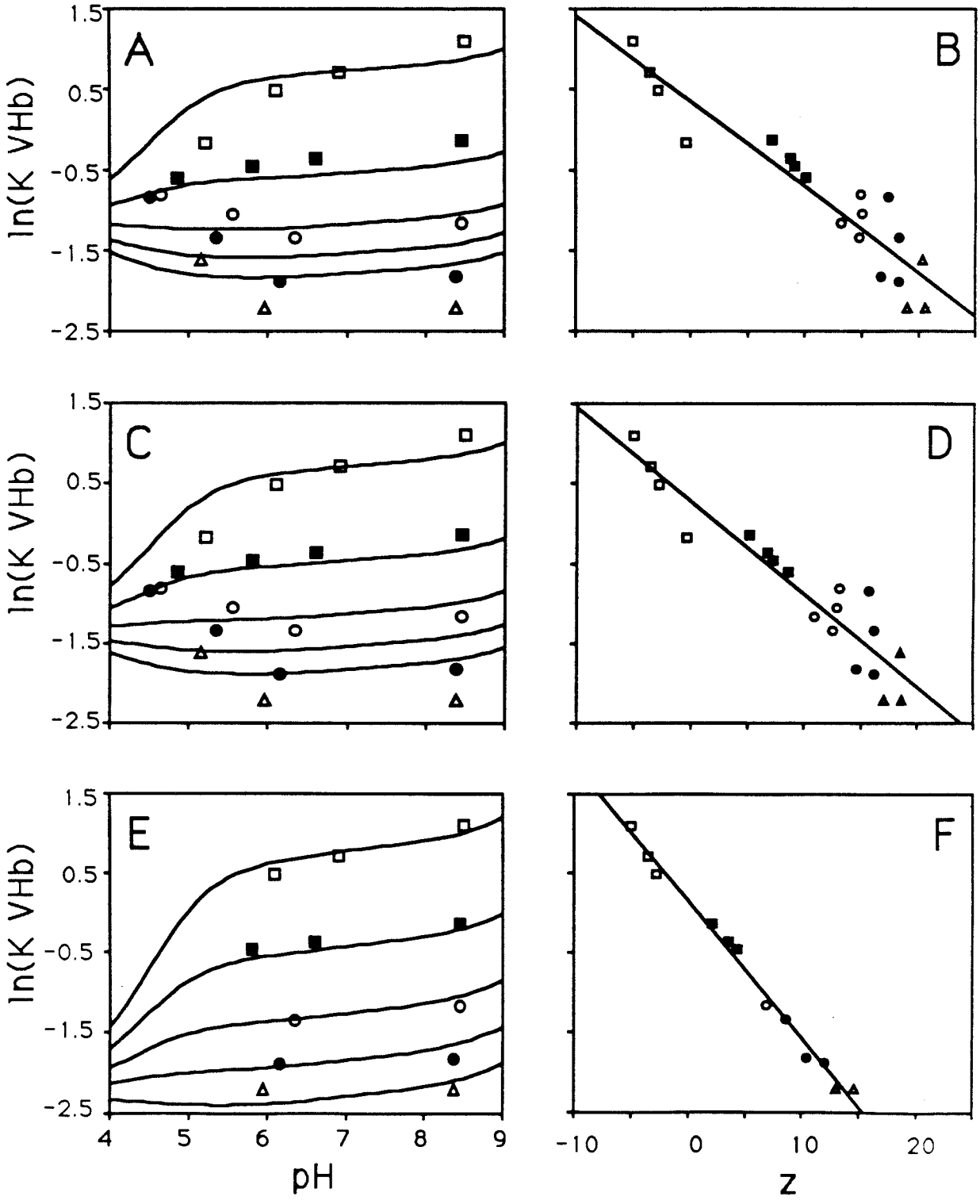

Figure 6.

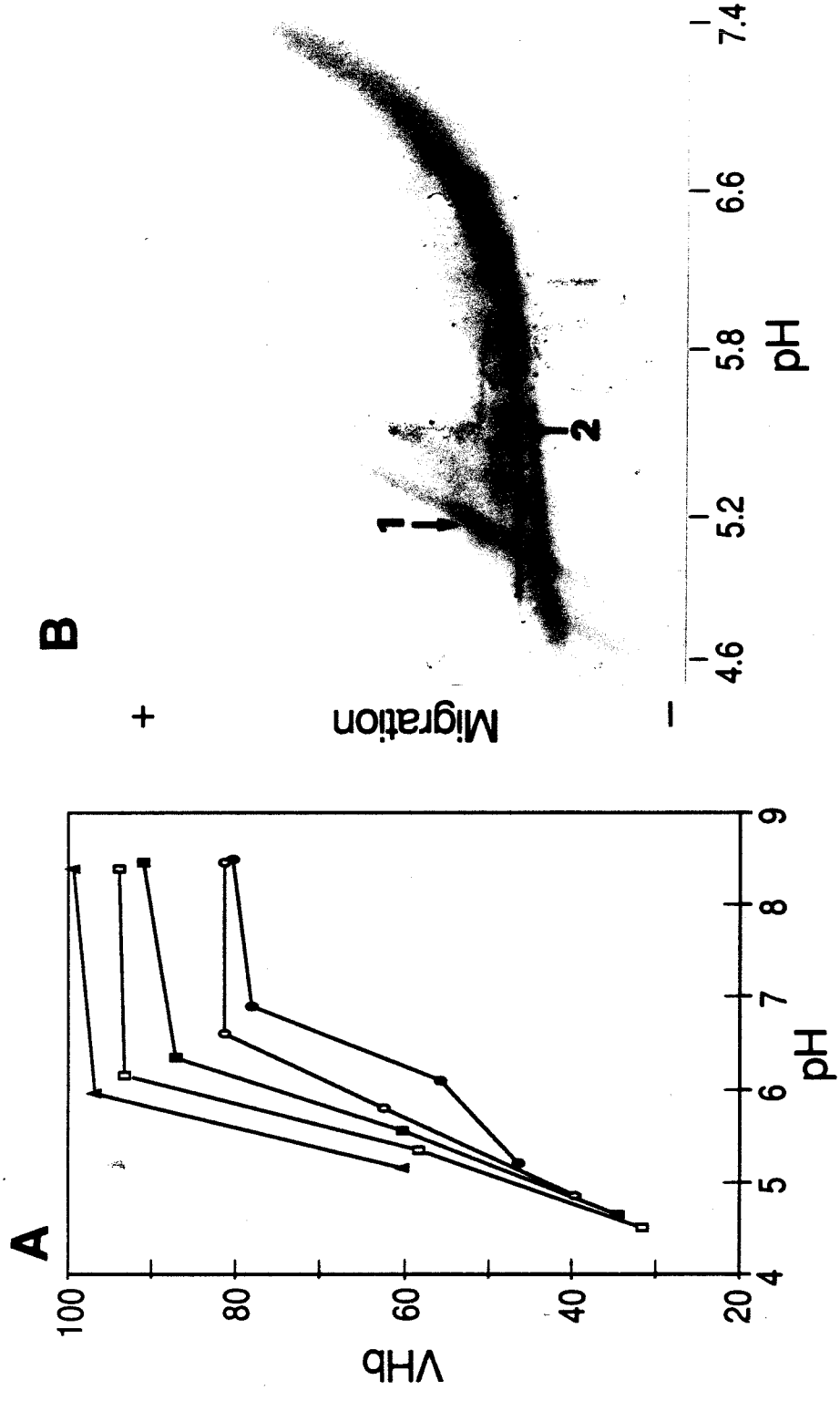

CHAPTER 3

Protein Composition of *Vitreoscilla* Hemoglobin Inclusion Bodies Produced in *Escherichia coli*

Source: Hart, R. A., Rinas, U., and J.E. Bailey (1990)

J. Biol. Chem., **265**, 12728 - 12733.

3.1 Summary

The protein composition of inclusion bodies produced in recombinant *Escherichia coli* overproducing *Vitreoscilla* hemoglobin (VHb) was analyzed by one-dimensional and two-dimensional electrophoresis techniques. Results indicate the presence of two types of cytoplasmic aggregates of differing morphology in single bacterial cells. These aggregates also differ in their relative content of VHb and pre-β-lactamase and are separable by differential centrifugation. Results further suggest that the cytoplasmic protein elongation factor Tu is integrated into VHb inclusion bodies. The presence of the outer membrane proteins OmpA and OmpF in inclusion body preparations is attributed to cell envelope contamination rather than specific involvement in inclusion bodies. The specificity of *in vivo* protein aggregation is discussed.

3.2 Introduction

The expression of a recombinant protein in the bacterial cell *E. coli* is often accompanied by the insolubilization of that protein *in vivo* into aggregates referred to as inclusion bodies. A large number of highly diverse proteins have been insolubilized in this way and it appears that the phenomenon of recombinant protein inclusion body formation is not unique to *E. coli* or for that matter to bacterial cells (Kitano *et al.*, 1987a). Several incisive reviews of the literature concerning inclusion body formation have been prepared (Kane and Hartley, 1988; Mitraki and King, 1989; and Schein, 1989).

Despite the abundance of recombinant systems which produce inclusion bodies, little is known concerning the properties of these aggregates or their fundamental mechanism of formation. The presence of ordinarily soluble proteins in insoluble aggregates, lacking measurable activity and requiring chaotropic agents for dissolution, suggested from the outset that inclusion body proteins lack native conformation. Indirect evidence provided by polyclonal antibody binding (Paul *et al.*, 1983) and non-denaturing solubilization techniques (Kronheim et al., 1986; Hoess *et al.*, 1988), however, indicated that inclusion body proteins possess aspects of native conformation. The first direct evidence concerning the conformational state of *in vivo* insolubilized protein was provided by King and his associates (Goldenberg and King, 1982; Goldenberg et al., 1983; Haase-Pettingell and King, 1988). Their findings indicate that aggregates derive from specific partially folded intermediates and not from mature or fully unfolded proteins.

Inclusion bodies are generally relatively devoid of contaminant proteins suggesting that *in vivo* association of misfolded protein species to form inclusion bodies is a highly specific process. The specificity of protein association in aggregation processes seemingly analogous to inclusion body formation has been discussed (Mitraki and King, 1989). Investigators have, however, reported finding specific protein contaminants in inclusion bodies such as the subunits of RNA polymerase and outer membrane proteins (Hartley and Kane, 1988). Proteins conferring antibiotic resistance for selection pressure are, as a class, most often cited as inclusion body contaminant proteins (Schoner *et al.*, 1985). Invariably, in these cases, the genes for the desired recombinant protein and the protein conferring antibiotic resistance are contained on the same plasmid. There is *a priori* no reason to expect specificity of association between the folding intermediates of this class of proteins and those of the reported desired proteins. Thus, this observation suggests that protein aggregation might occur in the vicinity of plasmid protein translation and be, at least in part, kinetically driven leading to an apparent loss of aggregation specificity. Following this logic, for fast aggregation kinetics, one might further expect to find numerous cellular macromolecules associated with protein expression as contaminants in inclusion bodies (Kane and Hartley, 1988; Hartley and Kane, 1988).

To investigate *in vivo* protein aggregation specificity and its role in inclusion body formation, we analyzed the protein composition of *Vitreoscilla* hemoglobin (VHb) inclusion bodies produced in *E. coli*. Proteins integrated into inclusion bodies were discerned from cell envelope contamination by detergent solubilization. Integral inclusion body proteins were identified by two-dimensional

electrophoresis and immunological staining. Our results indicate the presence of two types of cytoplasmic inclusion bodies differing in their relative content of VHb and pre-β-lactamase, both expressed from genes carried on the same plasmid.

3.3 Materials and Methods

Bacterial strains and plasmids - *Escherichia coli* JM101 was used as the host strain. The plasmid pRED2 is a derivative of pUC19 containing the VHb gene under the control of its native promoter (Khosla and Bailey, 1988).

Media and growth conditions - Complex growth medium containing 10 g/l bactotryptone, 5 g/l yeast extract, 5 g/l NaCl, 3 g/l K_2HPO_4, and 1 g/l KH_2PO_4 was used throughout. Growth medium for JM101:pRED2 was supplemented with 0.1 g/l ampicillin. Capped 2 liter flasks (Kimax) containing 1 liter medium were inoculated with 5 ml of overnight culture and grown in a Lab-Line Orbit Environ-Shaker at 225 rpm and 37 °C. After 15 hours of growth, each culture was supplemented with 10 ml of feed media consisting of 110 g/l bactotryptone, 110 g/l yeast extract, and 110 g/l glucose. Growth was continued for 6 additional hours with a reduced shaker speed of 175 rpm.

Isolation of soluble and insoluble fractions - Cell harvest, lysis and inclusion body isolation procedures are essentially as reported previously (Marston *et al.*, 1984). All procedures were carried out at 4 °C unless otherwise indicated. Cells were harvested by centrifugation, resuspended in buffer A, consisting of 100 mM Tris-HCl (pH 8), 50 mM NaCl, 1 mM EDTA, 1 mM dithiothreitol

(DTT), 0.1 mM phenylmethylsulfonyl fluoride, and lysed by sonication on ice. The crude lysate suspension was fractionated into soluble and insoluble fractions by differential centrifugation in a Beckman J2-21 Centrifuge with a JA20 rotor. Insoluble lysate fraction I was isolated by centrifugation of the crude lysate suspension at 6,000 g for 10 min. Centrifugation of the resulting supernatant at 12,500 g for 15 min yielded insoluble lysate fraction II. Centrifugation of the resulting supernatant at 40,000 g for 2 h yielded the soluble lysate fraction. Insoluble lysate fractions were washed twice with buffer A. All fractions were stored at -70 °C for further analysis.

Detergent extraction - Detergent extraction procedures are essentially as reported previously (Schnaitman, 1971b; Langley *et al.*, 1987). Insoluble lysate fractions were washed twice with 50 mM Tris-HCl (pH 8), 10 mM EDTA, resuspended in 50 mM Tris-HCl (pH 8), 10 mM EDTA, 1.6 g/l lysozyme and incubated at 25 °C for 40 min with periodic mixing. Resulting suspensions were then divided into two aliquots and made up to final concentrations of either 2% (v/v) Triton X-100 or 2% (w/v) sodium deoxycholate and incubated at 25 °C for 40 additional min with periodic mixing. Remaining particulate was isolated by centrifugation at 40,000 g for 30 min and washed once with 50 mM potassium phosphate (pH 7). All fractions were stored at -70 °C for further analysis.

Gel Electrophoresis - One-dimensional SDS polyacrylamide gel electrophoresis (SDS-PAGE) was performed according to the method of Laemmli (1970). Samples were prepared in 4% (w/v) SDS, 20% (w/v) glycerol, 12.5 mM DTT, 125 mM Tris-HCl (pH 6.8), sonicated several seconds, boiled for 10 min,

and electrophoresed on a 9 - 16 % acrylamide gradient gel. Two-dimensional electrophoresis was performed using the O'Farrell technique (1975) as modified by Hochstrasser *et al.*(1988). Samples were prepared in 2% SDS, 30 mM DTT, sonicated several seconds, boiled for 10 min and electrophoresed. Isoelectric focusing for the first dimension was performed to equilibrium (4 h 200 V, 4 h 500 V, and 8 h 2000 V) using the Bio-Rad model 175 chamber. The ampholine mixture used consisted of 2% (v/v) Serva pH 3 - 10, 2% (v/v) Bio-Rad pH 3 - 10 and 1% (v/v) Bio-Rad pH 5 - 7. SDS-electrophoresis for the second dimension was performed on a 9 - 16 % acrylamide gradient gel at constant current (40 mA per gel, 160 x 200 x 1.5 mm) using the Bio-Rad Protean II Multi-Cell electrophoresis apparatus.

Silver staining was performed according to the method of Hochstrasser *et al.* (1988). Electrophoretic transfer of protein for Western blotting was done according to the method of Towbin *et al.* (1979). Rabbit anti-RTEM-β-lactamase antiserum (J. Richards) and rabbit anti-VHb antiserum (Exogene Corp., Pasadena, Ca. USA) were used with a commercially available kit for immunodetection (Vectastain ABC Kit, Vector Labs, Burlingame, Ca. USA). Procedures for immunostaining supplied by Vector Labs were followed.

Microscopy - Sample preparation procedures for electron microscopy were essentially as reported previously (Kitano et al., 1987b). Cell samples were fixed with 2% (v/v) glutaraldehyde in 100 mM cacodylate (pH 7.4), post-fixed with 2% (w/v) osmium tetroxide, en-bloc stained with 1% (w/v) uranyl acetate in 100 mM malate (pH 5), dehydrated in a graded series of ethanol,

cleared with propylene oxide and embedded in Polysciences LR-White. Thin sections were stained with uranyl acetate and lead citrate. Samples were examined using a Phillips 420 Transmission Electron Microscope. Cells for phase contrast microscopy were viewed while in growth media with an Olympus BH light microscope.

3.4 Results

The recombinant *E. coli* strain JM101:pRED2 bears a high copy number plasmid encoding *Vitreoscilla* hemoglobin (VHb) under the control of its native promoter (Khosla and Bailey, 1988). When grown under microaerobic conditions, this strain is found to produce both soluble and insoluble forms of VHb. Microscopic examination of the recombinant cells grown under this condition reveals an abnormally elongated cell morphology and a large variety of cytoplasmic aggregates not found in plasmid lacking JM101 control cells grown under parallel conditions. The inclusion bodies, as seen in Figure 1, exhibit a large degree of heterogeneity whether viewed by phase contrast or transmission electron microscopy. In addition to the large, dense, spherical bodies generally termed refractile bodies, looser flocculated clusters with irregular boundaries are also seen.

In order to distinguish whether the two aggregate types seen by microscopy differ in composition, whole cell lysates of JM101:pRED2 were fractionated into two insoluble fractions by differential centrifugation and analyzed by SDS-PAGE with the results shown in Figure 2A. The two insoluble fractions, isolated as

described in the Materials and Methods section, differ from each other in protein composition as well as from comparable fractions of JM101 controls. The most notable differences between the two insoluble fractions from JM101:pRED2 (lanes 4 and 6 in Figure 2A) are produced by bands at 31.5 and 33 kDa which are present in fraction I but absent, or dramatically reduced, in fraction II. These proteins are not present in whole cell lysates of JM101 and are not present in the soluble fraction of JM101:pRED2. Insoluble fractions I and II from JM101:pRED2 additionally contain a band at 43 kDa not found in comparable insoluble fractions of JM101 but present in whole cell lysates of JM101 and the soluble fraction of JM101:pRED2 (data not shown). The only differences between the soluble fractions of JM101:pRED2 and JM101 are bands at 15.8 and 31 kDa (indicated by arrows in Figure 2A) attributable to VHb and β-lactamase, respectively; the proteins expected from expression of the recombinant plasmid.

To ascertain whether the compositional differences between insoluble fractions I and II were due to inclusion bodies or crude cell envelope, and more generally to identify integral inclusion body proteins, EDTA/lysozyme/detergent extraction was used for the selective solubilization of cell envelope proteins. The soluble and insoluble fractions resulting from these extractions were analyzed by SDS-PAGE (Figure 2B). The non-ionic detergent Triton X-100 effectively solubilizes cytoplasmic membrane proteins from cell envelope fractions (Schnaitman, 1971a). Pretreatment of envelope fractions with EDTA and lysozyme followed by extraction with Triton X-100 solubilizes about half of the cell wall proteins as well as the cytoplasmic membrane proteins (Schnaitman, 1971b). Inclusion bodies, on the other hand, have in general been found to be stable to Triton

X-100 extraction (Marston *et al.*, 1984). Treatment of insoluble fractions I and II with EDTA and lysozyme followed by extraction with 2% Triton X-100 partially solubilizes most of the proteins in these fractions. As VHb remains entirely insoluble, however, it is evident that inclusion body dissolution has not occurred; hence, proteins solubilized with this treatment clearly arise from the cell envelope.

The bile salt deoxycholate is a more powerful membrane solubilizing agent than Triton X-100 and tends to be more effective in dissociating protein aggregates such as those seen in membrane structures (Helenius and Simons, 1975; Helenius *et al.*, 1979). The use of EDTA/lysozyme/deoxycholate extraction for the removal of endotoxin, phospholipid and nucleic acid from inclusion body containing insoluble fractions with only slight solubilization of recombinant protein has been described (Langely *et al.*, 1987). Treatment of fractions I and II with EDTA and Lysozyme followed by extraction with 2% deoxycholate leads to greater protein solubilization than occurred with Triton X-100 extraction. Indeed, partial inclusion body dissolution is evident as some VHb is solubilized. Even when extracted with sodium deoxycholate, however, particular proteins are clearly more resistant to solubilization and are only liberated to the extent that VHb is. Such proteins are considered to be integral inclusion body proteins. Proteins demonstrating this behavior include those which migrate at 31.5, 33 and 43 kDa and distinguish JM101:pRED2 insoluble fractions I and II from comparable JM101 insoluble fractions.

A higher resolution analysis of the composition of the two different insoluble fractions is afforded by two-dimensional gel electrophoresis, as shown in Figure

3 (Two-dimensional electrophoresis gels were run by Ursula Rinas). These gels clearly indicate the differences between the fractions discussed earlier. Comparison of the two-dimensional electrophoresis protein patterns obtained with the protein index established by Neidhardt and coworkers (Phillips *et al.*, 1987) allows identification of several of the proteins present in the insoluble fractions of JM101:pRED2. The prominent spot migrating at 35 kDa is identified as OmpA and is present in all isolated insoluble fractions. This protein is partly solubilized by extraction with Triton X-100 and is not present at significantly higher levels in JM101:pRED2 than JM101; hence OmpA is not considered to be an integral inclusion body protein. The same observation is made concerning OmpF, a protein which migrates at 37 kDa but does not stain reproducibly with silver so is not apparent in all gels shown. The prominent spot migrating at 43 kDa is found at the same location as the cytoplasmic protein elongation factor Tu (EF-Tu). This protein is resistant to solubilization by EDTA/lysozyme/detergent extraction and is considered to be an integral inclusion body protein. VHb appears as a multiple spot pattern on two-dimensional gels (multiple isoelectric points). This pattern is the same for both soluble and insoluble fractions and is identical to that obtained for purified soluble VHb (data not shown).

Identification of the 31.5 and 33 kDa proteins in insoluble fraction I of JM101:pRED2 as VHb and β-lactamase variants, respectively, was initially made on the observation that they were found only in strains harboring the appropriate structural gene as discussed above. Evidence supporting this assignment is provided by the Western blots shown in Figure 4. The 33 kDa band reacts with antiserum raised against β-lactamase but not with antiserum raised against

VHb, clearly identifying the protein as the precursor form of β-lactamase (Sutcliffe, 1978). The 31.5 kDa band reacts with antiserum raised against VHb but not with antiserum raised against β-lactamase. Additionally, treatment with high amounts of reducing agent prior to electrophoresis leads to a dramatic reduction in the size of this spot on two-dimensional gels (Figure 5). Based on reactivity with antiserum raised against VHb, molecular weight, and behavior under extreme reducing conditions, this protein is identified as a disulfide-linked VHb dimer. Numerous other bands, including ones in the vicinity of both 31.5 and 43 kDa, appear with immunodetection by antiserum raised against either VHb or β-lactamase. The two-dimensional gels also show spot multiplicity in the vicinity of 31.5 and 43 kDa. These protein species are not affected by treatment with excess reducing agent prior to electrophoresis (data not shown). The identity of these proteins is unknown at this time.

3.5 Discussion

Microscopic analysis indicates that two types of inclusion bodies, differing in general morphology, are produced in single cells of JM101:pRED2. Fractionation of the insoluble material in whole-cell lysate suspensions by differential centrifugation followed by electrophoretic analysis shows that the isolated fractions contain two types of inclusion bodies differing in protein composition. There are two mechanisms one can envision for the production of different types of inclusion bodies in single recombinant *E. coli* cells. One mechanism is based on compartmentalization in which proteins partition between, and aggregate in, different cell compartments, namely the cytoplasm and the periplasm. This

mechanism appears to have been responsible for the presence of pre-β-lactamase in β-lactamase inclusion body fractions (Georgiou *et al.*, 1986; Bowden and Georgiou, 1988). This mechanism is not responsible, however, for the two types of inclusion bodies seen in JM101:pRED2 as aggregates are only seen in the cytoplasmic space.

Another mechanism is based on specificity of protein aggregation in which different proteins preferentially associate with themselves rather than with each other during insolubilization. Such a mechanism, in its extreme, would yield distinct aggregates of high purity for each of the species insolubilized. Specificity of association during aggregation has been seen in *in vitro* refolding studies of proteins in complex protein mixtures (London *et al.*, 1974). This type of mechanism is supported in this case by two observations: cytoplasmic pre-β-lactamase inclusion bodies, apparently lacking integral protein contaminants, are produced by JM101:pUC19, cells containing the parent plasmid of pRED2, when grown under the conditions described; and VHb inclusion bodies free of pre-β-lactamase can be produced in JM101:pRED2 when grown under different conditions from those described (data not shown). These two observations demonstrate that pre-β-lactamase and VHb can independently aggregate to form inclusion bodies under conditions similar to those described.

The observation that different pellet fractions contain different proteins indicates a correlation between aggregate colloidal properties and protein composition. Two possible processes which could account for this are: a temporal dependence of contaminant protein insolubilization, such that different proteins are insolubilized at different stages of inclusion body growth, and the selective

insolubilization of different proteins into different inclusion bodies. To determine the temporal dependence, the protein composition of insoluble lysate fraction I was examined at different stages of the cultivation. Results show that VHb, VHb dimer, pre-β-lactamase and EF-Tu are insolubilized in the same proportion throughout the entire cultivation. A dramatic increase in the amount of all species occurs following nutrient replenishment and concomitant aeration reduction, however, the increase is again proportional. To determine whether VHb and pre-β-lactamase were insolubilized selectively in different inclusion bodies, experiments were undertaken to determine whether insoluble lysate fraction I, which contains both VHb and pre-β-lactamase, could be further fractionated. Analytical techniques used to distinguish differences in particle size (Taylor *et al.*, 1986) and density (Schoner *et al.*, 1985; Taylor *et al.*, 1986) did not indicate the presence of two distinguishable aggregates in fraction I. These same techniques, however, did not indicate distinguishable differences between JM101:pRED2 insoluble fractions and JM101 insoluble fractions even when treated by EDTA/lysozyme/Triton extraction (data not shown). This is likely because of interactions between inclusion bodies and cell envelope or its components. Based on these experiments we are unable to determine the exact protein composition of the two aggregates seen by microscopy or determine if insoluble fraction I is composed of a mixture of these two aggregates. These experiments do, however, reinforce the need for the use of suitable controls when investigating inclusion bodies because of contamination of inclusion body preparations by cell envelope.

Our conclusions concerning what cellular proteins can be considered as integral inclusion body proteins differ in part from those of other authors. Hartley and Kane (1988) reported finding the four subunits of RNA polymerase (α, σ, β and β') as well as a combination of OmpA, OmpF and OmpC in inclusion bodies by analysis with SDS-PAGE. They note that these proteins were always present in inclusion bodies regardless of the cloned gene, promoter, plasmid vector, fermentation regimen, or media composition. No discussion is given, however, to the methods used to eliminate or at least account for crude cell envelope contaminants which are always present in the insoluble fraction of cell lysates. Veeraragavan (1989) reported finding OmpA and OmpF in inclusion bodies purified by density gradient centrifugation. As these proteins, however, were present in the processed form in cytoplasmic inclusion bodies, the conclusion made was that these proteins were deposited in inclusion bodies following or during lysis by sonication. This conclusion additionally implies that density gradient centrifugation is ineffective in removing crude cell envelope from inclusion body preparations.

We have identified OmpA and OmpF in insoluble fractions containing inclusion bodies by two-dimensional electrophoresis. Analysis of their solubilization properties with EDTA/lysozyme/detergent extraction relative to that for VHb leads us to conclude that OmpA and OmpF are not integral contaminants of VHb inclusion bodies, but rather are contributed to the insoluble fraction through their involvement with the cell envelope. This conclusion is further supported by the observation that OmpA and OmpF are mature outer membrane proteins formed by cotranslational cleavage of precursor species and therefore

not available for insolubilization in the cytoplasmic space (Silhavy *et al.*, 1983). Results suggest that the cellular protein EF-Tu may be an integral protein of VHb inclusion bodies. Analysis of inclusion bodies formed by aggregation of various forms of porcine somatotropin, however, indicates that EF-Tu may not be a general inclusion body contaminant but rather one specific to this system (data not shown). Elongation factor Tu is intimately involved in the elongation cycle during protein synthesis (Hershey, 1987) and is the most abundant protein in the *E. coli* cell.

Some discussion regarding the disulfide-linked VHb dimers found insolubilized is warranted. One would expect the probability of formation of this species would be low as monomeric VHb only contains one cysteine residue and native dimeric VHb does not contain a disulfide bond (Wakabayashi *et al.*, 1986). This species is found systematically only in insoluble fraction I despite the presence of considerable VHb in insoluble fraction II. Further, it is present in whole cell samples lysed by treatment with electrophoresis sample buffer containing SDS and DTT, conditions sufficient to solubilize inclusion bodies concurrent with cell lysis and inhibitory to disulfide bond formation. Overall, this type of behavior appears inconsistent with that expected for a species thought to be formed following cell lysis (Schoemaker *et al.*, 1985; Langley *et al.*, 1987; Tsuji *et al.*, 1987) but rather suggests that the species is formed *in vivo*. Such a process may be possible in this case as the recombinant cell contains very large amounts of an oxygen-binding protein, VHb, whose presence may tend to make the cellular environment more oxidative than usual.

Our observations regarding the state of protein structure in inclusion bodies are supportive of the well established view that inclusion body proteins are misfolded. Regardless of the mechanism for disulfide formation, the disulfide-linked VHb dimer found in inclusion bodies is clearly in a non-native state as VHb dimer isolated from *Vitreoscilla* lacks intermolecular disulfide cross-links. Additionally, spectroscopic analysis of inclusion body fractions and purified soluble fraction VHb indicates that the insoluble VHb lacks heme whereas the soluble form contains heme and appears properly folded (manuscript in preparation).

3.6 Acknowledgements

This research was supported by the National Science Foundation (Grant No. EET-8606179) and by a grant for predoctoral training in biotechnology from the National Institute of General Medical Sciences (National Research Service Award 1 $T32$ GM 08346 – 01, Pharmacology Sciences Program). The authors thank C. Khosla for providing bacterial strains, M. Harrington for instruction in two-dimensional gel electrophoresis, J. Richards for providing β-lactamase antiserum, Exogene Corporation for providing VHb antiserum, and J. Edens for technical assistance in electron microscopy. U. Rinas is the recipient of a postdoctoral fellowship from the Deutsche Akademische Austauschdienst (DAAD).

3.7 References

1. Bowden, G. A., and Georgiou, G. (1988) *Biotechnol. Prog.* **4**, 97 - 101

2. Georgiou, G., Telford, J. N., Schuler, M. L., and Wilson, D. B. (1986) *Appl. Envir. Microbiol.* **52**, 1157 - 1161

3. Goldenberg, D., and King, J. (1982) *Proc. Natl. Acad. Sci. USA* **79**, 3403 - 3407

4. Goldenberg, D. P., Smith, D. H., and King, J. (1983) *Proc. Natl. Acad. Sci. USA* **80**, 7060 - 7064

5. Haase-Pettingell, C. A., and King, J. (1988) *J. Biol. Chem.* **263**, 4977 - 4983

6. Hartley, D. L., and Kane, J. F. (1988) *Biochem. Soc. Trans.* **16**, 101 - 102

7. Helenius, A., and Simons, K. (1975) *Biochim. Biophys. Acta* **415**, 29 - 79

8. Helenius, A., McCaslin, D. R., Fries, E., and Tanford, C. (1979) *Methods Enzymol.* **56**, 734 - 749

9. Hershey, J. W. B. (1987) in *Escherichia coli and Salmonella typhimurium Cellular and Molecular Biology* (Neidhardt, F. C., editor in chief) Vol. 1, pp. 613 - 647, American Society for Microbiology, Washington, D. C.

10. Hochstrasser, D. F., Harrington, M. G., Hochstrasser, A. C., Miller, M. J., Merril, C. R. (1988) *Anal. Biochem.* **173**, 424 - 435

11. Hoess, A., Arthur, A. K., Wanner, G., and Fanning, E. (1988) *Bio/Tech nology* **6**, 1214 - 1217

12. Kane, J. F., and Hartley, D. L. (1988) *Trends in Biotechnol.* **6**, 95 - 101

13. Khosla, C., and Bailey, J. E. (1988) *Mol. Gen. Genet.* **214**, 158 - 161

14. Kitano, K., Nakao, M., Itoh, Y., and Fujisawa, Y. (1987a) *Bio/Technology* **5**, 281 - 283

15. Kitano, K., Fujimoto, S., Nakao, M., Watanabe, T., and Nakao, Y. (1987b) *J. Biotechnol.* **5**, 77 - 86

16. Kronheim, S. R., Cantrell, M. A., Deeley, M. C., March, C. J., Glackin, P. J., Anderson, D. M., Hemenway, T., Merriam, J. E., Cosman, D., and Hopp, T. P. (1986) *Bio/Technology* **4**, 1078 - 1082

17. Laemmli, U. K. (1970) *Nature* **227**, 680 - 685

18. Langley, K. E., Berg, T. F., Strickland, T. W., Fenton, D. M., Boone, T. C., and Wypych, J. (1987) *Eur. J. Biochem* **163**, 313 - 321

19. London, J., Skrzynia, C., Goldberg, M. E. (1974) *Eur. J. Biochem.* **47**, 409 - 415

20. Marston, F. A. O., Lowe, P. A., Doel, M. T., Schoemaker, J. M., White, S., and Angal, S. (1984) *Bio/Technology* **2**, 800 - 804

21. Mitraki, A., and King, J. (1989) *Bio/Technology* **7**, 690 - 697

22. O'Farrell, P. H. (1975) *J. Biol. Chem.* **250**, 4007 - 4021

23. Paul, D. C., Van Frank, R. M., Muth, W. L., Ross, J. W., and Williams, D. C. (1983) *Eur. J. Cell Biol.* **31**, 171 - 174

24. Phillips, T. A., Vaughn, V., Bloch, P. L., and Neidhardt, F. C. (1987) in *Escherichia coli and Salmonella typhimurium Cellular and Molecular Biology* (Neidhardt, F. C., editor in chief) vol. 2, pp. 919 - 966, American Society for Microbiology, Washington, D. C.

25. Schein, C. H. (1989) *Bio/Technology* **7**, 1141 - 1149

26. Schnaitman, C. A. (1971a) *J. Bacteriol.* **108**, 545 - 552

27. Schnaitman, C. A. (1971b) *J. Bacteriol.* **108**, 553 - 563

28. Schoner, R. G., Ellis, L. F., and Schoner, B. E. (1985) *Bio/Technology* **3**, 151 - 154

29. Schoemaker, J. M., Brasnett, A. H., and Marston, F. A. O. (1985) *EMBO J.* **4**, 775 - 780

30. Silhavy, T. J., Benson, S. A., and Emr, S. D. (1983) *Microbiol. Rev.* **47**, 313 - 344

31. Sutcliffe, J. G. (1978) *Proc. Natl. Acad. Sci. USA* **75**, 3737 - 3741

32. Taylor, G., Hoare, M., Gray, D. R., and Marston, F. A. O. (1986) *Bio/Technology* **4**, 553 - 557

33. Towbin, H., Staehelin, T., and Gordon, J. (1979) *Proc. Natl. Acad. Sci. U. S. A.* **76**, 4350 - 4354

34. Tsuji, T., Nakagawa, R., Sugimoto, N., and Fukuhara, K. (1987) *Biochemistry* **26**, 3129 - 3134

35. Veeraragavan, K. (1989) *FEMS Microbiol. Lett.* **61**, 149 - 152

36. Wakabayashi, S., Matsubara, H., and Webster, D. A. (1986) *Nature* **322**, 481 - 483

3.8 Figures

Figure 1. Photomicrographs of JM101:pRED2 cells. (**A**) Phase contrast micrograph (bar is 1 μm). (**B**) Transmission electron micrograph (bar is 1 μm). In addition to refractile type inclusion bodies (rIB), cells also contain floccule type inclusion bodies (fIB).

Figure 2. SDS-PAGE analysis of insoluble fractions. (**A**) Comparison of soluble and insoluble lysate fractions of JM101 (lanes 1, 3 and 5) and JM101:pRED2 (lanes 2, 4 and 6). The soluble lysate fraction (lanes 1 and 2) and insoluble lysate fractions I (lanes 3 and 4) and II (lanes 5 and 6) were obtained as described in the Materials and Methods section. Insoluble fractions are concentrated 4 times relative to respective soluble fractions. (**B**) EDTA/lysozyme/detergent extraction of JM101:pRED2 insoluble lysate fractions I (lanes 1 - 4) and II (lanes 5 - 8). Following extraction with EDTA/lysozyme/Triton X-100 (lanes 1, 2, 5 and 6) and EDTA/lysozyme/deoxycholate (lanes 3, 4, 7 and 8) insoluble proteins were separated from soluble ones by centrifugation as described in the Materials and Methods section. Inclusion body proteins were still largely insoluble and were found in the resulting pellet fraction (lanes 1, 3, 5 and 7), while most cell envelope proteins were solubilized and were found in the resulting supernatant fraction (lanes 2, 4, 6 and 8).

Figure 3. Two-dimensional electrophoresis of insoluble lysate fractions of JM101 and JM101:pRED2. Conditions for electrophoresis were as described in the Materials and Methods section. (**A**) Insoluble lysate fraction I of

JM101. (**B**) Insoluble lysate fraction I of JM101:pRED2. (**C**) Insoluble lysate fraction II of JM101:pRED2. The major proteins in insoluble lysate fraction I of JM101:pRED2, as identified in the figure, include: VHb (a), OmpA (b), OmpF (c), EF-Tu (d), disulfide-linked VHb dimer (e) and pre-β-lactamase (f). (Two-dimensional electrophoresis gels were run by Ursula Rinas)

Figure 4. Identification of disulfide-linked VHb dimer and pre-β-lactamase in inclusion bodies by Western blotting. The proteins in insoluble lysate fraction I of JM101 (lanes 1, 3 and 5) and JM101:pRED2 (lanes 2, 4 and 6) were resolved by SDS-PAGE. Replicate lanes were then silver stained (lanes 1 and 2) or electroblotted onto nitrocellulose for immunostaining with antiserum raised against either β-lactamase (lanes 3 and 4) or VHb (lanes 5 and 6).

Figure 5. Reduction of disulfide-linked VHb dimer in JM101:pRED2 insoluble lysate fraction I by treatment with DTT. (**A**) Preparation of fraction I in sample buffer lacking DTT (2% SDS). (**B**) Preparation of fraction I in sample buffer containing excess DTT (170 mM DTT, 2% SDS). The two-dimensional gel region shown is identified by the box in Figure 3B. The position of the disulfide-linked VHb dimer (e) is indicated. (Two-dimensional electrophoresis gels were run by Ursula Rinas)

Figure 1.

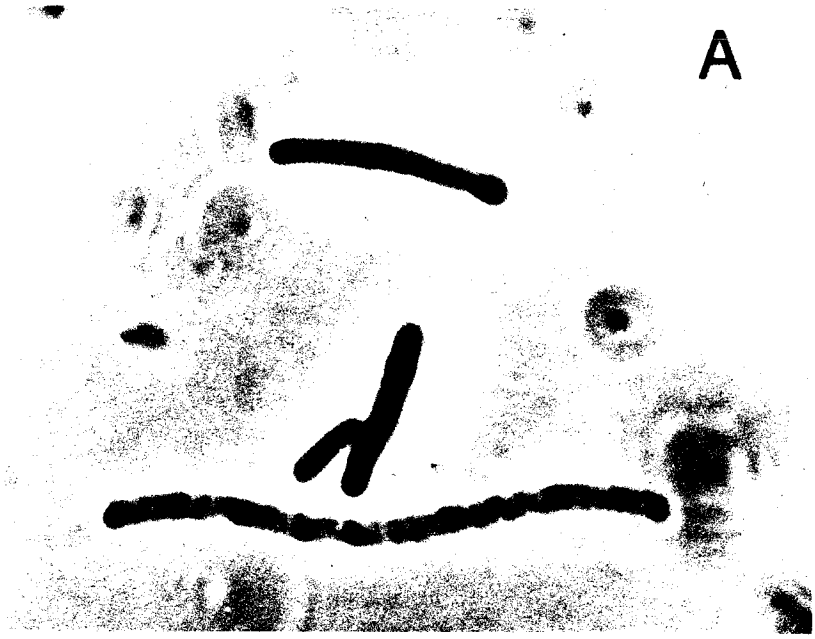

Figure 2.

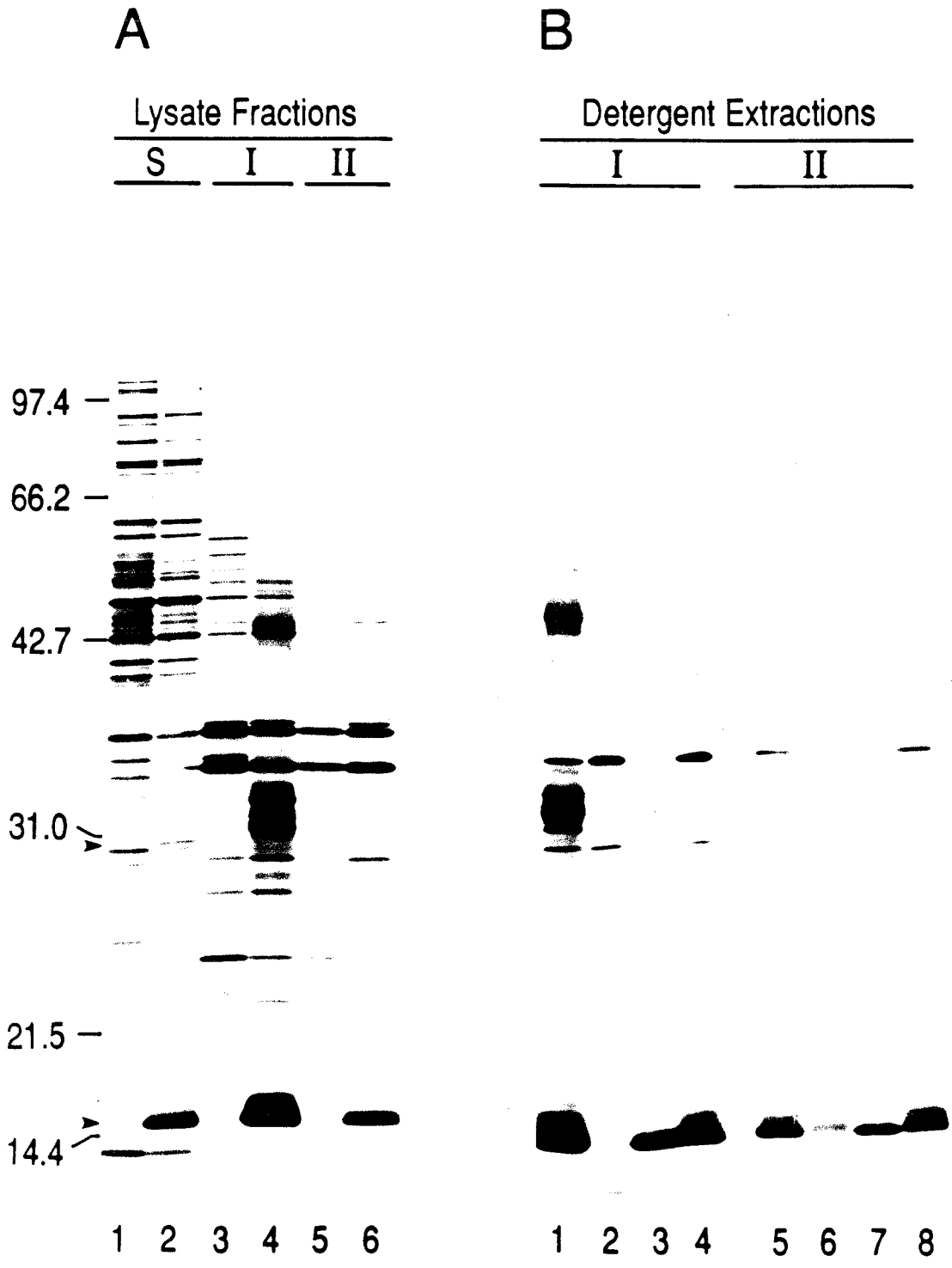
A
Lysate Fractions
S
I
II
B
Detergent Extractions
I
II
97.4
66.2
42.7
31.0
21.5
14.4
1 2 3 4 5 6
1 2 3 4 5 6 7 8

Figure 3.

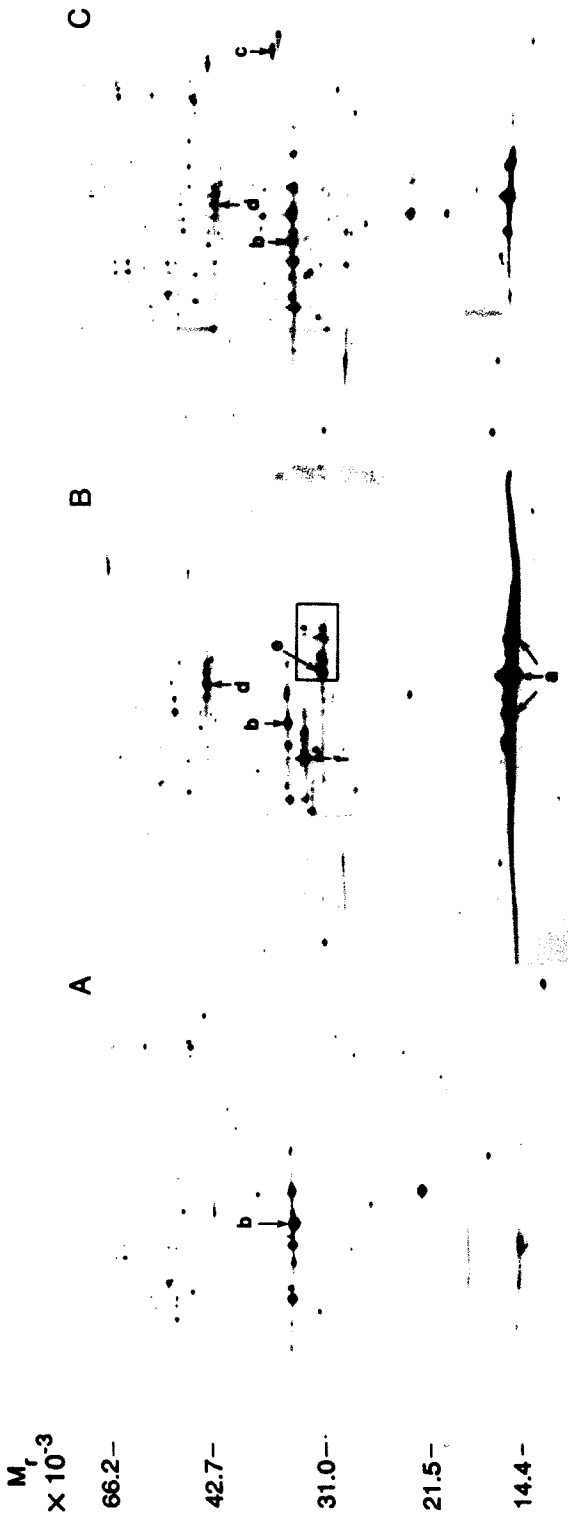

Figure 4.

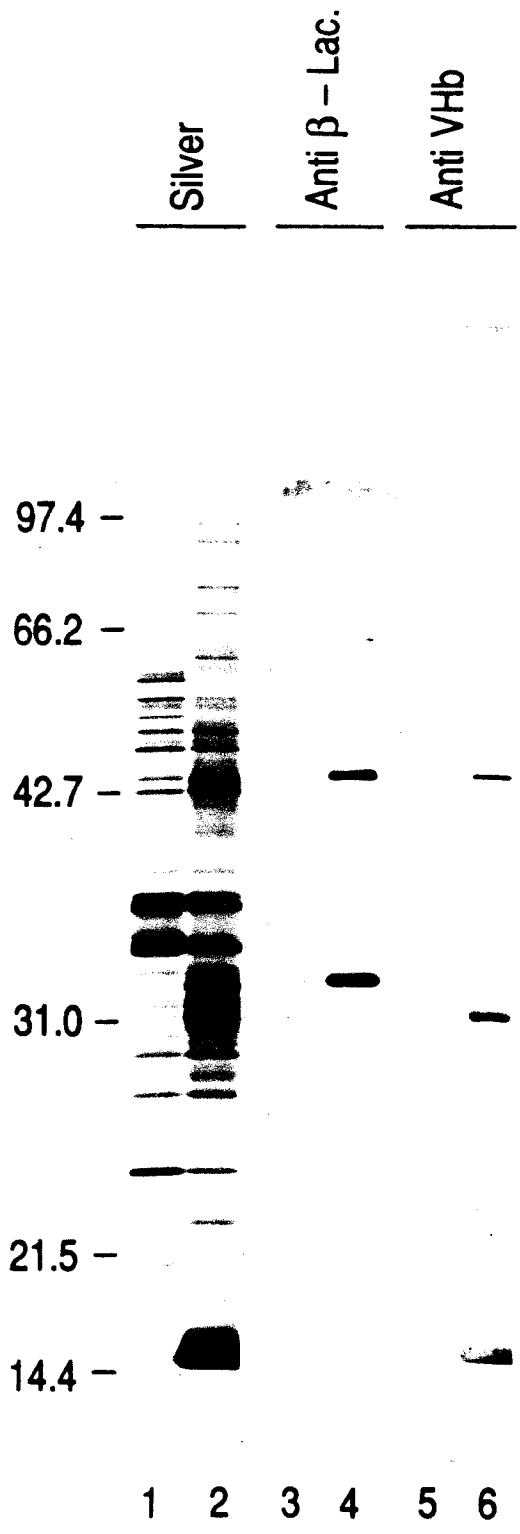

Figure 5.

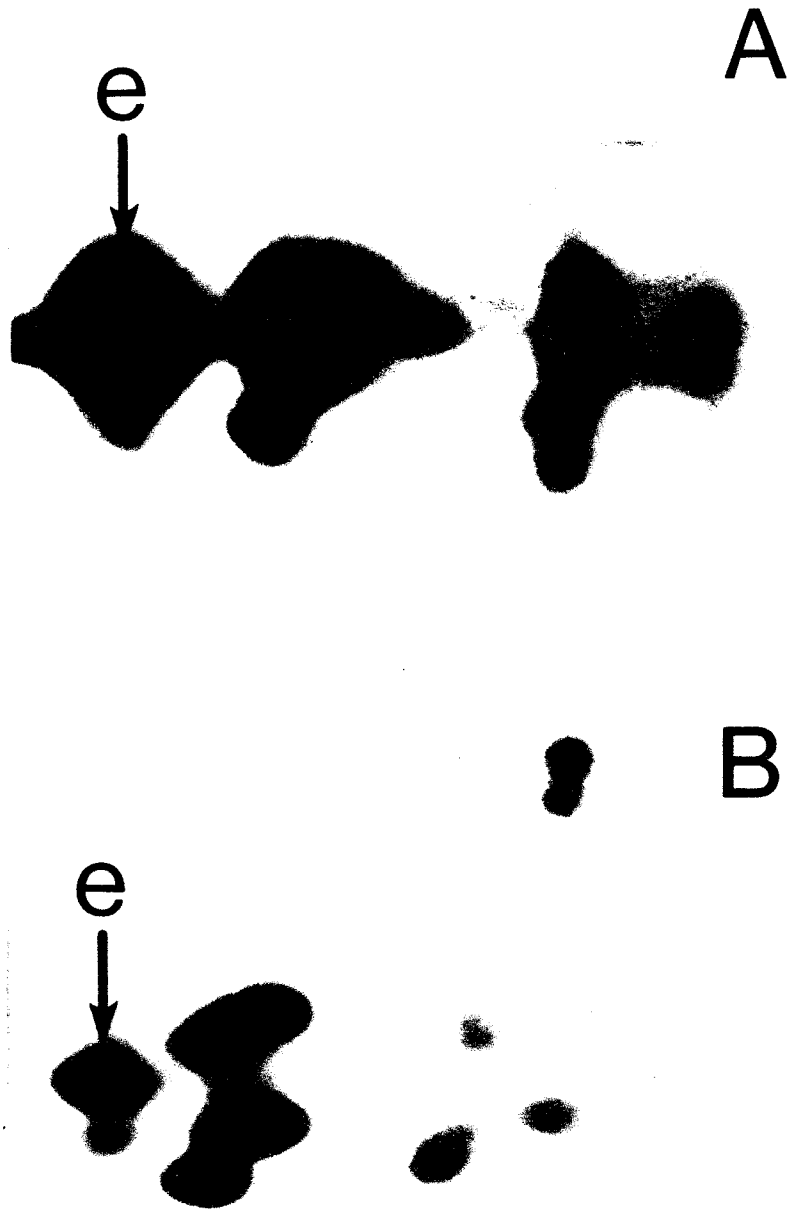

CHAPTER 4

Characterization of the Soluble and Insoluble Forms of *Vitreoscilla* Hemoglobin Produced in *Escherichia coli*

4.1 Summary

Vitreoscilla hemoglobin (VHb) is produced at high levels in both soluble and insoluble forms when expressed from its native promoter on a pUC19 derived plasmid in *Escherichia coli*. The soluble and insoluble forms of VHb exhibit identical migration properties during denaturing two-dimensional electrophoresis. The amino acid content and N-terminal sequence of purified soluble VHb is consistent with that of VHb purified from *Vitreoscilla*. Purified soluble VHb is dimeric and exhibits three high-spin resonances in the vicinity of g 6 when examined by electron paramagnetic resonance spectroscopy (EPR). These resonances are attributed to inequivalency of the two heme centers in dimeric VHb. One center is axial and gives rise to a resonance at g 6.00. The second is rhombic and gives rise to resonances at g 5.50 and 6.39. Inclusion body isolates containing the insoluble form of VHb exhibit a single resonance in the vicinity of g 6 when examined by EPR. This resonance, found at g 5.98, is also present in control cell debris fractions and is attributed to the membrane-bound cytochrome d complex. Iron quantitation by atomic absorption spectroscopy demonstrates that inclusion body VHb lacks heme. Titration of insoluble lysate fractions with monomeric ferrous heme followed by difference absorption spectroscopy suggests that some inclusion body VHb is competent for heme binding.

4.2 Introduction

Intracellular aggregation is a common fate of heterologous recombinant proteins (Kane and Hartley, 1988; Schein, 1989; Mitraki and King, 1989). Despite the prevalence of this phenomenon, the fundamental mechanisms underlying this intracellular aggregation are poorly understood. Protein misfolding is generally believed to be the major contributor to the process. Unfortunately, there is very little information available to support or dispute this view. The protein insolubilized by this process has been subjected to direct conformational analysis on only one occasion. In this case, the protein was shown to be a "thermolabile intermediate in the productive folding pathway" (Haase-Pettingell and King, 1988). Activity measurements have been used for inference of protein structure. In some cases, the insoluble protein lacked activity and was considered incorrectly folded (Sharma *et al.*, 1987; Kepetzki *et al.*, 1989). Significant activity of inclusion body protein has also been reported (Dhurjati *et al.*, 1990). Activity measurements, however, cannot provide a complete picture of the conformational state of inclusion-body-bound protein as steric hindrance, substrate diffusion limitations and constrained protein flexibility can all affect the activity measurement (Kennedy and Cabral, 1983). Further, activity may be absent although substantial folded structure exists (Mitraki *et al.*, 1987).

Understanding the conformational properties of inclusion body protein is important for two reasons. First, this information can provide clues concerning the underlying mechanisms of the aggregation process and the extent to which aberrant protein folding is responsible. In particular, the existence of a dis-

tinct conformational state in the inclusion body might indicate that this species, or a variant thereof, precedes the rate determining step in folding or maturation (Horowitz and Criscimagna, 1986; Horowitz and Criscimagna, 1990). This species might also represent the terminal product of folding within the host recombinant cell. Second, this information may be used to guide the development of dissolution and renaturation strategies necessary for active protein recovery.

Inclusion body preparations generally contain contaminant proteins due to the presence of cell wall debris, loss of specificity during the intracellular aggregational process, or both (Hart *et al.*, 1990). Analysis of inclusion body protein conformation requires either the removal of contaminant proteins or resolution of the properties of the target protein from those of the contaminants. Progress has been made in analyzing the properties of the tailspike variant which is aggregated into inclusion bodies (Haase-Pettingell and King, 1988). This has been possible because the stability properties of this protein allow for its separation from contaminants without structural perturbation. Unfortunately, most recombinant proteins which aggregate into inclusion bodies lack these stability properties. *In situ* analytical techniques which allow resolution of the target protein's properties relative to those of contaminants can be used to analyze inclusion body protein properties. The term *in situ* is used here to refer to analysis of protein aggregated in inclusion bodies removed from the cell. One such technique involves the use of probes specific to the target protein which may be analyzed spectroscopically. Ideal probes include those indigenous to the recombinant protein but not particularly prevalent in contaminant proteins. Spectroscopic techniques have previously been used to analyze proteins in non-native immo-

bilized states. Examples include protein attached to chromatographic matrices (Clark and Bailey, 1983; Clark and Bailey, 1984) and protein in salt precipitated aggregates (Przybycien and Bailey, 1989; Przybycien and Bailey, 1991). To investigate this approach, we have utilized a variety of spectroscopic techniques for the comparative analysis of the soluble and insoluble forms of *Vitreoscilla* hemoglobin (VHb) produced in *Escherichia* coli.

VHb is a soluble homodimeric heme protein expressed by the obligate aerobic bacterium *Vitreoscilla* in response to low oxygen conditions (Wakabayashi *et al.*, 1986). The protein can be expressed from its native promoter in recombinant *E. coli* under similar hypoxic conditions (Khosla and Bailey, 1989a; Dikshit and Webster, 1988). VHb is accumulated concurrently in both soluble and insoluble forms when expressed from a high copy number plasmid under the control of its native promoter (Hart *et al.*, 1990). The soluble form is found to partition between the cytoplasmic and periplasmic spaces despite the absence of a processed N-terminal signal peptide (Khosla and Bailey, 1989b). Similar compartmentalization is observed in the native host *Vitreoscilla.* In contrast, the insoluble form is only found aggregated in cytoplasmic inclusion bodies (Hart *et al.*, 1990). Integral protein contaminants of VHb inclusion bodies include the precursor form of β-lactamase, an aberrant disulfide-linked dimer of VHb and a protein identified by two-dimensional electrophoresis as elongation factor TU. The principle contaminants of VHb inclusion body preparations are derived from cell wall debris which cosediment with inclusion bodies during centrifugation (Hart *et al.*, 1990).

In this report we show that purified soluble VHb produced in *E. coli* possess

the same amino acid content, heme stoichiometry, and optical spectra as VHb isolated from *Vitreoscilla*. Electron paramagnetic resonance spectroscopy (EPR) of purified soluble dimeric VHb shows the protein to possess two inequivalent heme centers. The insoluble form of VHb yields the same multiple spot pattern as purified soluble VHb during denaturing two-dimensional gel electrophoresis suggesting the polypeptides are identical. *In situ* EPR and atomic absorption spectroscopy of the insoluble form of VHb proves it uniformly lacks heme. Titration of insoluble VHb with heme suggests some protein is competent for heme binding *in situ*.

4.3 Materials and Methods

Bacterial growth, lysis and fractionation - The recombinant *E. coli* strain JM101:pRED2 was grown by a fed-batch procedure, harvested, washed, lysed and fractionated by differential centrifugation as described previously (Hart *et al.*, 1990). This procedure leads to the accumulation of soluble VHb (representing 10% of soluble protein) and insoluble VHb at comparable levels. Two insoluble lysate fractions were obtained, each containing VHb inclusion bodies but differing in the relative content and type of contaminating proteins (Hart *et al.*, 1990). Control soluble and insoluble lysate fractions were prepared under identical conditions from JM101:pUC19, the host strain containing the parent plasmid of pRED2.

Insoluble lysate sample preparation - Insoluble lysate fractions were obtained from late stationary phase cultures having the same optical density. With the exception of Figure 1c, all data shown were obtained from the fraction

previously identified as insoluble lysate fraction I (Hart *et al.*, 1990). Identical results were observed for the fraction previously identified as insoluble lysate fraction II. In some cases insolubles were subjected to EDTA and lysozyme followed by Triton-X100 extraction to partially solubilize membrane contaminants by methods described previously (Hart *et al.*, 1990). Stocks were prepared from the insoluble lysate fraction by washing extensively with 50 mM potassium phosphate (pH 7.0), 10 mM EDTA followed by washing and resuspension in 50 mM potassium phosphate (pH 7.0). The resulting JM101:pRED2 debris stock contained approximately 0.5 mM VHb polypeptide as determined by quantitative SDS-PAGE. Resulting JM101:pUC19 debris stock contained the same amount of cell wall material as judged by the content of the outer membrane proteins OmpA, OmpF and OmpC. For EPR analysis, 0.5 ml of debris stock was oxidized with ammonium persulfate or reduced with sodium dithionite and placed in an EPR tube. For atomic absorption spectroscopy, inclusion body analogues were prepared by titrating purified VHb stock into JM101:pUC19 debris stock to achieve a protein composition comparable to that of JM101:pRED2 debris stock. To investigate insoluble VHb heme binding competency, debris stocks were diluted 200 fold with 100 mM potassium phosphate (pH 7.0) and titrated with heme from a 15 mM heme, 0.1 N NaOH stock solution.

Soluble VHb purification - VHb was purified from the soluble lysate fraction of JM101:pRED2 (Hart and Bailey, 1991). The soluble lysate (L) was extracted in an aqueous two-phase system consisting of 12% (w/w) dextran T-500, 7.7% (w/w) PEG 4000, 20 mM Tris-HCl (pH 8.0), and 10 mM NaCl and the PEG-rich phase was collected (E1). This fraction was then extracted

in a two-phase system consisting of 12.4% (w/w) Na_2SO_4, 11.8% (w/w) PEG 4000, and 20 mM Tris-HCl and the PEG-rich phase was collected (E2). The PEG-rich fraction was then extracted in a two-phase system consisting of 9.7% (w/w) $MgSO_4$, 10.8% (w/w) PEG 4000, and 50 mM Tris-HCl and the $MgSO_4$ fraction was collected (E3). The resulting salt fraction was dialyzed against 20 mM sodium phosphate (pH 7.5), 0.5 M NaCl and subjected to metal affinity chromatography (Pharmacia Chelating Sepharose Fast Flow, immobilized Cu^{+2}) with 3.5 mM Nα-acetyl-L-histidine elution (M1). Further purity was obtained by subjecting the resulting eluent to gel permeation chromatography (Pharmacia Sephadex G-75 Superfine) (GPC). The purified VHb was dialyzed against distilled water, lyophilized, and stored at -70°C.

Purified soluble VHb sample preparation - For extinction coefficient determination, an 11 μM stock solution of VHb in distilled water was prepared for amino acid analysis and UV-visible absorption spectroscopy. Various dilutions of the VHb stock solution were prepared and buffered with 50 mM potassium phosphate (pH 7.0). Reduced VHb was prepared by the addition of sodium dithionite. Oxidized VHb was prepared by the addition of ammonium persulfate. Carbon monoxide bound VHb was prepared by reduction with sodium dithionite followed by incubation in CO at 4 psig for 30 min. For EPR analysis a 35 μM VHb stock solution was prepared by dialyzing purified protein against 50 mM potassium phosphate (pH 7.0), 10 mM EDTA followed by dialysis against 50 mM potassium phosphate (pH 7.0). Purified VHb exists naturally in the ferric state presumably due to the absence of a naturally occurring reductase present in both *Vitreoscilla* and *Escherichia coli* (Dikshit and Webster, 1988).

Amino acid analysis - Amino acid analysis was carried out with an Applied Biosystems Inc. Model 420A/130A Amino Acid Derivatizer-Analyzer System. Protein was hydrolyzed in the vapor phase under vacuum (constant boiling HCl, 1 h, 165 °C) and derivatized with phenylisothiocyanate.

Visible difference absorption spectroscopy - Samples were analyzed with a Shimadzu UV260 Spectrophotometer interfaced to an IBM-XT computer. Matching 1 cm. path length quartz microcuvettes were used with a temperature controlled platform maintained at 25 °C. Difference spectra relative to suitable buffer blanks were obtained in all cases. Serial dilution was used to ensure linearity of absorbance measurements.

Electron paramagnetic resonance spectroscopy - Prepared samples were transferred to 4 mm quartz EPR tubes (Wilmad) and deoxygenated by argon replacement. EPR spectra were recorded on a Varian E-Line Century series X band spectrometer (Varian Instruments, Palo Alto, Ca) equipped with an Oxford Model ESR-900 Cryostat and Model 3120 Digital Temperature Controller (Oxford Instruments, Bedford, Ma). The relative receiver gain was 5 for oxidized debris, 2 for reduced debris and 1 for purified VHb. Spectra were obtained at nonsaturating microwave power (typically below 8 mW) and 4 degrees Kelvin.

Atomic absorption spectroscopy - Cell debris stocks, purified VHb stock and inclusion body analogues were prepared for analysis by one of two methods. In the first method, samples were diluted with ultrapure HCL (Baker Ultrex Ultrapure HCl) and glass distilled water to give a final HCl concentra-

tion of 1.2 N. In the second method, samples were hydrolyzed by vapor phase hydrolysis in constant boiling HCl at 165 °C for 1 hour, resuspended in 1.2 N Ultrapure HCl, and 0.22 μm filtered. Resulting samples were analyzed with an Instrumentation Laboratory Atomic Absorption Spectrometer following Instrumentation Laboratory suggested procedures. Samples analyzed by the first method systematically gave lower measurements (typically by 20%) than samples analyzed by the second method. This error is attributed to reduced flow rate through the needle orifice for samples containing particulate matter.

Analytical techniques - VHb concentration was determined by visible difference spectroscopy (carbon monoxide minus reduced) using the extinction coefficients determined for purified protein. Total protein was measured by the Bradford dye binding assay using a commercially available kit (Bio-Rad, Richmond CA). Two-dimensional electrophoresis and SDS-PAGE were conducted as previously described (Hart *et al.*, 1990). Proteins were visualized by either Coomassie blue or silver staining. For protein quantitation, Coomassie blue stained gels were scanned with a LKB Ultroscan XL Scanning Densitometer.

4.4 Results

To provide a basis for the *in situ* analysis of inclusion body VHb produced by JM101:pRED2, soluble VHb coincidentally produced was purified to homogeneity and examined by a variety of spectroscopic techniques. Difference visible absorption spectroscopy was used throughout the purification to monitor protein structural integrity. The amino acid content of the purified soluble VHb, given in table 1, is consistent with the previously reported amino acid sequence

of VHb isolated from *Vitreoscilla* (Wakabayashi, 1986). The sequence of the first 15 amino acids of this protein was previously shown to be identical to that reported for VHb isolated from *Vitreoscilla* (Khosla and Bailey, 1989). Examination of purified VHb by denaturing two-dimensional electrophoresis revealed a distinctive multi-spot pattern along the isoelectric focusing direction as shown in Figure 1a (Two-dimensional gels were run by Ursula Rinas). Similar examination of crude insoluble lysate fractions obtained from JM101:pRED2 revealed the identical spot pattern as shown in Figures 1b and 1c. The migration of a protein during denaturing isoelectric focusing is determined by the protein's charged residue content and its stability properties (Bravo, 1984). The migration of a protein during SDS-PAGE is determined by the protein's stability properties and its molecular weight (Bravo, 1984). The identity of the two-dimensional electrophoresis spot patterns derived from purified VHb, crude soluble VHb and insoluble VHb is strong evidence for the identity of the respective VHb polypeptide species. This is important as changes in amino acid sequence can lead to inclusion body formation (Krueger, 1990). In the case of hemoglobins, a number of disease states are known to arise from globin aggregation and this aggregation has been linked to single amino acid substitutions (Dickerson and Geis, 1983; Pagnier *et al.*, 1990). Interestingly, norleucine is known to be incorporated into recombinant proteins (Chang *et al.*, 1986; Lu *et al.*, 1988). Norleucine is not present in soluble VHb as determined by amino acid analysis.

To examine the heme environment of the respective forms of VHb each was analyzed by electron paramagnetic resonance spectroscopy (EPR). The EPR spectrum of purified ferric VHb, shown in figure 2a, has features which dis-

tinguish it from published spectra of many other hemeproteins including those contained in *E. coli* membranes. Three peaks in the vicinity of g 6 derived from high-spin ferric heme are discernable. One peak is centered at g 6.00 and arises from an axial heme center. The other two peaks are centered at g 6.39 and 5.50 and arise from a rhombic heme center. The calculated high-spin rhombicity (Palmer, 1979) of this resonance is compared with values previously reported for related hemeproteins in Table 2. VHb is a dimeric heme protein composed of identical subunits having distinctly different iron redox potentials (Webster, 1988). These results suggest that the two heme centers of VHb are magnetically inequivalent, presumably due to heme pocket distortion upon dimerization. The EPR spectrum of crude soluble VHb obtained from JM101:pRED2 also has peaks centered at g 6.0 and 6.39. The peak at 5.50 cannot be observed in crude soluble lysate samples due to the presence of numerous contaminating resonances (data not shown).

The insoluble form of VHb produced by JM101:pRED2 was investigated *in situ* by EPR analysis of insoluble lysate fractions containing inclusion bodies. Control insoluble lysate fractions obtained from JM101:pUC19 were likewise analyzed to account for membrane contaminants present in inclusion body preparations. EPR spectra obtained from the respective insoluble lysate fractions, shown in Figures 2b and 2c, are virtually identical both in terms of resonance content and relative resonance intensity. Further, the spectra of JM101:pRED2 insoluble lysate lacks the distinctive triple resonance pattern produced by active dimeric VHb. To determine the relative contribution of different proteins to the observed spectra, samples containing differing amounts of VHb and membrane

material were prepared from JM101:pRED2 insoluble lysate by differential centrifugation and EDTA/lysozyme/detergent extraction (Hart *et al.*, 1990). Results indicate that the intensities of the resonances observed under oxidizing conditions scale with the quantity of membrane protein rather than VHb (data not shown). EPR spectra of insoluble lysate from JM101:pUC19 and JM101:pRED2 in the reduced state, shown in Figures 3a and 3b, are likewise virtually identical in terms of resonance content and relative resonance intensity. HoloVHb is diamagnetic in the reduced state and does not exhibit an EPR resonance. Results suggest that the EPR resonances observed in insoluble lysate fractions arise from membrane protein contaminants. A list of the resonances previously observed for *E.* coli membrane proteins is given in Table 3.

The absence of the triplet structure in JM101:pRED2 insoluble lysate taken with the observation that resonance intensity scales with membrane protein content rather than VHb content, strongly suggests that the insoluble form of VHb lacks heme. To further test this possibility, the quantity of iron in each insoluble lysate fraction was determined by atomic absorption spectroscopy. All measurements were normalized by the amount of the outer membrane proteins OmpA and OmpF in the sample to account for varying membrane content. To determine how much iron would be present if all insoluble VHb contained iron, inclusion body analogues were prepared by titrating purified VHb into JM101:pUC19 insoluble lysate as shown in Figure 4b. To ensure that titrated iron arose only from VHb, the iron to polypeptide stoichiometry of the VHb stock was determined by amino acid analysis and atomic absorption spectroscopy. The membrane-normalized iron content of JM101:pUC19 insolu-

ble lysate, JM101:pRED2 insoluble lysate and VHb inclusion body analogues is shown in Figure 4a. Results show that purified soluble VHb contains stoichiometric heme. This is evident in Figure 4 by the fact that the curves for the iron content of inclusion body analogues predicted by amino acid analysis and atomic absorption spectroscopy of the purified VHb titration stock are coincident. The curve determined by analysis of inclusion body analogues has a reduced slope relative to the predicted curve. Results from analysis of JM101:pRED2 insoluble lysate show the iron content is at least six-fold less than expected for lysate containing VHb with incorporated heme. Further, the membrane normalized iron content of JM101:pRED2 insoluble lysate is the same as that of JM101:pUC19 insoluble lysate. These results clearly show that the insoluble form of VHb produced in JM101:pRED2 uniformly lacks heme.

To determine if the insoluble form of VHb is competent for heme binding, monomeric heme was titrated into insoluble lysate fractions and monitored by difference visible absorption spectroscopy. During titration, heme to VHb polypeptide ratios ranged from 0.2 to 1.4. The difference visible extinction spectra of purified soluble VHb (carbon monoxide minus reduced) is shown in Figure 5a. The extinctions and positions of the alpha, beta and Soret peaks of oxidized, reduced and carbon monoxide forms of purified VHb are given in Table 3 along with those for related hemeproteins. The visible difference absorption spectra of JM101:pUC19 insoluble lysate titrated with heme is shown in Figure 5b. The position of the Soret peak in these samples does not vary with heme content and is found at 422.8 nm. The visible difference absorption spectra of JM101:pRED2 insoluble lysate titrated with heme is shown in Figure 5c. The

position of the Soret peak in these samples varies systematically with heme content. At a heme to VHb polypeptide ratio of 0.2, the Soret peak maximum is found at 422.8nm. At a heme to VHb ratio of 1.4, the Soret peak maximum is found at 424.5 nm. These results show that JM101:pRED2 insoluble lysate provides a different environment for heme than JM101:pUC19 insoluble lysate and suggests that some insoluble VHb is competent for heme binding. If this is true, the conformation of the heme pocket of inclusion body VHb must differ significantly from that present in soluble VHb to account for the differences in the observed spectra. Additionally, it must have a low binding constant as the observed spectral changes occur at high heme to VHb polypeptide ratios.

4.5 Discussion

Vitreoscilla hemoglobin (VHb) is a soluble homodimeric heme protein produced by the obligate aerobic bacterium *Vitreoscilla* when grown under oxygen limiting conditions (Webster, 1988). The amino acid sequence of this protein has a striking homology to lupin leghemoglobin and several other globin proteins (Wakabayashi *et al.*, 1986). The most notable divergence of the sequence of this hemoglobin from that of eucaryotic hemoglobins lies in the N-terminal region. It is possible that VHb lacks the N-terminal helix, referred to as the A helix, which other globins possess (Wakabayashi *et al.*, 1986). This helix, when present, is not directly involved in heme pocket formation (Lesk and Chothia, 1980). VHb also appears to have a glutamine as the distal heme ligand in contrast to the usual histidine (Wakabayashi *et al.*, 1986). Substitution of the distal histidine in human hemoglobin with glutamine by site-directed mutagenesis yields a protein

with similar oxygen binding characteristics and X-ray crystal structure to native hemoglobin (Nagai *et al.*, 1987)

Previous studies have shown that the two heme centers of dimeric VHb have vastly different redox potentials (Webster, 1988). Our results from EPR analysis of VHb confirm this heme center inequivalency. Previous studies have also shown cooperativity of carbon monoxide binding (Webster, 1988). A possible cause of the rhombicity of one VHb heme center is heme pocket distortion upon dimerization. Our results suggest cooperativity in binding may be manifest through a relaxation in the distortion of this heme pocket. Further, VHb is partitioned to both the cytoplasmic and periplasmic spaces in *E.* coli and *Vitreoscilla* (Khosla and Bailey, 1989). It is possible that the inequivalency of the two heme centers allows VHb to be active in both these compartments despite their different redox states.

Hemeproteins as a class have historically been very heavily studied proteins. They continue to be heavily studied today and are routinely mutagenized for structure, function and folding analysis (Nagai and Thogersen, 1984; Nagai *et al.*, 1985; Nagai *et al.*, 1987; Springer and Sligar, 1987; Dodson *et al.*, 1988; Shimada *et al.*, 1989; Simons and Satterlee, 1989; Kraus and Wittenberg, 1990; Pagnier *et al.*, 1990; Hoffman *et al.*, 1990). Given this cloning activity, one would expect sufficient information would have emerged concerning inclusion body formation to allow an inference of mechanism. Unfortunately, this is not the case. The principle reason for this is the small number of cloning strategies employed. The most commonly used cloning vector is the λ cII fusion protein vector developed by Nagai and Thogersen (1984). Protein is produced with this

system by induction at 42°C and the expressed λ cII - hemoglobin fusion protein invariably aggregates. It is likely that the expressed fusion protein is incapable of folding correctly.

Fortunately, some of the expression vectors used for producing hemeproteins do lead to the formation of soluble protein. Sperm whale myoglobin was expressed in *E. coli* from a totally synthetic gene inserted into the expression vector pUC19 (Springer and Sliger, 1987). The protein is expressed from the *lac* promoter and accumulates as a holoprotein in soluble form to a level of 10% of total soluble protein. Apparently no insoluble myoglobin was produced with this vector. The formation of high levels of soluble holoprotein was attributed to the use of *E. coli* preferred codons in the synthetic gene.

Human hemoglobin was expressed in *E. coli* from a synthetic operon composed of synthetic genes encoding α- and β-globin (Hoffman *et al.*, 1990). This operon was inserted into the expression vector pKK223-3, a derivative of pUC19. Both α- and β-globin are expressed from the *tac* promoter and soluble $\alpha_2\beta_2$ hemoglobin accumulates to a level of $\geq 5\%$ of total protein. Interestingly, expression of β-globin alone results in high-level accumulation of insoluble β-globin. Expression of α-globin alone results in a marked decrease of soluble α-globin levels relative to those obtained with coexpression of α- and β-globin. These results clearly show that intramolecular association of globin chains *in vivo* aids in folding and/or stabilization of the individual chains.

Expression of VHb in JM101:pRED2 is controlled by the native VHb promoter. This promoter has been shown to be regulated by dissolved oxygen levels with expression occurring under hypoxic conditions (Khosla and Bailey,

1989a). During shake flask cultivation on complex media, these conditions are manifest during stationary phase. JM101:pRED2 grown on complex media accumulates soluble VHb during stationary phase at a fairly constant rate of 0.2 μmole/(gmdw hr) to a final concentration of 3.0 μmole/gmdw. Soluble VHb is fairly equally distributed between the periplasmic and cytoplasmic spaces and represents approximately 10% of total soluble protein at the end of stationary phase.

Expression of VHb in *E.* coli from a pUC19-derived plasmid also leads to a concurrent accumulation of insoluble VHb. The accumulation rate of insoluble VHb during stationary phase varies but is generally highest during phases exhibiting metabolic acids accumulation. ***In situ*** examination of this insoluble form of VHb by EPR and atomic absorption spectroscopy clearly shows that it uniformly lacks heme. Analysis of soluble and insoluble VHb by two-dimensional electrophoresis indicates that they do not otherwise differ. Other investigators have reported observing an absence of heme in hemeprotein inclusion bodies; however, as yet no direct evidence has been presented in support of this contention (Smith *et al.*, 1990). In this case the hemeprotein was accumulated only in an insoluble form.

In an insightful review, Mitraki and King discussed the role of cofactors in protein folding and speculated that their absence during ***in vivo*** protein folding could lead to aggregation and inclusion body formation (Mitraki and King, 1989). As an extension of this thought, one might expect apoprotein aggregation whenever the ratio of net polypeptide synthetic rate to net cofactor synthetic rate exceeds their stoichiometric binding ratio. Such a state would arise if the

cofactor biosynthetic pathway were saturated and consequently unable to respond to a demand for increased flux. A mechanism such as this would lead to the simultaneous accumulation of both soluble and insoluble hemeprotein with the only determinant between the two forms being heme content. To investigate this possible mechanism we are currently examining the influence of heme biosynthesis of VHb inclusion body formation *in vivo*.

The origins of several resonances observed in the EPR of *E coli* insoluble lysate fractions can be identified by reference to the literature. The resonance at 5.98 is attributed to the cytochrome d complex due to its tendency to become rhombic with a distinguishable side resonance at 5.71 following membrane detergent extraction (Hata *et al.*, 1985; Finlayson and Ingledew, 1985). This identification is consistent with previous observations that the cytochrome d complex is produced in response to low oxygen tension (Hata *et al.*, 1985). The resonance at 2.03, attributed to the succinate dehydrogenase and nitrate reductase complex (Condon *et al.*, 1985) as it was readily lost with detergent extraction and was not observable above 30 K. Normalization of EPR signal intensity with Omp levels indicates that the amounts of cytochrome d complex, succinate dehydrogenase and nitrate reductase complex are comparable in both JM101:pUC19 and JM101:pRED2. This view is supported by the observation that membrane-normalized iron levels are likewise comparable for the two strains.

4.6 Acknowledgements

This research was supported by the National Science Foundation (Grant No. EET-8606179). R. H. was supported in part by a predoctoral training grant in biotechnology from the National Institute of General Medical Sciences (National Research Service Award 1 T32 GM 08346-01, Pharmacology Sciences Program).

4.7 References

1. Adar, F. (1978) in *The Porphyrins* (Dolphin, D., ed.) **3**, 167 - 209

2. Appleby, C. A., Blumberg, W. E., Peisach, J., Wittenberg, B. A., and Wittenberg, J. B. (1976) *J. Biol. Chem.* **251**, 6090 - 6096

3. Bravo, R. (1984) in *Two-Dimensional Gel Electrophoresis of Proteins* (Celis, J. E., and Bravo, R., ed.) Academic Press, pp. 3 - 36

4. Chang, J. Y-H *et al.* (1986) *Microbiology (ASM)* 324 - 329

5. Clark, D. S., and Bailey, J. E. (1984) *Biotech. Bioeng.* **26**, 231 - 238

6. Clark, D. S., and Bailey, J. E. (1983) *Biotech. Bioeng.* **25**, 1027 - 1047

7. Condon, C., Cammack, R., Patil, D. S., and Owen, P. (1985) *J. Biol. Chem.* **260**, 9427 - 9434

8. Dickerson, R. E., Geis, I. (1983) *Hemoglobin*, Benjamin Cummings, Menlo Park, CA

9. Dhurjati, P., Tokatlidis, K., Millet, J., Beguin, P., Tremel, R., Longin, R., and Aubert, J. P. (1990) Presentation number 82, Symposium on Protein Refolding, 199th National Meeting American Chemical Society, Boston Mass.

10. Dikshit, K. L., and Webster, D. A. (1988) *Gene* **70**, 377 - 386

11. Dodson, G., Hubbard, R. E., Oldfield, T. J., Smerdon, S. J., and Wilkinson, A. J. (1988) *Prot. Engr.* **2**, 233 - 237

12. Finlayson, S. D., Ingledew, W. J. (1985) *Biochem. Soc. Trans.*

13. Godfrey, C., Coddington, A., Greenwood, C., Thomson, A. J., and Gadsby, P. M. A (1987) **Biochem. J. 243**, 225 - 233

14. Haase-Pettingell, C. A., and King, J. (1988) *J. Biol. Chem.* **263**, 4977 - 4983

15. Hart, R. A., Rinas, U., and Bailey, J. E. (1990) *J. Biol. Chem.* **265**, 12728 - 12733

16. Hart, R. A., and Bailey, J. E. (1991) Material in Chapter 2.

17. Hata, A., Kirino, Y., Matsuura, K., Itoh, S., Hiyama, T., Konishi, K., Kita, K., and Anraku, Y. (1985) *Biochem. Biophys. Acta* **810**, 62 - 72

18. Hoffman, S. J., Looker, D. L., Roehrich, J. M., Cozart, P. E., Durfee, S. L., Tedesco, J. L., and Stetler, G. L. (1990) *Proc. Natl. Acad. Sci. USA* **87**, 8521 - 8525

19. Horowitz, P. M., and Criscimagna, N. L. (1990) *J. Biol. Chem.* **265**, 2576 - 2583

20. Horowitz, P., and Criscimagna, N. L. (1986) *J. Biol. Chem.* **261**, 15652 - 15658

21. Lu, H. S., Tsai, L. B., Kenney, W. C., and Lai, P-H (1988) *Bioch. Biophy. Res. Comm.* **156**, 807 - 813

22. Kane, J. F., and Hartley, D. L. (1988) *Trend. Biotechnol* **6**, 95 - 101

23. Kennedy, J. F., and Cabral, J. M. S. (1983) *Solid Phase Biochemistry* **66**, 253 - 391

24. Khosla, C., and Bailey, J. E. (1988) *Mol. Gen. Genet.* **214**, 158 - 161

25. Khosla, C., and Bailey, J. E. (1989a) *J. Bacteriol.* **171**, 5995 - 6004

26. Khosla, C., and Bailey, J. E. (1989b) *J. Mol. Biol.* **210**, 79 - 89

27. Kopetzki, E., Schumacher, G., and Buckel, P. (1989) *Mol. Gen. Genet.* **216**, 149 - 155

28. Kraus, D. W., and Wittenberg, J. B. (1990) *J. Biol. Chem.* **265**, 16043 - 16053

29. Krueger, J. K., Stock, A. M., Schutt, C. E., and Stock, J. B. (1990) in *Protein Folding* (Gierasch, L.M., King, J., ed.) American Association for the Advancement of Science

30. Lesk, A. M., and Chothia, C. (1980) *J. Mol. Biol.* **136**, 225 - 270

31. Mitraki, A., and King, J. (1989) *Bio/Technology* **7**, 690 - 697

32. Mitraki, A., Betton, J-M, Desmadril, M., and Yon, J. M. (1987) *Eur. J. Biochem.* **163**, 29 - 34

33. Nagai, K., *et al.* (1987) *Nature* **329**, 858 - 860

34. Nagai, K., Perutz, M. F., and Poyart, C. (1985) *Proc. Natl. Acad. Sci. USA* **82**, 7252 - 7255

35. Nagai, K., and Thorgersen, H-C. (1984) *Nature* **309**, 810 - 812

36. Nagai, K., Thorgersen, H-C., and Luisi, B. F. (1988) *Biochem. Soc. Trans.* **16**, 108 - 110

37. Pagnier, J., Baudin-Chich, V., Lacaze, N., Bohn, B. and Poyart, C. (1990) *Brit. J. Haem.* **74**, 531 - 534

38. Palmer, G. (1979) in *The Porphyrins* (Dolphin, D., ed) Vol. 4, pp. 313 - 353, Academic Press

39. Peisach, J., Blumberg, W. E., Ogawa, S., Rachmilewitz, E. A., and Oltzik, R. (1971) *J. Biol. Chem.* **246**, 3342 - 3355

40. Przybycien, T., and Bailey, J. E. (1989) *Bioc. Biop. A.* **995**, 231 - 245

41. Przybycien, T., and Bailey, J. E. (1991) *Bioc. Biop. A.* **1076**, 103 - 111

42. Schein, C. H. (1989) *Bio/Technology* **7**, 1141 - 1149

43. Sharma, S. K., Evans, D. B., Tomich, C-S. C., Cornette, J. C., and Ulrich, R. G. (1987) *Biotech. Appl. Biochem.* **9**, 181 - 193 (1987)

44. Shimada, H., Fukasawa, T., and Ishimura, Y. (1989) *J. Biochem.* **105**, 417 - 422

45. Simons, P. C., and Satterlee, J. D. (1989) *Biochemistry* **28**, 8525 - 8530

46. Smith, A. T. *et al.* (1990) *J. Biol. Chem.* **265**, 13335 - 13343

47. Springer, B. A., and Sligar, S. G. (1987) *Proc. Natl. Acad. Sci. USA* **84**, 8961 - 8965

48. Wakabayashi, S., Matsubara, H., and Webster, D. A. (1986) *Nature* **322**, 481 - 483

49. Webster. D. A. (1988) *Adv. Inorg. Biochem.* **7**, 245 - 265

4.8 Tables

Table 1: Amino acid content of VHb

Amino Acid	Sequence	Recombinant VHb
Asp	12	13.0
Glu	18	16.7
Lys	10	10.8
Arg	2	2.4
His	4	4.6
Phe	4	4.0
Tyr	4	4.0
Gly	8	8.2
Ala	23	19.0
Val	14	12.3
Leu	14	12.2
Ile	12	10.8
Ser	1	1.8
Thr	8	6.4
Cys	1	0.0
Met	3	3.0
Pro	7	6.5

Table 2: Hemeprotein high-spin rhombicity

Hemeprotein	% Rhombicity	Reference
Sperm whale myoglobin	0.8	Peisach *et al.*,, 1971
Human hemoglobin A	0.8	"
Leghemoglobin	4.6	Appleby *et al.*, 1976
Vitreoscilla hemoglobin	5.6	This work
Bacterial catalase	6.5	Peisach *et al.*, 1971
E. coli sulfite reductase	8.9	"

Table 3: *E. coli* membrane protein EPR resonances.

Membrane protein	EPR Resonances		Reference
	Oxidized	Reduced	
Cytochrome b-556	6.0		Hata *et al.*, 1985
Cytochrome b-562-o	6.0,3.0,2.26		"
Cytochrome b-558-d	6.0,3.0,2.26		"
Succinate Dehydrogenase	2.02	2.03,1.94	Condon *et al.*, 1985
Formate Dehydrogenase	3.77	2.044,1.943,1.903	Godfrey *et al.*, 1987
Nitrate Reductase	2.01	2.054,1.952,1.878	"

Table 4: Electronic absorption band positions (nm) and extinction coefficients (mM^{-1})

Hemeprotein	a	B	Soret	Reference
Sperm whale myoglobin				Adar, 1978
ferric	632 (3.55)	504 (9.47)	409 (157)	
carboxy	579 (12.2)	542 (14.0)	423 (187)	
ferrous	556 (11.8)		434 (115)	
Human hemoglobin A				Adar, 1978
ferric	*	*	*	
carboxy	569 (13.4)	540 (13.4)	419 (191)	
ferrous	555 (12.5)		430 (133)	
Vitreoscilla hemoglobin				This work
ferric	*	*	405 (69)	
carboxy	565 (10.9)	539 (11.7)	420 (138)	
ferrous	556 (9.9)		427 (67)	
Leghemoglobin				Appleby, 1977
ferric	627 (3.5)	496 (8.5)	409 (*)	
carboxy	*	*	*	
ferrous	*	*	*	

4.8 Figures

Figure 1: Two-dimensional electrophoresis migration pattern of soluble and insoluble VHb. (a) Pattern of purified soluble VHb. (b) Pattern of inclusion body VHb contained in insoluble lysate fraction I. (c) Pattern of inclusion body VHb contained in insoluble lysate fraction II.

Figure 2: EPR spectra of oxidized soluble VHb and insoluble lysate fractions. (a) Spectrum of purified soluble VHb. (b) Spectrum of JM101:pUC19 insoluble lysate fraction I. (c) Spectrum of JM101:pRED2 insoluble lysate fraction I.

Figure 3: EPR spectra of reduced insoluble lysate fractions. (a) Spectrum of JM101:pUC19 insoluble lysate fraction I. (b) Spectrum of JM101:pRED2 insoluble lysate fraction I.

Figure 4: (a) Membrane normalized iron content of JM101:pUC19 insoluble lysate, JM101:pRED2 insoluble lysate and various inclusion body analogues. Open symbols represent data determined by AA analysis of respective samples. Filled symbols represent values expected from amino acid analysis (circle) and iron analysis (square) of purified VHb used for analogue preparation. (b) SDS-PAGE of purified soluble VHb (lane 1), JM101:pUC19 insoluble lysate (lane 2), JM101:pRED2 insoluble lysate (lane 3) and various inclusion body analogues (lanes 4 through 6).

Figure 5: Difference absorption spectra (carbon monoxide bound minus reduced) of purified soluble VHb and heme titrated insoluble lysate fractions. (a) Spectrum of purified soluble VHb. (b) Spectra of heme titrated JM101:pUC19 insoluble lysate. (c) Spectra of heme titrated JM101:pRED2 insoluble lysate

Figure 1.

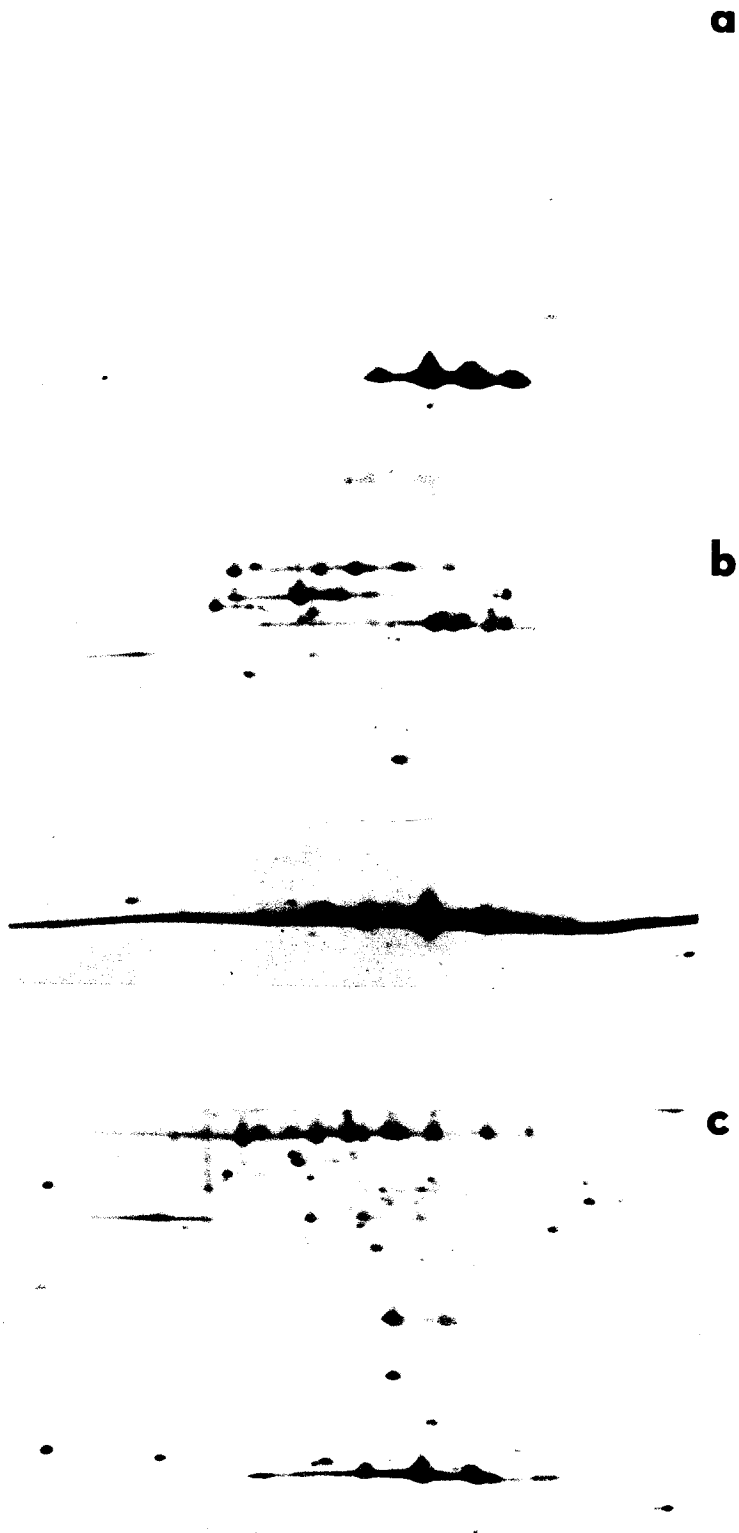

Figure 2.

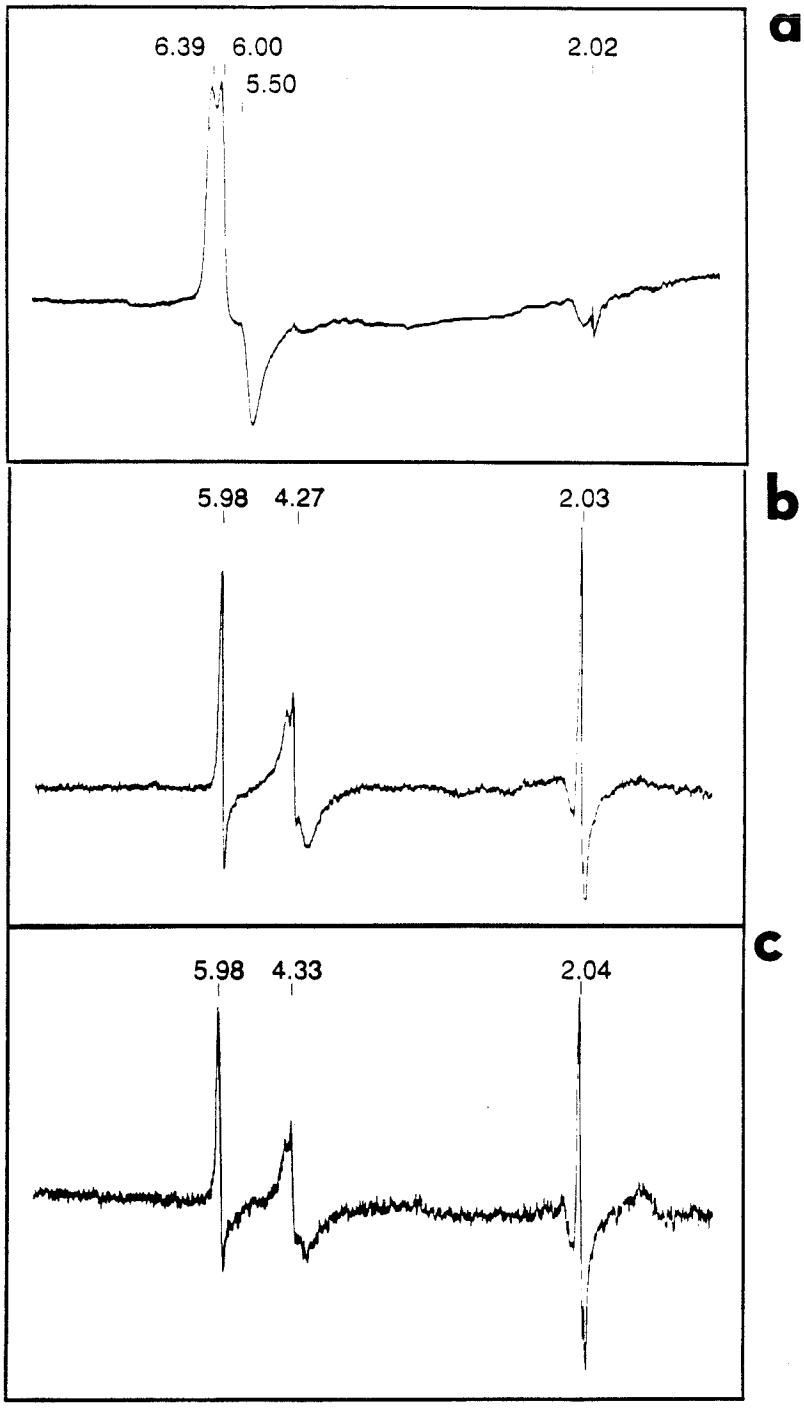

Figure 3.

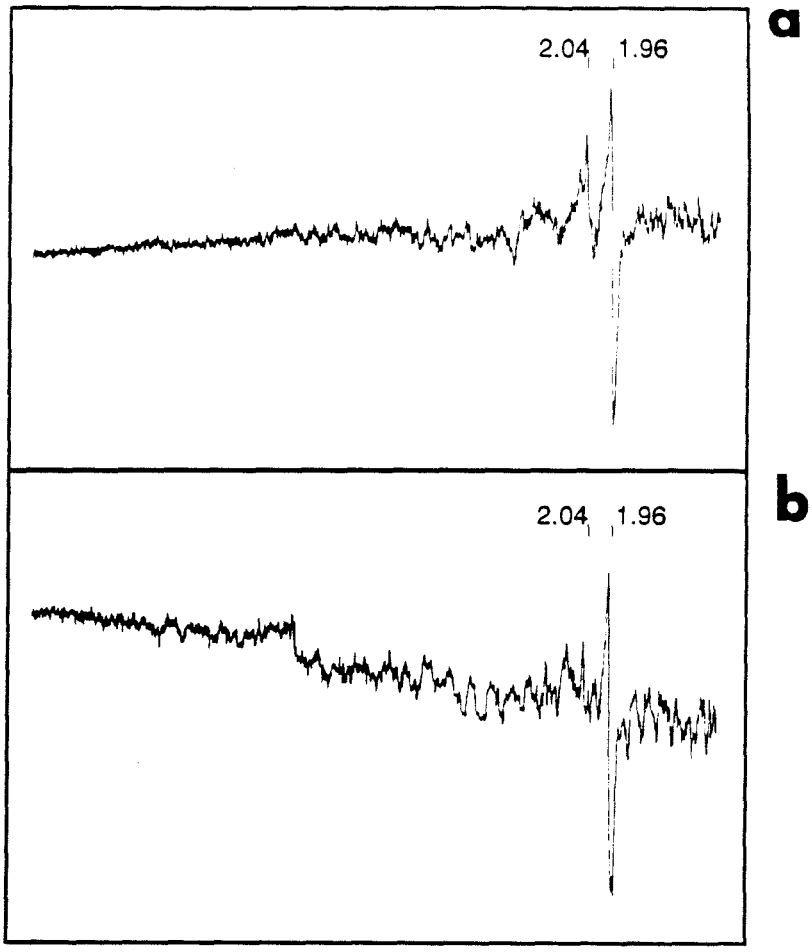

Figure 4.

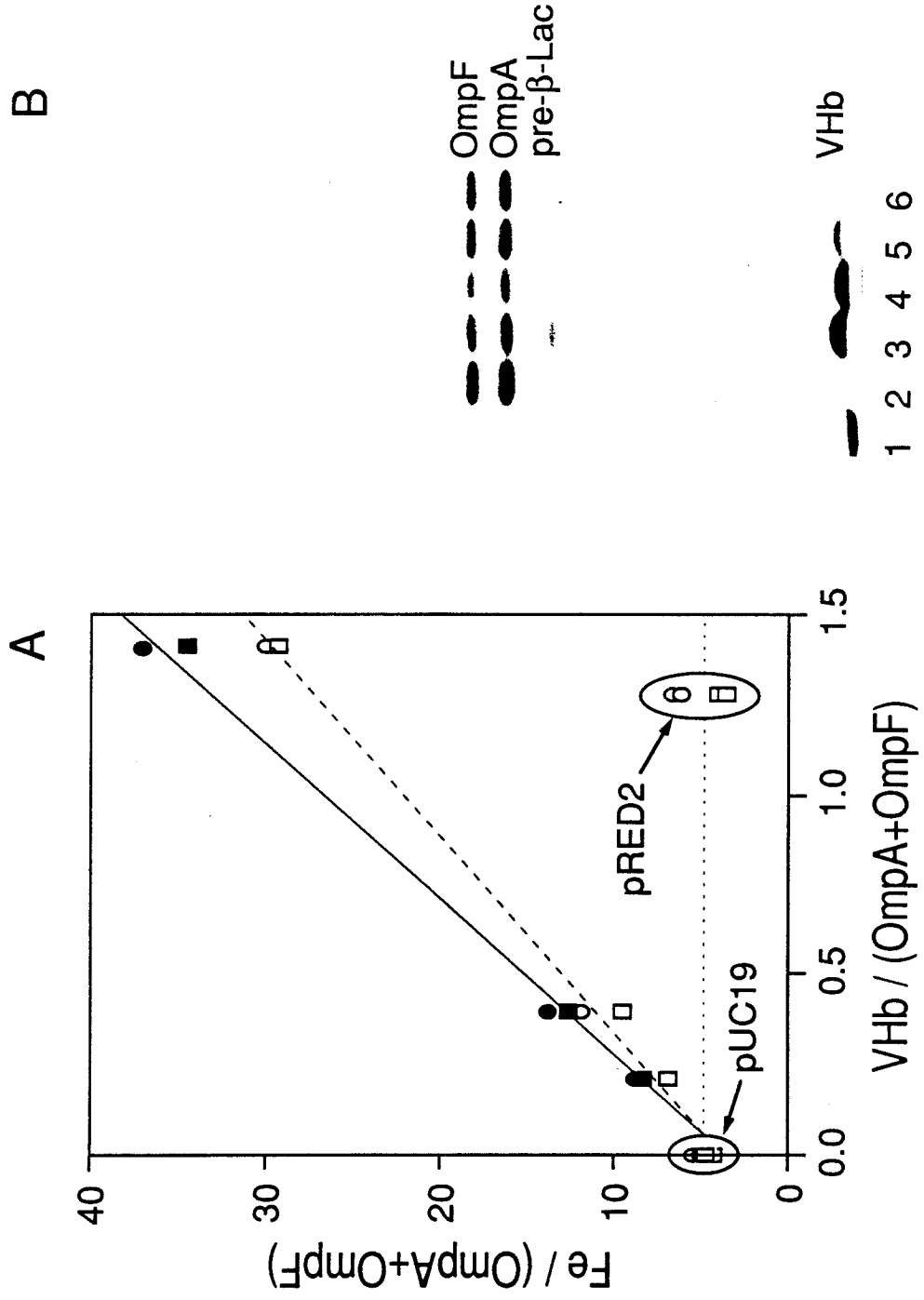
A
B
Fe / (OmpA+OmpF)
VHb / (OmpA+OmpF)
pRED2
pUC19
OmpF
OmpA
pre-β-Lac
VHb
1 2 3 4 5 6

Figure 5.

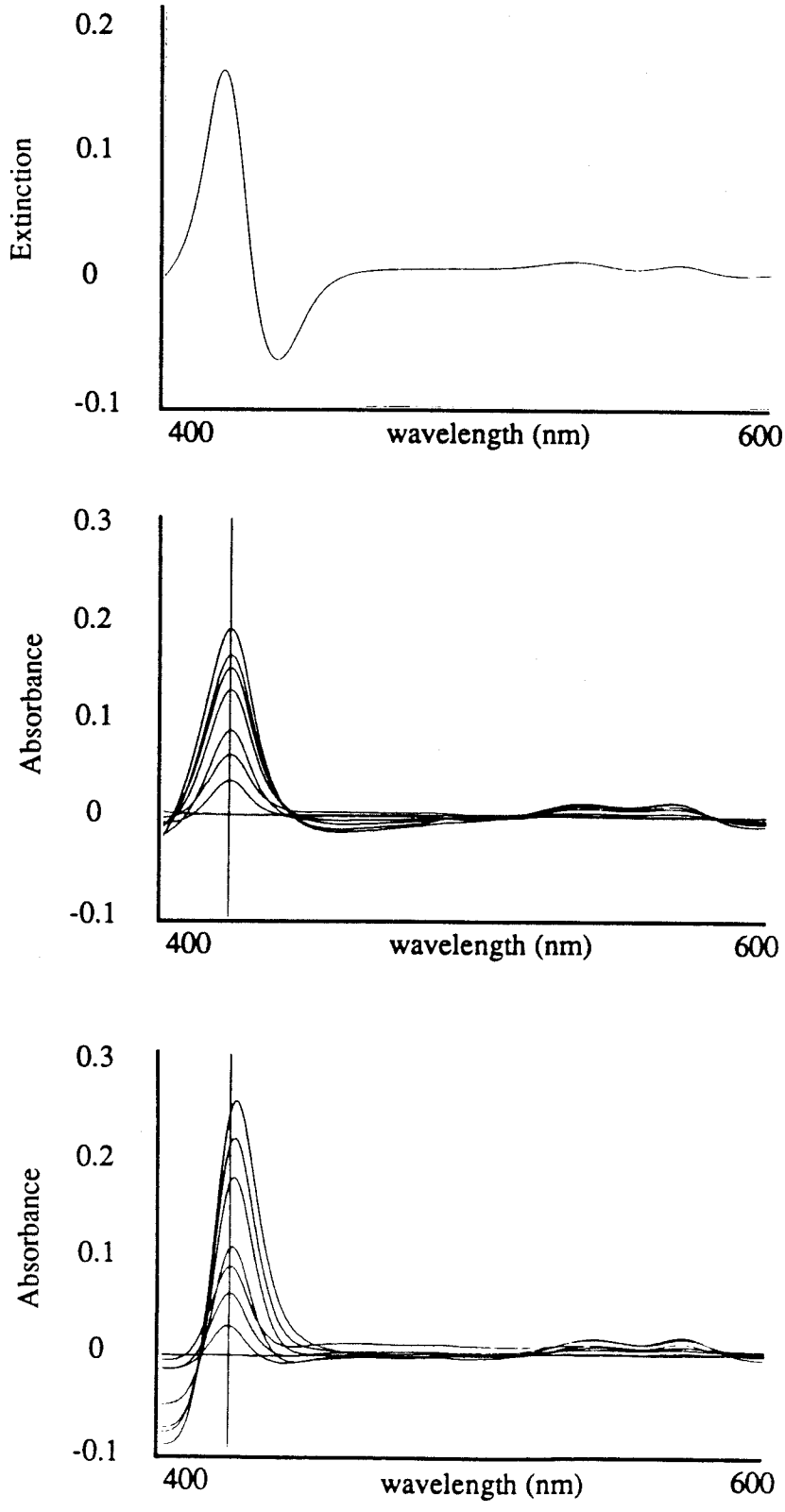
0.2
0.1
0
-0.1
Extinction
400
wavelength (nm)
600
0.3
0.2
0.1
0
-0.1
Absorbance
400
wavelength (nm)
600
0.3
0.2
0.1
0
-0.1
Absorbance
400
wavelength (nm)
600

CHAPTER 5

Solubilization and Regeneration of *Vitreoscilla* Hemoglobin Isolated from Protein Inclusion Bodies

5.1 Summary

Vitreoscilla hemoglobin (VHb) in its native, active state is a homodimer containing two heme groups. High-level expression of VHb in recombinant *E. coli* results in its accumulation in heme-free inclusion bodies. VHb can be solubilized from these inclusion bodies with relatively low concentrations of urea. The midpoint of VHb inclusion body dissolution occurs at approximately 3.2 M urea. Dissolution in the presence of stoichiometric heme shifts the dissolution midpoint to approximately 4.5 M urea. The presence of heme does not influence the dissolution properties of contaminant proteins, as determined by SDS-PAGE, suggesting the effect is specific for VHb. Denaturation of apoVHb obtained from purified native VHb has a midpoint of 2.9 M urea and follows a two-state model. The midpoint of denaturation of holoVHb obtained from purified native VHb occurs at 5.1 M urea. The denaturation of holoVHb in urea does not follow a two-state model. VHb solubilized from inclusion bodies with urea at concentrations from 0 to 3.5 M urea can be regenerated by heme addition without dilution to yield active holoVHb. The fraction of solubilized VHb reconstituted upon heme addition is maximum when solubilization and reconstitution is conducted in less than 1 M urea. At these low urea concentrations, approximately 5% of inclusion body VHb is solubilized. Of this solubilized VHb, approximately 30% is reconstituted upon heme addition.

5.2 Introduction

Many proteins aggregate intracellularly when expressed at high levels in heterologous hosts (Kane and Hartley, 1988; Mitraki and King, 1989; Schein, 1989). For subsequent recovery of the desired recombinant protein, the aggregated form may represent either an advantage or a disadvantage. Inclusion bodies may be advantageous for downstream processing as the insoluble protein can be substantially concentrated and purified with low-speed centrifugation (Marston *et al.*, 1984; Schoner *et al.*, 1985). Inclusion bodies may be very disadvantageous, however, if the insolubilized protein cannot be renatured. In most cases, the extent of advantage afforded downstream processing by inclusion bodies is determined by the technological difficulty of refolding/renaturation steps and the resulting yield of active product (Kenten *et al.*, 1984; Tsuji *et al*, 1987).

The standard approach to recovering protein from inclusion bodies involves dissolving the protein aggregates with high concentrations of denaturants followed by a refolding process based on systematic removal of the denaturing solute (Builder and Ogez, 1985; Olson and Pai, 1985; Marston and Hartley, 1990). The governing premise of this approach is absence of desired conformation in the insolubilized protein which is worth preserving. This premise has not been shown to be uniformly true and a few reported cases contradict it directly (Kronheim *et al.*, 1986; Hoess *et al.*, 1988). If the insoluble protein does possess useful conformational attributes, greater progress in developing suitable recovery strategies may be made by utilizing minimal denaturant concentrations during dissolution. We have adopted this approach in the recovery and reactivation of

Vitreoscilla hemoglobin (VHb) from inclusion bodies produced in *Escherichia* coli.

VHb represents a good model system for investigating this approach. It spans the entire hierarchy of protein structure (Jaenicke, 1987) as it is dimeric and each protomer incorporates a heme prosthetic group. Thus, this system affords new challenges in the form of prosthetic group incorporation and oligomerization not encountered in previous inclusion body processing reports (Marston *et al.*, 1984; Kronheim *et al.*, 1986; Lowe *et al.*, 1987). VHb is a useful model of such complex proteins since it is homodimeric and each protomer is relatively small and largely helical (Wakabayashi *et al.*, 1986).

Previous studies of VHb inclusion bodies by EPR and atomic absorption spectroscopy demonstrated that insoluble VHb uniformly lacks heme (Hart and Bailey, 1991b). Concurrently produced soluble VHb, however, contains heme and is active. Two-dimensional electrophoresis and amino acid analysis demonstrated that the soluble and insoluble forms of VHb do not otherwise differ. Further, heme titration studies suggest some insoluble VHb is competent for heme binding (Hart and Bailey, 1991b). In this report we show that VHb can be solubilized from inclusion bodies with low concentrations of denaturant and subsequently regenerated by heme addition in the presence of denaturant to yield active protein. Further, observations of the response of inclusion bodies and soluble VHb to the presence of heme and denaturant offer general insights into the complex phenomena encountered in inclusion body processing.

5.3 Materials and Methods

Cell growth and inclusion body harvesting - *E.* coli strain JM101: pRED2 which overproduces VHb from a pUC19-derived plasmid was grown as previously described (Hart *et al.*, 1990). Cells were washed, lysed by sonication and fractionated by centrifugation. Inclusion bodies were washed, resuspended in buffer and stored at - 70°C as previously described (Hart *et al.*, 1990).

VHb inclusion body dissolution - Stock inclusion body suspensions, in which VHb constitutes approximately one third of total protein, had a VHb monomer concentration of approximately 0.5 mM. Inclusion bodies from 0.1 ml of inclusion body stock suspension were pelleted by centrifugation and resuspended in 1.0 ml of X M urea, 100 mM potassium phosphate (pH 7.0), 1 mM DTT and incubated for 1 hour at 25°C. Dissolution in the presence of heme was conducted identically except the dissolution buffer in this case also contained 50 μM hemin chloride. Heme was added to the dissolution buffer from a 15 mM hemin chloride, 100 mM NaOH stock solution (Sano, 1979). Following incubation, remaining insolubles were removed by centrifugation at 14,000 g for 5 min. Solubilized proteins were then precipitated with 10% TCA and the recovered pellets washed extensively with ethanol:ethyl ether (1:1). All samples were stored at - 70°C for later analysis. Soluble and insoluble fractions were analyzed by SDS-PAGE with Coomassie blue staining. The amount of VHb per band was determined by scanning densitometry.

Conformational stability of holoVHb and apoVHb - HoloVHb and apoVHb stock solutions were prepared from a common 1 mM stock solution of

purified VHb in 50 mM potassium phosphate (pH 7.0) (Hart and Bailey, 1991a). The holoVHb stock solution was prepared by diluting 0.1 ml of the 1 mM VHb stock to 2.0 ml with 0.1 M potassium phosphate (pH 7.0) to achieve a final holoVHb concentration of 50 μM. The apoVHb stock solution was prepared by diluting 0.1 mL of the 1 mM VHb stock solution to 0.5 ml with distilled water. The resulting VHb solution was then added dropwise to 10 mL of ice cold acidified acetone (3 ml of 2 N HCl/liter acetone) and the precipitated apoVHb was isolated by centrifugation at 10,000 g, - 20°C for 30 min (Sano, 1979). The precipitated apoVHb was resuspended in 1 ml of ice cold distilled water and dialyzed extensively against 0.1 M potassium phosphate (pH 7.0) at 4°C. Following dialysis, irreversibly precipitated protein was removed by centrifugation and the supernatant was diluted to 2.0 ml with 0.1 M potassium phosphate (pH 7.0) to achieve a final apoVHb concentration of approximately 50 μM. Yield of apoVHb was estimated to be approximately 70% with remaining holoVHb representing less than 3% of VHb. Stability was determined by adding 0.1 ml of prepared holoVHb or apoVHb stock solution to 1.9 ml of a denaturation buffer containing X M urea, 0.1 M potassium phosphate (pH 7.0), incubating at 25°C for 5 min, and measuring sample fluorescence.

VHb regeneration - The starting material was the soluble fraction isolated by inclusion body dissolution as described above. The soluble fraction was diluted 1:2 with a regeneration buffer containing X M urea, 0.1 M potassium phosphate (pH 7.0), 1 mM DTT, 50 μM heme (equimolar urea). VHb concentration at this point ranged from 50 μg/ml to 1 mg/ml. Sodium dithionite was added to a concentration of 2.5 mg/ml and the protein was incubated at 25°C

for 4 hours. Unbound heme was removed by ultrafiltration, the retained protein was resuspended in X M urea, 0.1 M potassium phosphate (pH 7.0), 1 mM DTT (equimolar urea) and the difference absorption spectrum was collected.

Difference absorption spectroscopy - Difference absorption spectra (carbon monoxide minus reduced) were obtained with a Shimadzu UV-260 dual beam spectrophotometer interfaced to an IBM XT computer (Hart and Bailey, 1991b). The spectrophotometer cell was maintained at 25°C. Reduced VHb was produced by addition of 2.5 mg/ml sodium dithionite. Carbon monoxide-bound VHb was produced by addition of 2.5 mg/ml sodium dithionite followed by incubation in CO at 3 psig for 30 min.

Fluorescence spectroscopy - Fluorescence emission spectra were obtained with a Shimadzu RF-540 spectrofluorometer interfaced to an IBM XT computer. The spectrofluorometer cell was maintained at 25°C with a recirculating water temperature controller. The excitation wavelength was set at the absorption maximum of 290 nm. Spectral resolution was 0.1 nm with excitation and emission slit widths of 2 nm. The fluorescence spectra of suitable buffer controls were collected and subtracted digitally.

Electrophoresis - SDS-PAGE was conducted using the BioRad Protein II Multi Cell Electrophoresis system according to the method of Laemmli (1970). Resolving gradient slab gels were composed from 10% - 20% acrylamide, 0.3% - 0.6% bisacrylamide and 0.1% SDS. Gels were run at 32.5 mA/gel, 4°C for 6 hours and stained with Coomassie blue R 250. VHb internal standard was included throughout to correct for variations in staining. For quantitative analysis, gels

were scanned while wet using an LKB Ultroscan XL Scanning Densitometer.

5.4 Results

VHb Inclusion Body Dissolution

Dissolution of protein inclusion bodies is usually accomplished by incubation in buffer containing high concentrations of the denaturants urea or guanidine hydrochloride (Marston and Hartley, 1990). *Vitreoscilla* hemoglobin (VHb) is solubilized from inclusion bodies with comparatively low concentrations of urea as shown in Figure 1a. The midpoint of VHb dissolution occurs at approximately 3.2 M urea. Essentially all VHb is solubilized by 5 M urea and some is solubilized by incubation in buffer containing no urea.

Inclusion body VHb uniformly lacks heme (Hart and Bailey, 1991b). Active VHb, by definition, contains heme. To determine whether heme may influence the solubilization of inclusion body VHb, we repeated the experiments described above using buffers containing urea and heme. All buffers contained the same amount of heme which was stoichiometric with the total amount of VHb polypeptide present. Including heme in the dissolution buffer results in less VHb solubilization at intermediate concentrations of urea as shown in Figure 1b.

VHb solubilization in urea buffers and urea buffers containing heme was determined by quantitative SDS-PAGE. Thus, we were able to monitor the solubilization properties of all proteins contained within insoluble lysates simultaneously. Interestingly, only the solubilization properties of VHb are affected by including heme in the dissolution buffers (data not shown). That is, the effect

appears specific to VHb. The midpoint of dissolution of VHb in the presence of heme occurs at approximately 4.5 M urea.

VHb Denaturation

Treatment of inclusion bodies with denaturant can cause protein unfolding as well as protein solubilization. To resolve these potentially simultaneous processes, it is useful to determine the stability properties of VHb. The closest analogue of inclusion body VHb available is apoVHb produced from purified soluble VHb by heme extraction as described in Materials and Methods. Purified soluble VHb was previously shown to be active and homogeneous (Hart and Bailey, 1991a). Fluorescence spectroscopy was used to determine the denaturation properties of apoVHb and holoVHb. Each VHb monomer contains 1 tryptophan, 4 tyrosine and 4 phenylalanine residues. Of these potential fluorophores, the only one expected to have appreciable fluorescence under these experimental conditions is tryptophan.

Fluorescence emission spectra of apoVHb in various denaturation buffers are shown in Figure 2a. The excitation wavelength was 290 nm. Results show apoVHb has an emission maximum at 320 nm. Upon denaturation, the emission maximum shifts to 348 nm. Previous studies on tryptophan fluorescence have shown the wavelength of the emission maximum to be dependent on the polarity of the solvent (Demchenko, 1986). In particular, tryptophan in a polar environment has an emission maximum near 350 nm while tryptophan in an apolar environment has an emission maximum between 320 and 340 nm (Demchenko, 1986). Thus, the fluorescence spectrum of apoVHb in buffer, shown in

Figure 2a, reveals that apoVHb possesses a hydrophobic core. Detailed analysis of apomyoglobin has shown that it also possesses a hydrophobic core (Griko *et al.*, 1988).

Examination of the urea denaturation curve of apoVHb, shown in Figure 3a, shows the midpoint of denaturation occurs at 2.9 M urea. Assuming two-state denaturation, the free energy of apoVHb denaturation can be determined (Pace, 1986). A plot of the calculated free energy values is shown in Figure 3b. Using the linear extrapolation method, the free energy of denaturation in the absence of denaturant can be determined. This value, referred to as the conformational stability, is a measure of the free energy required to unfold a protein in the absence of denaturant. The conformational stability of apoVHb determined by this method is 2.4 kcal/mole. The conformational stability of apomyoglobin, determined by more accurate means, is reported to to be 2.6 kcal/mole (Griko *et al.*, 1988). The linearity of the free energy curve shown in Figure 3b indicates validity of the two-state model assumption for the denaturation of apoVHb.

Fluorescence emission spectra of holoVHb in various denaturant buffers are shown in Figure 2b. The presence of heme in holoVHb efficiently quenches tryptophan fluorescence as it does with other hemeproteins (Kawamura-Konishi *et al.*, 1988). Consequently, the fluorescence of holoVHb in buffer is weak with the emission maximum occurring at 348 nm. The intensity of fluorescence increases with denaturation due to the loss of the heme group.

The urea denaturation curve of holoVHb, shown in Figure 4a, reveals that the midpoint of holoVHb denaturation occurs at approximately 5.1 M urea. Employing the same analytical assumptions as with apoVHb, the free energy of

denaturation of holoVHb was determined and is plotted in Figure 4b. Linear extrapolation to zero denaturant concentration gives an estimate of the conformational stability of holoVHb of 3.1 Kcal/mole. In this case, however, examination of the free energy curve reveals the presence of two distinct linear regions indicating existence of an intermediate and failure of the two-state model assumption. Consequently, 3.1 kcal/mole must be considered a low estimate of the actual conformational stability (Pace, 1986). The conformational stability of holomyoglobin, for example, is 8.1 kcal/mole (Griko, 1988).

Regeneration of VHb Solubilized from Inclusion Bodies

Results from dissolution studies show that VHb can be solubilized from inclusion bodies by incubation in relatively low concentrations of urea. Previous studies suggest some inclusion body VHb is competent for heme binding (Hart and Bailey, 1991b). At the low concentrations of urea required for VHb solubilization from inclusion bodies, holoVHb is essentially stable. These observations suggest a possible strategy for recovering VHb from inclusion bodies. In this strategy, VHb is solubilized from inclusion bodies using low concentrations of urea and subsequently stabilized by heme binding. It is possible that the stabilizing action of heme may alleviate the need for extensive dilution.

To test this strategy, inclusion body samples were incubated in buffer containing urea at the concentrations indicated in Figure 1a. After one hour incubation, the solubilized protein was separated from remaining aggregate. The isolated soluble fractions were then diluted (1:2) into regeneration buffers containing equimolar urea and stoichiometric levels of heme. VHb concentration at

this point varied from 50μg/ml to 1 mg/ml. Sodium dithionite was added to reduce the heme and the solution was allowed to incubate for 4 hours. Later, unbound heme was removed by ultrafiltration against a buffer containing equimolar urea. The samples were then analyzed by difference absorption spectroscopy (carbon monoxide minus reduced) to examine the extent of renaturation and the properties of the renatured protein. Special care was taken to ensure that a given protein sample only encountered one urea concentration throughout its manipulation.

Visible difference spectra of regenerated VHb are shown in Figure 5b. Results show that VHb solubilized and regenerated in less than 4 M urea has a difference absorption spectrum indistinguishable from that of native soluble VHb (Figure 5a). Note that the sample resulting from solubilization and regeneration in buffer containing no urea also yields the same difference absorption spectrum as native VHb. Spectral analysis of controls produced by eliminating heme from the regeneration buffer shows the spectrum is not due to the presence of residual active VHb in inclusion body preparations (data not shown). Further, parallel treatment of control cell debris shows the spectrum is not derived from solubilized membrane cytochromes (data not shown). Consequently, the spectrum is attributed entirely to regenerated VHb.

Evidence of the invariance of VHb conformation among samples arising from solubilization and regeneration in less than 4 M urea is provided by the existence of isosbestic points at 405 nm and 428 nm in the spectrum of the respective samples (Figure 5b). Native VHb has isosbestic points at these same wavelengths (Figure 5a). Isosbestic points are the frequencies at which the dif-

ference extinction coefficient equals zero. The frequency at which an isosbestic point occurs is sensitive to heme pocket conformation and heme electronic state (Smith and Williams, 1970; Adar, 1978). VHb in samples resulting from dissolution and regeneration in urea concentrations greater than 4 M shows evidence of denaturation as these isosbestic points are absent in spectra of such samples. (Figure 5b).

By assuming the regenerated form of VHb has the same extinction as purified soluble VHb, it is possible to calculate the yield resulting from the reconstitution strategy. The results from this yield determination are shown in Figure 6. Results show that the fraction of solubilized VHb reconstituted upon heme addition is maximum for samples incubated in 1 M urea or less. At this low urea concentration, approximately 30% of solubilized VHb is reconstituted upon heme addition. Overall recovery yield in this regime is low, below 5%, due to the relatively low solubilization achieved under these conditions. Improved yields, approaching 10%, are obtained when VHb is solubilized and reconstituted in urea concentrations near 4 M.

5.5 Discussion

Most strategies for recovering protein from inclusion bodies begin with a solubilization step employing high concentrations of denaturant, typically 8 M urea or 6 M guanidine hydrochloride (Marston and Hartley, 1990). Few investigators, however, report the actual concentration of denaturant required for solubilizing the target protein (Lowe *et al.*, 1987). We have found that *Vitreoscilla* hemoglobin is solubilized from inclusion bodies with relatively low

concentrations of urea. The midpoint of VHb solubilization occurs at 3.2 M urea. Interestingly, some VHb, approximately 5%, is solubilized by treatment with buffer containing 1 M urea or less. The midpoint of apoVHb denaturation occurs at 2.9 M urea. The similarity between the midpoints of VHb solubilization and apoVHb denaturation suggest that denaturation may be an important component of the solubilization mechanism at higher denaturant concentrations.

Contacts between the heme prosthetic group and neighboring polypeptide structures generally stabilize the holo form of heme proteins relative to the apo form (Griko, 1988). This stabilization generally shifts the polypeptide unfolding equilibrium to favor the folded state. Due to this interaction, we initially thought it possible that including heme in VHb inclusion body dissolution buffers would influence the underlying solubilization process so as to favor the soluble holoVHb state. Through such a mechanism, we expected that the midpoint of VHb solubilization in buffers containing heme would be less than the midpoint of VHb solubilization in buffers lacking heme. Results show, however, that the opposite of this is true. That is, including heme in dissolution buffers makes VHb more difficult to solubilize. In particular, the midpoint of dissolution in the presence of heme occurs at approximately 4.5 M urea while dissolution in the absence of heme occurs at approximately 3.2 M urea. The midpoint of VHb dissolution in the presence of heme occurs at a urea concentration between the midpoint of denaturation of apoVHb (2.9 M urea) and the midpoint of denaturation of holoVHb (5.1 M urea).

One possible mechanism to explain this behavior is heme stabilization of insoluble inclusion body protein through nonspecific hydrophobic contacts. With

this mechanism, one would expect that the solubilization properties of all aggregated proteins in the inclusion bodies would be similarly affected. Results indicate, however, that the solubilization properties of contaminant proteins are unaffected by the presence of heme. Another possible mechanism to explain this behavior is interaction of heme specifically with VHb, at a site perhaps similar to the hydrophobic pocket of apoVHb, and thereby stabilizing VHb in the insoluble state by stabilizing the molecule to denaturation. Such a mechanism appears plausible based on observations from heme titration studies which suggest that some inclusion body VHb is competent for heme binding (Hart and Bailey, 1991a).

Results from dissolution and reconstitution studies show that VHb can be solubilized and reconstituted using low concentrations of urea. Interestingly, some VHb can be solubilized and reconstituted in buffer lacking urea. Results further show that the fraction of soluble VHb reconstituted by heme addition is maximum at or below 1 M urea. At these low urea concentrations, approximately 30% of solubilized VHb is reconstituted upon heme addition. VHb reconstituted in this regime has the same difference absorption spectrum as native VHb. Interestingly, at these low urea concentrations, apoVHb is relatively stable with approximately 90% existing in the native state. Thus, it is possible that the protein solubilized in this concentration range is not denatured upon solubilization.

Overall recovery yields are higher when VHb is solubilized and reconstituted in greater than 3.5 M urea. This is due to the larger extent of solubilization with these higher urea concentrations. At these higher urea concentrations,

solubilized VHb is undoubtedly denatured. Thus, reconstitution in this regime is likely due to heme-induced protein refolding. Dissolution and reconstitution in greater than 4 M urea yields a form of holoVHb which does not have the same difference absorption spectrum as native VHb. The difference absorption spectrum of native VHb denatured by incubation in greater than 4 M urea is similar to that obtained from VHb solubilized and reconstituted in greater than 4 M urea (data not shown). Interestingly, the urea concentration at which the difference absorption spectrum of holoVHb is disrupted (approximately 4 M urea) coincides with the point at which the fluorescence spectrum of holoVHb is disrupted (see Figure 2b, emission wavelength of 300 nm). This also corresponds to the point of discontinuity between two linear regimes in the holoVHb free energy of denaturation curve. It is possible that all these changes are due to a dimer to monomer transition occurring during denaturation.

An advantage to the solubilization and regeneration strategy used here is minimal solubilization of membrane proteins in low concentrations of denaturants. In particular, the outer membrane proteins OmpA, OmpF and OmpC, the most prevalent protein contaminants in inclusion body preparations, are not solubilized by incubation in urea concentrations less than 5 M (data not shown). This is important as these proteins can readily foul ultrafiltration membranes due to their high tendency for aggregation.

5.6 Acknowledgements

This research was supported by the National Science Foundation (Grant No. EET-8606179). R. H. was supported in part by a predoctoral training grant in biotechnology from the National Institute of General Medical Sciences (National Research Service Award 1 T32 GM 08346-01, Pharmacology Sciences Program)

5.7 References

1. Adar, F. (1978) in *The Porphyrins* (Dolphin, D., ed.), **3**, 167 - 209

2. Builder, S. E., Ogez, J. R. (1985) U.S. Patent 4511502

3. Demchenko, A. P. (1986) *Ultraviolet Spectroscopy of Proteins.* Springer Verlag, New York

4. Griko, Y.V., Privalov, P. L., and Venyaminov, S. Y. (1988) *J. Mol. Biol.* **202**, 127 - 138

5. Hart, R. A., Rinas, U., and Bailey, J. E. (1990) *J. Biol. Chem.*, **265**, 12728 - 12733

6. Hart, R. A., and Bailey, J. E. (1991a) Material in Chapter 2. Accepted by *Enzyme and Microbial Technology*

7. Hart, R. A., and Bailey, J. E. (1991b) Material in Chapter 4.

8. Hoess, A., Arthur, A. K., Wanner, G., and Fanning, E. (1988) *Bio/Technology* **6**, 1214 - 1217

9. Jaenicke, R. (1987) *Prog. Biophys. Molec. Biol.* **49**, 117 - 237

10. Kane, J. F., and Hartley, D. L. (1988) *Trends in Biotechnol.*, **6**, 95 - 101

11. Kawamura-Konishi, Y., Kihara, H., Suzuki, H. (1988) *Eur. J. Biochem.* **170**, 589 - 595

12. Kenten, J., Helm, B., Ishizaki, T., Cattini, P., and Gould, H. (1984) *Proc. Natl. Acad. Sci. USA* **81**, 2955 - 2959

13. Kronheim, S. R., Cantrell, M. A., Deeley, M. C., March, C. J., Glackin, P. J., Anderson, D. M., Hemenway, T., Merriam, J. E., Cosman, D., and Hopp, T. P. (1986) *Bio/Technology* **4**, 1078 - 1082

14. Laemmli, U. K. (1970) *Nature*, **227**, 680 - 685

15. Lowe, P. A., Rhind, S. K., Sugrue, R., and Marston, F. A. O. (1987) in *Protein Purification: Micro to Macro.* Alan R. Liss Inc.

16. Marston, F. A. O., Lowe, P. A., Doel, M. T., Schoemaker, J. M., White, S., and Angal, S. (1984) *Bio/Technology* **3**, 800 - 804

17. Marston, F. A. O., and Hartley, D. L. (1990) *Meth. Enzymol.* **182**, 264 - 276

18. Mitraki, A., and King, J. (1989) *Bio/Technology* **7**, 690 - 697

19. Olson, N.C., and Pai, D. C., (1985) U.S. Patent 451103

20. Pace, C. N. (1986) *Meth. Enzymol.* **131**, 266 - 280

21. Sano, S. (1979) in *The Porphyrins* (Dolphin, D., ed) **7**, 377 - 402, Academic Press

22. Schein, C. H. (1989) *Bio/Technology* **7**, 1141 - 1149

23. Schoner, R. G., Ellis, L. F., and Schoner, B. E. (1985) *Bio/Technology* **3**, 151 - 154

24. Smith, D. W., and Williams, R. J. P. (1970) *Struct. Bond.*, **7**, 1 - 45

25. Tsuji, T., Nakagawa, R., Sugimoto, N., and Fukuhara, K. (1987) *Biochemistry* **26**, 3129 - 3134

26. Wakabayashi, S., Matsubara, H., and Webster, D. A. (1986) *Nature* **322**, 481 - 483

5.8 Figures

Figure 1: Solubilization of VHb inclusion bodies in buffer containing urea and buffer containing urea and stoichiometric ferrous heme. (a) Fraction VHb found soluble (open) and insoluble (filled) following incubation in urea. (b) Fraction VHb found soluble (open) and insoluble (filled) following incubation in urea containing heme.

Figure 2: Fluorescence spectra of apoVHb and holoVHb with urea denaturation. (a) Changes in fluorescence upon apoVHb denaturation. (b) Changes in fluorescence upon holoVHb denaturation. Bold line indicates fluorescence of apoVHb in buffer.

Figure 3: Denaturation of apoVHb in urea. (a) Fraction apoVHb remaining native following incubation in urea. (b) Free energy change upon denaturation of apoVHb in urea.

Figure 4: Denaturation of holoVHb in urea. (a) Fraction holoVHb remaining active following incubation in urea. (b) Free energy change upon denaturation of holoVHb in urea.

Figure 5: Regeneration of VHb solubilized from inclusion bodies. (a) Difference extinction spectrum of purified soluble VHb. (b) Difference absorption spectra of inclusion body VHb following solubilization and regeneration in 0, 1, 2, 2.5, 3.0, 3.5, 4.0 and 4.5 M urea.

Figure 6: Inclusion body VHb renaturation yields. Fraction inclusion body VHb solubilized by incubation in buffers containing urea shown with open symbols. Fraction of solubilized VHb reconstituted following heme addition shown with filled symbols.

Figure 1.

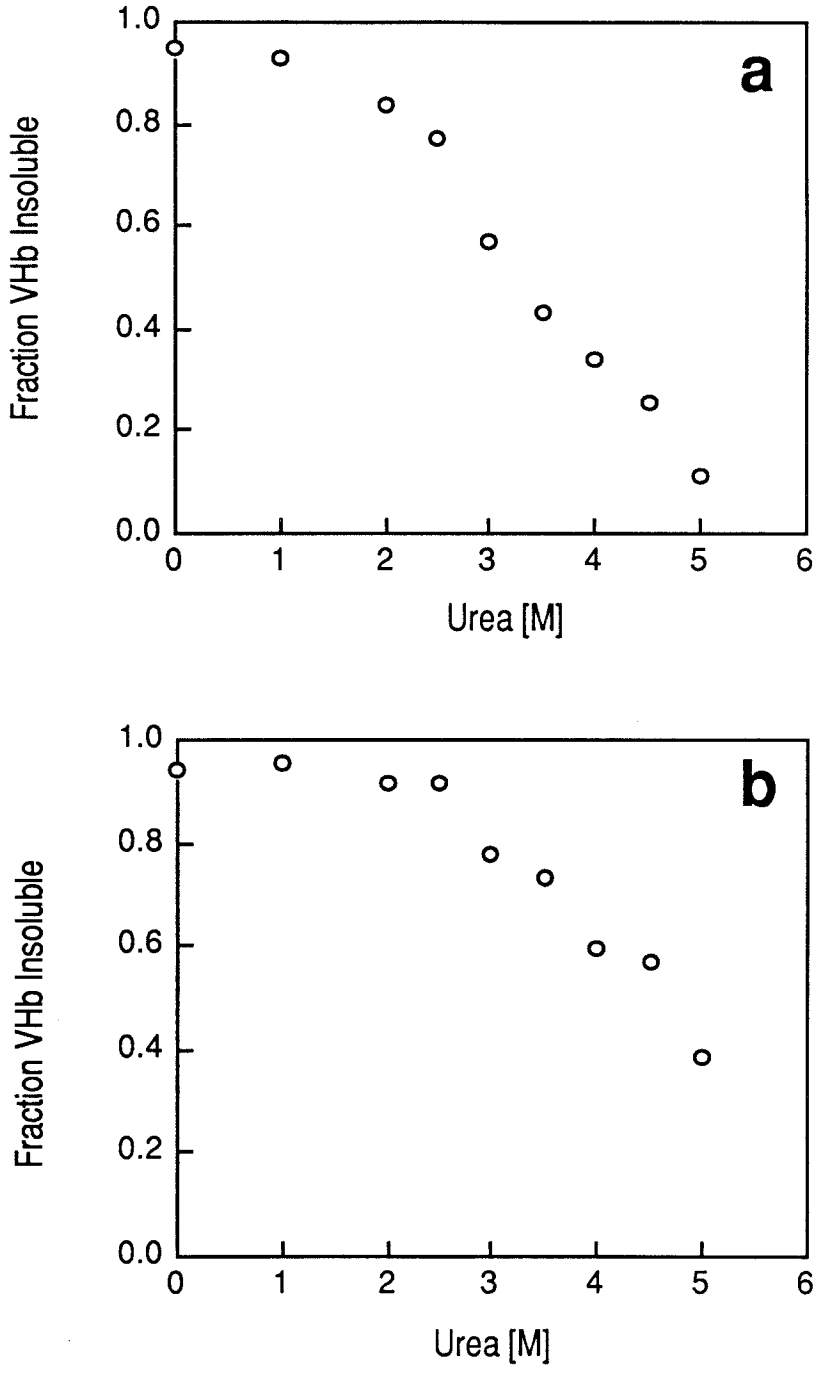
a
Fraction VHb Insoluble
1.0
0.8
0.6
0.4
0.2
0.0
0
1
2
3
4
5
6
Urea [M]
b
Fraction VHb Insoluble
1.0
0.8
0.6
0.4
0.2
0.0
0
1
2
3
4
5
6
Urea [M]

Figure 2.

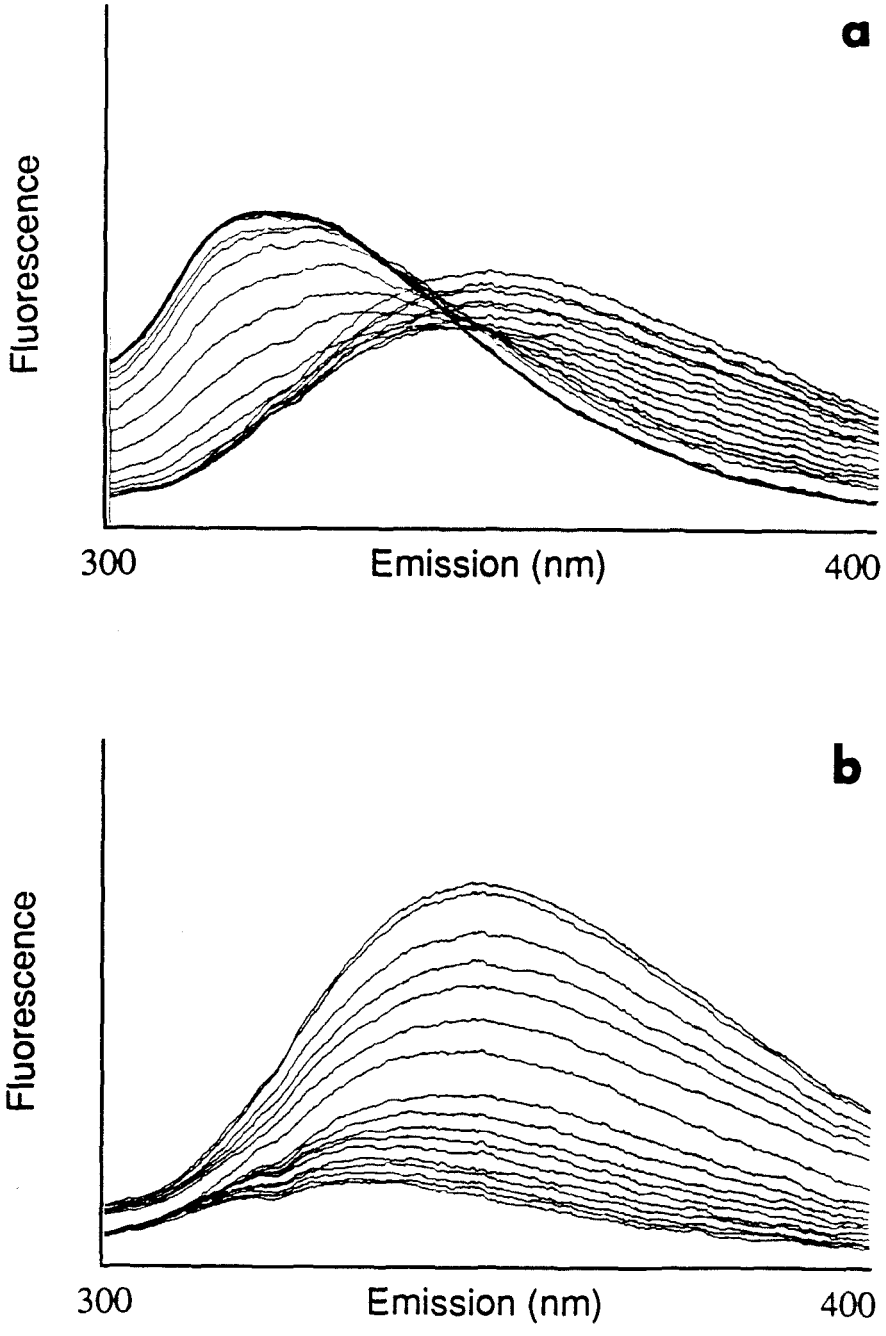
a
Fluorescence
300
Emission (nm)
400
b
Fluorescence
300
Emission (nm)
400

Figure 3.

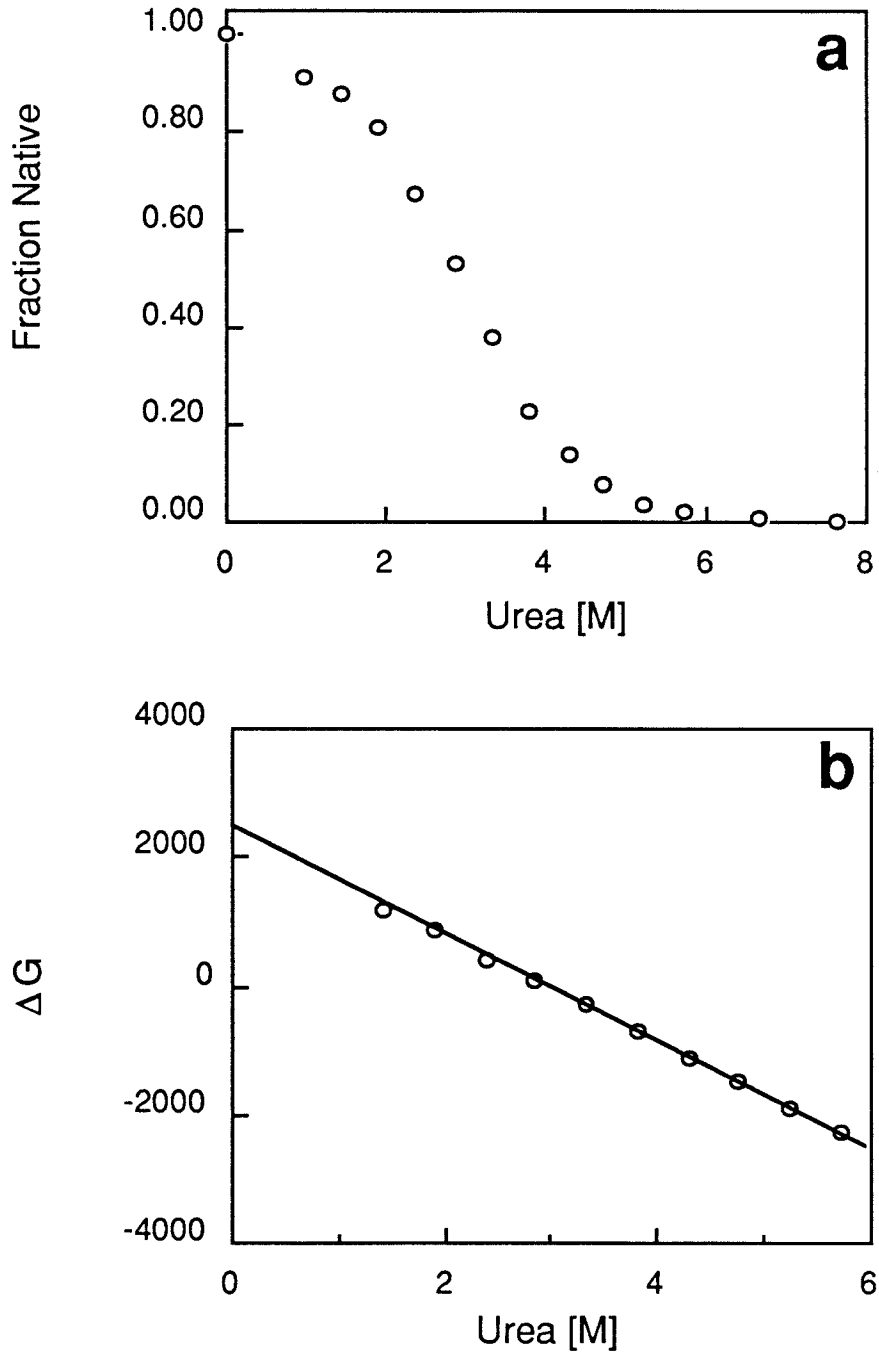
a
Fraction Native
1.00
0.80
0.60
0.40
0.20
0.00
0
2
4
6
8
Urea [M]
b
ΔG
4000
2000
0
-2000
-4000
0
2
4
6
Urea [M]

Figure 4.

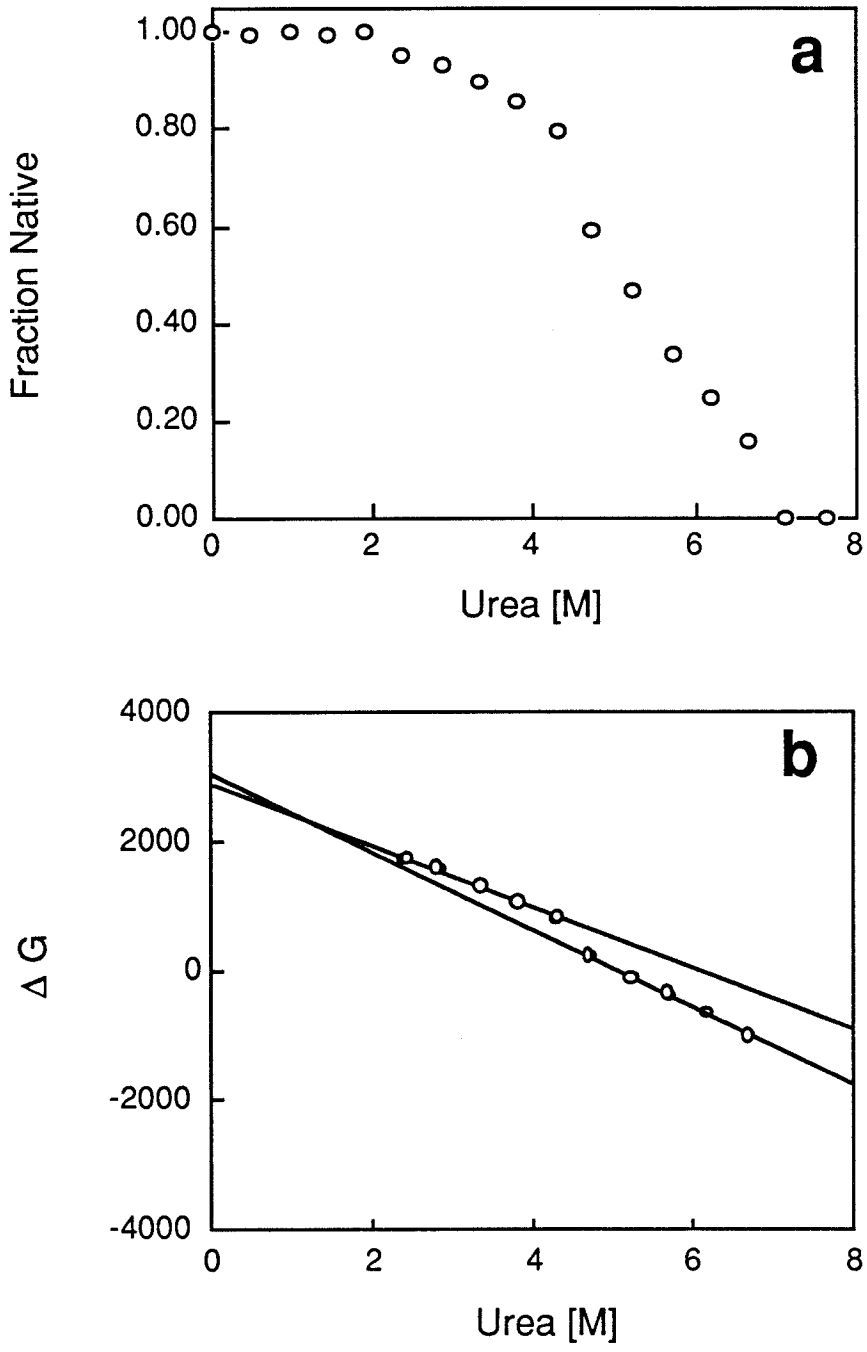
a
Fraction Native
1.00
0.80
0.60
0.40
0.20
0.00
0
2
4
6
8
Urea [M]
b
Δ G
4000
2000
0
-2000
-4000
0
2
4
6
8
Urea [M]

Figure 5.

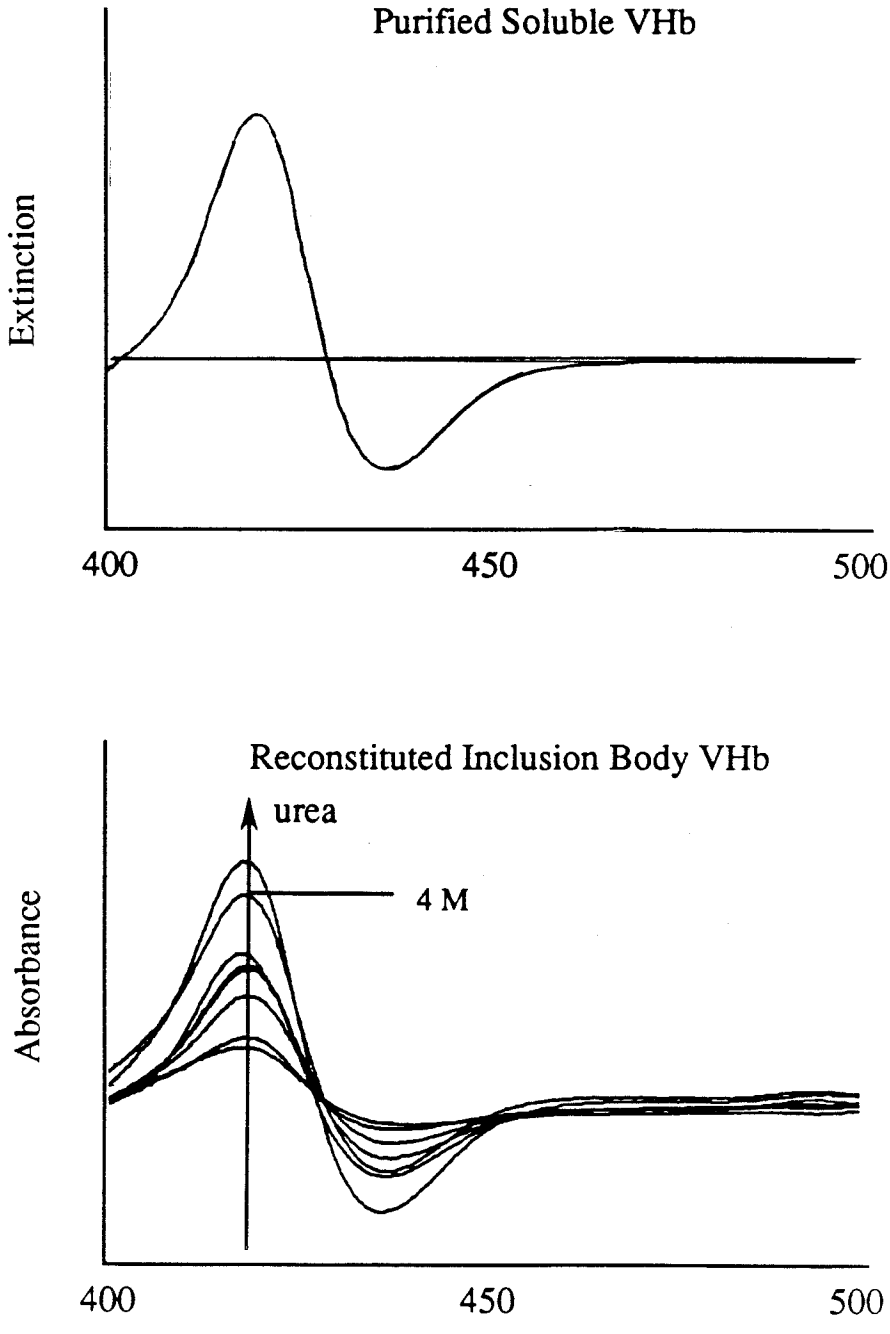
Purified Soluble VHb
Extinction
400
450
500
Reconstituted Inclusion Body VHb
urea
4 M
Absorbance
400
450
500

Figure 6.

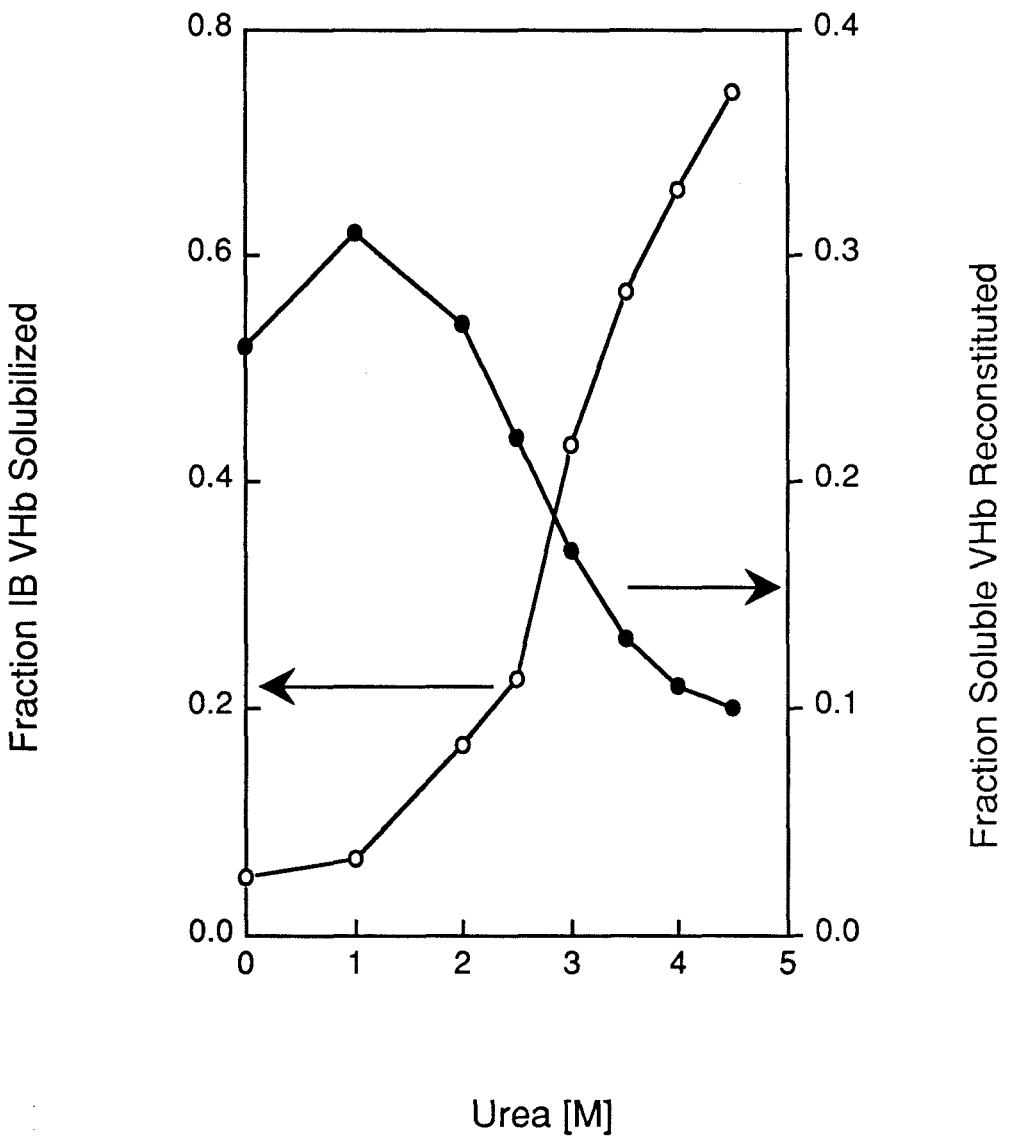
0.8
0.6
0.4
0.2
0.0
0.4
0.3
0.2
0.1
0.0
0
1
2
3
4
5
Fraction IB VHb Solubilized
Fraction Soluble VHb Reconstituted
Urea [M]

CHAPTER 6

Factors Influencing *Vitreoscilla* Hemoglobin Inclusion Body Formation in Recombinant *Escherichia coli*

6.1 Summary

A series of perturbation-response experiments was conducted to elucidate cellular processes which influence *Vitreoscilla* hemoglobin (VHb) inclusion body formation in *E. coli*. The effect of VHb accumulation rate was examined by using pUC19 and pBR322-derived expression plasmids, varying induction level through aeration and supplementing readily metabolized sugars to the medium. The effect of heme biosynthetic rate was investigated through supplementation of the heme pathway intermediates glutamate and δ-aminolevulinic acid (ALA) and the heme pathway inhibitor levulinic acid. Attempts were also made to increase heme biosynthetic capacity through the genetic amplification of ALA synthase and ALA dehydratase levels. The influence of chaperone protein levels was examined by varying temperature and inducing the heat shock response through genetic amplification of *E. coli* σ^{32}. Results show that VHb inclusion body formation is highly influenced by plasmid vector construction and the heme biosynthetic capacity. The level of induction and accumulation rate appear less important than the general metabolic state of the culture. Temperature and chaperone protein levels have little effect. Efforts of reduce inclusion body formation through genetic amplification of ALA synthase and ALA dehydratase levels were unsuccessful, presumably due to interaction with regulation.

6.2 Introduction

Many heterologous proteins aggregate intracellularly when expressed in recombinant hosts (Kane and Hartley, 1988; Schein, 1989; Mitraki and King, 1989). This phenomenon is best documented for protein expression in the gram-negative bacterial host *Escherichia coli*. However, inclusion body formation is not confined exclusively to this bacterium or for that matter to procaryotic hosts (Kitano *et al.*, 1987a; Kitano *et al.*, 1987b; Wang *et al.*, 1989). The mechanisms underlying this intracellular aggregation are not well understood and may vary with protein and recombinant host. A common theme, however, may be malfunction or disruption of intracellular protein folding. A summary of the various ways intracellular protein folding may malfunction and lead to insolubilization has been presented previously (Mitraki and King, 1989).

The study of *in vivo* protein folding is new in comparison to that of protein secretion and degradation. From the investigation of these related phenomena it is clear that the fate of an intracellular protein is determined both by its properties and those of the host cell (Hartl *et al.*, 1989). Early analysis of inclusion body formation concentrated on determining what protein properties influence intracellular aggregation (Kane and Hartley, 1988; Schein, 1989; King, 1989; Krueger, *et al.* 1990). Recently, more attention has been given to determining what cellular properties influence the event (Schein, 1989; Mitraki and King, 1989). The most potentially important work in this area concerns a class of proteins referred to as molecular chaperones which appear capable of preventing partially folded protein chains from aggregating *in vivo* (Gatenby, 1990). In

our investigations on inclusion body formation we have examined the influence of both protein and host properties (Hart and Bailey, 1991a; Hart and Bailey, 1991b).

6.3 Model Development

In the systems examined, VHb, a homodimeric hemeprotein, is produced from multicopy plasmids with expression regulated by the native VHb promoter (Hart *et al.*, 1990). This promoter is regulated by dissolved oxygen levels with maximal expression occurring in a narrow window commonly described as the microaerobic region (Khosla and Bailey, 1989; Dikshit *et al.*, 1990). During batch shake flask cultivation, VHb is accumulated during stationary phase in both soluble and insoluble forms.

We have previously examined many properties of the soluble and insoluble forms of VHb accumulated in *E. coli*. The purified soluble form of VHb is properly folded, dimeric and contains heme in the correct stoichiometry (Hart and Bailey, 1991a). The insoluble form of VHb, however, uniformly lacks heme (Hart and Bailey, 1991a) and is aggregated into inclusion bodies which are relatively devoid of contaminants (Hart *et al.*, 1990). The insoluble form is not solubilized by incubation in the presence of heme although it does appear to bind the prosthetic group (Hart and Bailey, 1991b). Refolding studies have shown that VHb polypeptide does fold in the absence of heme to yield a species possessing a hydrophobic core. However, heme binding dramatically affects polypeptide folding and stability as shown by the observation that refolding of the denatured polypeptide occurs in the presence of denaturants following heme addition (Hart

and Bailey, 1991b). Available evidence indicates that some inclusion body VHb polypeptide bears conformational similarity to apoVHb.

To provide a basis for analyzing cellular influences on VHb aggregation, we developed a conceptual model of the process as shown in Figure 1. In this model, the pathway for insolubilization intersects that of maturation at an intermediate believed similar to apoVHb. This intersection definitely occurs prior to heme incorporation but follows initial polypeptide folding. The intermediate is postulated to be monomeric. Globin subunit association has previously been shown to be important for maturation of human hemoglobin expressed in *E. coli* (Hoffman *et al.*, 1990) Quantitative VHb maturation clearly requires availability of heme in stoichiometric proportion to VHb polypeptide. Aggregation processes typically have a higher reaction order than folding processes (Zettlmeissl *et al.*, 1979); consequently, factors which increase intermediate concentration are expected to increase aggregation. In this case, the intermediate is believed similar to apoVHb; the apo forms of hemeproteins are known to have a high tendency for aggregation (Sano, 1979). Factors expected to increase the concentration of apoVHb include high polypeptide synthetic rate and low heme biosynthetic rate. By analogy with their other established functions (Gatenby *et al.*, 1990), chaperone proteins may influence this process by shielding apoVHb from aggregation.

We have examined these model predictions through a series of perturbation-response experiments. Specifically, synthesis rate perturbations were made through the use of different plasmid constructs, supplementation of sugars to the growth media and modulation of aeration to effect induction level. Heme

biosynthesis perturbations were made through supplementation of heme pathway intermediates and inhibitors and through genetic amplification of two heme biosynthetic enzymes. Chaperone protein level perturbations were made through genetic amplification of the heat shock regulator protein σ^{32}.

6.4 Materials and Methods

Bacterial strains and plasmids - *E. coli* strain JM101, genotype *supE thi* Δ*(lac-proAB) [F' traD36 proAB lacI^q ZΔM15]* was used as the host strain throughout (Yanisch-Perron *et al.*, 1985). Plasmid pRED2 was constructed from pUC19 (Yanisch-Perron *et al.*, 1985) by insertion of a 2.2 kb HindIII fragment containing the gene which encodes VHb under the control of its native promoter (Khosla and Bailey, 1988). Plasmid pINT2 was constructed from pBR322 (Bolivar *et al.*, 1977) by insertion of a 2.2 kb HindIII-BamHI fragment containing the gene which encodes VHb under the control of its native promoter (Khosla and Bailey, 1989). Plasmid pVSP1 was constructed from pRED2 by insertion of a 2.9 kb BamHI- HindIII fragment isolated from pJL68 (Li *et al.*, 1989c) which contains the *hemA* gene under the control of its native promoter. Plasmid pVDP1 was constructed from pRED2 by insertion of a 1.6 kb PstI fragment isolated from pJL2 (Li *et al.*, 1988) which contains the *hemB* gene under the control of its native promoter. Plasmid pHP1 was constructed from pUC18 by insertion of a 1.3 kb EcoRI- BamHI fragment isolated from pDS2 (Grossman *et al.*, 1987) which contains the *rpoH* gene under the control of the tac promoter. Plasmid pVHP1 was constructed from pHP1 by insertion of a 2.2 kb HindIII fragment isolated from pRED2 which contains the gene encoding VHb under

the control of its native promoter. Plasmids pVSP1, pVDP1, and pVHP1 were constructed by Pauli Kallio.

Media and growth conditions - Phosphate buffered LB medium supplemented with 100 μg/ml ampicillin was used as the basal medium in all cases. Capped side-arm shake flasks (300 ml; Belco) containing 50 ml medium were inoculated with 0.5 ml of overnight culture and shaken at 250 rpm in a rotary shaker (New Brunswick) at the indicated temperature. When the Klett absorbance of the culture reached 150, cells were harvested by centrifugation at the culture growth temperature and resuspended in pre-warmed fresh media to the same absorbance. The resulting stock culture was then divided into aliquots, placed in culture tubes (Kimax) to the indicated volume, and grown in a reciprocating water bath shaker (Reichert-Jung) at 150 cycles/min and the indicated temperature. For all cells investigated, a Klett absorbance cell density of 150 is obtained in shake flask cultivation during the later stage of exponential growth. Test tube cultures grown from colony inocula, however, only reach a cell density of 150 Klett units in late stationary phase, presumably due to oxygen transfer limitations. Consequently, culture tubes inoculated with stock culture having a cell density of 150 Klett units are considered microaerobic. Parallel analysis of culture tubes prepared without replenishing medium shows that cell harvest and resuspension steps involved in stock culture preparation are not detrimental to either cell growth or VHb production. For carbon source perturbations, the culture tubes were additionally supplemented to the indicated final concentration with glucose, lactose, glycerol or sucrose from a 50% stock solution. For heme intermediate perturbations, the culture tubes were additionally supplemented

with monosodium glutamate, levulinic acid, δ-aminolevulinic acid or ferric citrate to the indicated final concentration from a 1 M stock solution neutralized with ammonium hydroxide.

Cell harvesting and sample preparation - Following cultivation, culture density was determined and 3 ml samples were collected. Cells were isolated by centrifugation, washed with a buffer consisting of 100 mM Tris-HCl, 50 mM NaCl, 1 mM EDTA, 1 mM DTT and 0.1 mM PMSF, and resuspended in 1 ml of the same buffer. Cells were lysed by sonication on ice using a Heat Systems Ultrasonicator. Soluble and insoluble fractions were separated by centrifugation at 14,000 g for 5 min. Soluble fractions were assayed for soluble VHb content and insoluble fractions were immediately frozen. The protein from soluble fractions was then isolated by precipitation with 10% TCA and the resulting pellets were washed extensively with ethanol:ethyl ether (1:1). Resulting samples were stored at -70°C for electrophoretic analysis.

VHb determination - Soluble VHb was determined by visible absorption spectroscopy of soluble lysate fractions and SDS-PAGE. The Soret peak of VHb in these samples uniformly had its maximum at 415 nm indicating the protein was present in the oxygenated state (Orii and Webster, 1986). Baseline values, determined from analysis of the soluble lysate from various cells lacking the gene encoding VHb, range between 2.7 and 3.0 A(415)/Klett units. The plotted activity units are 10^4 times calculated activity units. Insoluble VHb was determined by SDS-PAGE.

Electrophoresis - SDS-PAGE was conducted using the BioRad Protein II

Multi Cell Electrophoresis system. Resolving gradient slab gels were composed from 10% - 20% acrylamide, 0.3% - 0.6% bisacrylamide, and 0.1% SDS and topped with a discontinuous buffer stacking gel (Laemmli, 1970). Pellets from soluble and insoluble fractions were resuspended in sample buffer to a constant biomass concentration. Gels were run at 32.5 mA/gel, 4°C for 6 hours and stained with Coomassie blue. VHb internal standard was included throughout to correct for variations in staining.

6.5 Results

The following studies were conducted in culture tubes to insure uniform microaerobic conditions necessary for controlled activation of the VHb promoter in large numbers of samples. Culture tubes were inoculated with moderate cell density stock culture as described under Materials and Methods. As all cells lacked VHb at the time of tube inoculation, the culture tube results shown represent the entire temporal accumulation phase of VHb in *E. coli* when expressed from its native promoter under microaerobic conditions. Cell growth and VHb accumulation was monitored for all strains over a 12 hour time period. For chemical perturbations, cells were grown for 6 hours in 5 ml volume, defined as the standard state, and compared to cells not treated with the perturbant.

Plasmid Vector

The type of plasmid used for the expression of recombinant proteins can have a large effect on growth, protein synthesis (Seo and Bailey, 1985) and metabolic activity. To examine this influence, we have investigated VHb inclusion body formation in JM101 carrying plasmids of different construction.

Plasmid pRED2 was derived from the high copy number plasmid pUC19 by insertion of the gene encoding VHb under the control of its native promoter. Plasmid pINT2 also carries the gene encoding VHb under the control of its native promoter but was derived from the moderate copy number plasmid pBR322.

The strain JM101:pRED2 accumulates soluble VHb fairly rapidly upon induction acquiring 75 percent of its final level within 3 hours. Insoluble VHb accumulates much more slowly and is not present 3 hours after induction as shown in Figure 2. The growth rate is fairly linear for the first 6 hours and decreases thereafter. Cultures of 3 ml volume grow faster, reach a higher final cell density and accumulate higher levels of both soluble and insoluble VHb than 5 ml cultures.

The strain JM101:pINT2 accumulates soluble VHb during the first 3 hours at approximately the same rate as JM101:pRED2. However, soluble VHb accumulation continues for a longer period of time such that much higher levels are obtained after 12 hours. This strain does not accumulate insoluble VHb as indicated in Figure 3. This strain also grows faster and to a significantly higher final cell density than does JM101:pRED2. Cultures of 3 ml volume grow faster and reach a higher final cell density than those of 5 ml; however, they accumulate lower levels of soluble VHb.

Results clearly show that plasmid construction dramatically effects VHb inclusion body formation. This effect, however, is only significant 3 hours after induction. As the two strains produce similar specific amounts of VHb prior to this time and are derived from the same host, the significantly lower growth rate of JM101:pRED2 indicates it is more burdened by plasmid maintenance.

This is consistent with earlier fed-batch fermentations showing significant growth inhibition of JM101:pUC19 relative to JM101 (Khosla and Bailey, 1988).

Temperature

Temperature has a profound effect on the stability of proteins with denaturation typically occurring above 50°C (Privalov, 1982). In the case of sperm whale apomyoglobin, maximum stability at physiological pH occurs at 30°C; denaturation occurs above 50°C (Griko *et al.*, 1988). While most proteins are stable below 50°C, the occurrence of the highly conserved heat shock response below this temperature (Craig, 1985) suggests lower temperatures may generally affect intracellular protein folding. Indeed, protein mutations which affect the thermal sensitivity of folding but do not affect thermal stability are known to occur (King, 1986). Temperature has previously been shown to be an important variable in inclusion body formation (Schein and Noteborn, 1988). The need to understand the influence of temperature on inclusion body formation is punctuated by the prevalent use of thermally inducible promoters. To investigate this influence we have examined VHb inclusion body formation in JM101:pRED2 and JM101:pINT2 grown and induced at 42°C.

Growth and soluble VHb accumulation in JM101:pRED2 at 42°C are comparable to that at 37°C for the first 3 hours. Thereafter, growth and soluble VHb accumulation at 42°C decrease (Figure 4) relative to these trajectories at 37°C. Interestingly, specific soluble VHb levels fall after 6 hours despite minimal growth. Insoluble VHb is accumulated earlier at 42°C than 37°C but not to higher final levels.

Growth and soluble VHb accumulation in JM101:pINT2 at 42°C (Figure 5) are comparable for the first 3 hours to culture behavior at 37°C. Thereafter, increases in cell density and soluble VHb are less than those at 37°C. JM101:pINT2 does not produce insoluble VHb at 37°C or 42°C. Results suggest that higher temperatures have little affect on the insolubilization of VHb but do affect the level of expression.

Supplementary Carbon Source

Metabolizable sugars are commonly supplemented to fed batch media to enhance recombinant protein accumulation during the production phase (Tsai, 1987). This is in part due to the high energy yield obtained through their catabolism (Stouthamer, 1973). We have investigated the effect of supplementing glucose, lactose, glycerol and sucrose at 0.5, 1.0, 1.5 and 2.0% concentrations on VHb inclusion body formation.

The VHb promoter is believed to have a CAP binding site and be susceptible to catabolite repression (Khosla and Bailey, 1989). Supplementation of glucose to JM101:pRED2 cultures has little effect on growth or soluble VHb accumulation. It does, however, significantly decrease the accumulation of insoluble VHb as shown in Figure 6. Interestingly, supplementation of glucose to JM101:pINT2 decreases the accumulation of soluble VHb to a level comparable to that of JM101:pRED2 (data not shown). The effect of glucose is approximately the same over the concentration range tested.

Supplemented glycerol, which can be metabolized by JM101:pRED2, has little effect on growth, soluble VHb accumulation and insoluble VHb accumu-

lation. Its addition, however, does elicit accumulation of a number of distinct cellular proteins which are also accumulated with glucose addition (Figure 6). These proteins are also accumulated in insoluble fractions of control strains which do not produce VHb. The small improvement in growth and VHb production seen with glycerol addition suggests cell metabolism is limited by oxygen rather than nutrient level in the basal medium. Supplemented lactose and sucrose have no effect on growth, soluble VHb accumulation, insoluble VHb accumulation or cellular protein content. These sugars cannot be metabolized by JM101:pRED2 and were included as controls to account for osmolarity or related effects (Bowden and Georgiou, 1988)

Chemical Perturbation of Heme Biosynthesis

Heme biosynthesis involves the condensation of 8 molecules of δ-aminolevulinic acid (ALA) to form the tetrapyrrole protoporphyrin IX. The structure of the heme biosynthetic pathway is very well conserved among the plant, animal, and protista kingdoms (Bogorad, 1979), and portions of the pathway are also utilized for vitamin B-12 and chlorophyll biosynthesis. The most notable difference in the pathway among different organisms occurs in the synthesis of ALA. *E. coli* synthesizes ALA by the C-5 pathway from the intact five carbon chain of glutamate (Li *et al.*, 1989b). The enzyme which catalyzes this transformation, ALA synthase, shows no amino acid homology with any other cloned ALA synthase (Li *et al.*, 1989c). Other facultative aerobic bacteria synthesize ALA by the C-4 pathway from succinyl coenzyme A and glycine (Li *et al*, 1989b). *Vitreoscilla* appears to utilize the C-4 pathway (Dikshit *et al.*, 1989).

The pathway for heme biosynthesis in *E. coli* is shown schematically in Figure 7 (Bogorad, 1979; Li *et al.*, 1989).

Under hypoxic conditions, *Vitreoscilla* synthesizes VHb polypeptide, NADH-methemoglobin reductase, and δ-aminolevulinic acid (ALA) synthase (Dikshit *et al.*, 1989). The increase in ALA synthase levels with VHb polypeptide synthesis presumably allows the heme biosynthetic pathway to respond to the greater demand for heme. Expression of VHb in *E. coli* leads to increased production of heme (Khosla and Bailey, 1988; Dikshit and Webster, 1988). It is not known if this is accomplished by derepression of heme synthesis or by an amplification of ALA synthase levels as occurs in *Vitreoscilla.* Previous studies on *E. coli* suggest ALA synthesis is the rate limiting step in the heme biosynthetic pathway (Ishida and Hino, 1972; Hino and Ishida, 1973). Upon alleviating the limitation in ALA synthesis, the new limiting step is believed to lie at porphobilinogen (PBG) synthesis (personal communication, Dr. Alexander Sassarman). ALA Dehydratase, the enzyme responsible for this latter conversion, is competitively inhibited by levulinic acid (Li *et al.*, 1988). To examine the influence of heme biosynthesis on VHb insolubilization in *E. coli*, we conducted titration experiments on the strain JM101:pRED2 with glutamate, ALA, levulinic acid, and ferric citrate.

Glutamate was previously shown to effect VHb synthesis in *Vitreoscilla* (Lamba and Webster, 1980). Supplementing glutamate to JM101:pRED2 cultures, however, has no effect on growth, soluble VHb accumulation, or insoluble VHb accumulation as shown in Figure 8. In this basal medium, glutamate is the most prevalent carbon source available prior to supplementation (Difco

Laboratories, 1953). The basal level of glutamate in the medium used for the *Vitreoscilla* studies is unknown.

Iron concentration was also previously shown to effect VHb synthesis in *Vitreoscilla* (Lamba and Webster, 1980). We have used ferric citrate as an iron supplement as its uptake pathway is well understood (Van Hove *et al.*, 1990). Ferric citrate addition has no effect on growth or soluble VHb accumulation as shown in Figure 9. It does, however, decrease insoluble VHb accumulation monotonically when supplemented at concentrations in excess of 0.8 mM. The basal medium contains approximately 40 μM iron and the total iron required to meet VHb stoichiometric requirements under these conditions is approximately 5 μM iron. Given this, it is likely that ferric citrate addition at these much greater levels reduces insoluble VHb accumulation by affecting VHb synthesis. Such a perturbation is possible given the importance of the citric acid cycle in cellular metabolism.

To determine whether a reduction in heme biosynthesis would lead to greater VHb insolubilization, we titrated JM101:pRED2 cultures with levulinic acid, a competitive inhibitor of ALA dehydratase. Supplementation of levulinic acid does not effect the growth of JM101:pRED2 as shown in Figure 10. A monotonic decrease is observed, however, in the level of soluble VHb accumulated when the concentration of levulinic acid exceeds of 10 mM. The level of insoluble VHb accumulated under these conditions increases in apparent proportion. A concentration of 5 mM levulinic acid is commonly used for ALA dehydratase inhibition in cell extracts from *E. coli* (Li *et al.*, 1989b)

If heme biosynthesis in JM101:pRED2 is limited by the synthesis of ALA,

supplementing this intermediate should increase flux. ALA supplementation has previously been shown to increase heme biosynthesis in anaerobically or aerobically grown *E. coli* when incubated under aerobic conditions (Ishida and Hino, 1972). ALA addition has no effect on the growth of JM101:pRED2 as shown in Figure 11. At concentrations below 10 mM, ALA addition leads to an increase in the level of soluble VHb accumulated and an apparent proportional decrease in the accumulation of insoluble VHb. At concentrations above 10 mM, however, ALA appears inhibitory to VHb production as the accumulation levels of both soluble and insoluble VHb decrease.

Genetic Perturbation of Heme Biosynthesis

To further investigate the importance of heme biosynthesis in VHb inclusion body formation, we have inserted the genes for ALA Synthase and ALA Dehydratase separately into the plasmid pRED2. Expression of the heme biosynthetic enzymes is controlled by their respective native promoters.

The strain JM101:pVSP1 contains a plasmid derived from pRED2 encoding both VHb and ALA synthase. This strain produces dramatically greater quantities of insoluble VHb than does JM101:pRED2 as shown in Figure 12. The level of soluble VHb produced, as indicated by activity measurements, reaches its maximum within 3 hours. This maximum is approximately 30% of the maximum reached by JM101:pRED2. Interestingly, the level of soluble VHb produced, as indicated by electrophoresis, is much greater and falls after 3 hours. Also, in the electrophoresis results, the increase in insoluble VHb levels occurring after 3 hours appears proportional to the decrease in soluble VHb levels. These results

suggest that some of the soluble VHb produced in the initial 3 hours following induction is apo VHb and this protein is either degraded or insolubilized over subsequent hours.

The strain JM101:pVDP1 contains a plasmid derived from pRED2 which encodes both VHb and ALA dehydratase. This strain produces dramatically less soluble and insoluble VHb than JM101:pRED2 as shown in Figure 13. Levulinic acid supplementation does not affect the growth of this strain or its accumulation of soluble or insoluble VHb as shown in Figure 14. ALA supplementation at concentrations in excess of 10 mM, however, appears to inhibit VHb production in this strain as shown in Figure 15. This effect was also seen with JM101:pRED2.

Genetic Perturbation of Chaperone Protein Levels

The heat shock proteins hsp60 and hsp70, represented in *E. coli* by GroEL and DnaK, respectively, have been implicated in the intracellular folding of proteins (Gatenby *et al*, 1990). Enhanced expression of GroEL has been shown to reduce ribulose-bisphosphate carboxylase inclusion body formation in *E. coli* (Goloubinoff *el al.*, 1989). The intracellular levels of GroEL and DnaK are increased during heat shock through the action of the protein σ^{32} (Grossman *et al.*, 1987). Enhanced expression of σ^{32} has been shown to elicit the heat shock response at low temperature (Grossman *et al.*, 1987). We have enhanced the levels of the chaperone proteins GroEL and DnaK by inserting a fusion of the *tac* promoter and the *rpoH* gene, which encodes σ^{32}, into the plasmid pRED2.

The strain JM101:pVHP1 carries a plasmid similar to pRED2 which encodes

both VHb and σ^{32}. This strain produces dramatically greater levels of insoluble VHb than does JM101:pRED2 whether or not IPTG is added to the medium (Figures 16 and 17). Comparison of VHb activity results and electrophoretic results again suggests some soluble apoVHb is produced early in the cultivation which is subsequently degraded or insolubilized.

6.6 Discussion

A number of experimental results agree with trends expected based on the folding and aggregation model depicted in Figure 1. The strain JM101:pRED2 does produce less insoluble VHb with lower-level expression. This is apparent through perturbations with glucose and ferric citrate where, in each case, reduced inclusion body formation coincided with reduced total VHb accumulation. The same result was seen with studies using 1 ml culture to increase aeration and, consequently, reduce VHb expression (data not shown). The level of VHb inclusion body formation in JM101:pRED2 can also be modulated through chemical perturbation of heme biosynthesis. Titrations with ALA and levulinic acid reduced and increased inclusion body formation, respectively, without changing total VHb accumulation.

Other results do not agree with the model. In particular, total VHb accumulation in the the strain JM101:pINT2 is comparable to that in the strain JM101:pRED2 yet JM101:pINT2 does not produce inclusion bodies. This result suggests that the increased burden placed on the cell for maintenance of the plasmid pRED2, evidenced by the lower growth rate, is influencing VHb aggregation.

The results from chemical perturbations suggest one approach to increasing soluble VHb accumulation under high-expression conditions may be enhancement of heme biosynthesis. There are two mechanisms by which heme amplification may act to increase soluble VHb accumulation. First, the root cause of VHb insolubilization may be a limitation in heme availability. Such a mechanism is plausible given the observation that inclusion body VHb bears conformational similarity to apoVHb (Hart and Bailey, 1991a). Additionally, it is not clear whether the coupling between ALA synthase expression and VHb expression which exists in *Vitreoscilla* is present in *E. coli*. Second, heme may act as a template for VHb folding *in vivo* and consequently "rescue" VHb which would otherwise be insolubilized.

Some comments concerning leghemoglobin biosynthesis are of interest regarding the first of these mechanisms. Leghemoglobin has the closest amino acid sequence homology to VHb of known globins (Wakabayashi *et al*, 1986). Leghemoglobin production is a symbiotic process as globin polypeptide is produced by legume root nodules, and its heme prosthetic group is produced by the legumes symbiont *Rhizobium* (O'Brian *et al.*, 1987). Legume root nodules will synthesize apoleghemoglobin in the absence of bacterial heme synthesis (O'Brian *et al.*, 1987).

Genetic amplification of ALA synthase and ALA dehydratase levels did not increase soluble VHb accumulation. Genetic modulation of the heme biosynthetic pathway was expected to be difficult as it is not only complex but also tightly regulated at the protein level.

The finding that overexpression of chaperone proteins may reduce inclusion

body formation has prompted suggestion that these proteins may be a general solution to inclusion body formation (Goloubinoff *et al.*, 1989). At this time, it is unclear whether this approach to reducing inclusion body formation will be generally effective (Gatenby *et al.*, 1990). We have constructed a plasmid bearing both *rpoH* and the gene encoding VHb to investigate the influence of chaperone protein levels on VHb insolubilization. The only difference between the resulting strain and JM101:pRED2 is the increased *rpoH* gene dosage. This strain shows enhanced expression of two proteins found only in the soluble fraction. The molecular weights of these proteins are the same as those of the heat shock proteins GroEL and DnaK. Comparison of the protein pattern of this strain with that of JM101 following heat shock supports this assignment. Interestingly, this strain produces greater amounts of insoluble VHb than JM101:pRED2. The increased insolubilization of VHb may be due to changes in the regulation of expression or simply the nature of the plasmid construct. In any case, enhanced levels of GroEL and DnaK clearly do not reduce VHb insolubilization.

Some comments regarding the validity of perturbation-response experiment interpretation are appropriate. The chemical supplements investigated lead to small changes in the relative levels of soluble and insoluble VHb while not apparently influencing cell growth or protein composition. That is, these agents constitute a small perturbation and elicit a small response. From an analytical point of view this is desired as it simplifies the assignment of cause and effect. Genetic alterations, however, can clearly elicit large perturbations and make causal assignment vastly more difficult. The VHb accumulation behavior of the strain JM101:pVDP1, for example, is dramatically different from all other

strains discussed. Results from test tube cultivations and shake flask cultivations suggest that this genetic alteration may affect regulation of the VHb promoter. It is possible that similar effects are manifest with the strains JM101:pVSP1 and JM101:pVHP1.

6.7 Acknowledgements

This research was supported by the National Science Foundation (Grant No. EET-8606179) and by a grant for predoctoral training in biotechnology from the National Institute of General Medical Sciences (National Research Service Award 1 T32 GM 08346-01, Pharmacology Sciences Program).

6.8 References

1. Bogorad, L. (1979) in *The Porphyrins* (Dolphin, D., ed) Vol. 6, pp. 125 - 178, Academic Press

2. Bolivar, F., *et al.* (1977) *Gene* **2**, 95 - 113

3. Bowden, G. A., and Georgiou, G. (1988) *Biotech. Progress* **4**, 97 - 101

4. Craig, E. A. (1985) *CRC Crit. Rev. Biochem.* **18**, 239 - 280

5. Difco Laboratories (1953) Difco Manual, 9th edition, Difco Laboratories, Detroit MI

6. Dikshit, K. L., and Webster, D. A. (1988) *Gene* **70**, 377-386

7. Dikshit, K. L., Spaulding, D., Braun, A., and Webster, D. A. (1989) *J. Gen. Micro.* **135**, 2601 - 2609

8. Dikshit, K. L., Dikshit, R. P., and Webster, D. A. (1990) *Nucl. Acids Res.* **18**, 4149 - 4155

9. Gatenby, A. A., Viitanen, P. V., and Lorimar, G. H. (1990) *Trend Biotech* **8**, 354 - 358

10. Goloubinoff, P., Gatenby, A. A., and Lorimar, G. H. (1989) *Nature* **337**, 44 -47

11. Griko, Y. V., Privalov, P. L., Venyaminov, S. Y. (1988) *J. Mol. Biol.* **202**, 127 - 138

12. Grossman, A. D., Straus, D. B., Walter, W. A., and Gross, C. A. (1987) *Genes Dev.* **1**, 179 - 184

13. Hart, R. A., Rinas, U., and Bailey, J. E. (1990) *J. Biol. Chem.* **265**, 12728 - 12733

14. Hart, R. A., and Bailey, J. E. (1991a) Material in Chapter 4.

15. Hart, R. A., and Bailey, J. E. (1991b) Material in Chapter 5.

16. Hartl, F., Pfanner, N., Nicholson, D. W., Neupert, W. (1989) *Biochim. Biophys. Acta* **988**, 1 - 45

17. Hino, S., and Ishida, A. (1973) *Enzyme* **16**, 42 - 49

18. Hoffman, S. J., Looker, D. L., Roehrich, J. M., Cozart, P. E., Durfee, S. L., Tedesco, J. L., and Stetler, G. L. (1990) *Proc. Natl. Acad. Sci. USA* **87**, 8521 - 8525

19. Ishida, A., and Hino, S. (1972) *J. Gen. Appl. Microbiol.* **18**, 225 - 237

20. Kane, J. F., and Hartley, D. L. (1988) *Trend Biotech* **6**, 95 - 101

21. Khosla, C., and Bailey, J. E. (1989) *J. Bacteriol.* **171**, 5995 - 6004

22. Khosla, C., and Bailey, J. E. (1988) *Nature* **331**, 633 - 635

23. King, J. (1989) *Chem. Eng. News* **67**, 32 - 54

24. King, J. (1986) *Bio/Technology* **4**, 297 - 303

25. Kitano, K., Nakao, M., Itoh, Y., and Fujisawa, Y. (1987a) *Bio/Technology* **5**, 281 - 283

26. Kitano, K., Fujimoto, S., Nakao, M., Watanabe, T., and Nakao, Y. (1987b) *J. Biotechnol.* **5**, 77 - 86

27. Krueger, J. K., Stock, A. M., Schutt, C. E., and Stock, J. B. (1990) in *Protein Folding. Deciphering the Second Half of the Genetic Code* (Gierasch, L. M., King, J., ed.), American Association for the Advancement of Science, Washington DC

28. Lamba, P., and Webster, D. A. (1980) *J. Bacteriol.* **142**, 169 - 173

29. Li, J-M., Umanoff, H., Proenca, R., Russell, C. S., and Cosley, S. D. (1988) *J. Bacteriol.* **170**, 1021 - 1025

30. Li, J-M., Russell, C. S., and Cosley, S. D. (1989a) *Gene* **82**, 209 - 217

31. Li, J-M., Brathwaite, O., Cosloy, S. D., and Russell, C. S. (1989b) *J. Bacteriol.* **171**, 2547 - 2552

32. Li, J-M., Russell, C. S., and Cosley, S. D. (1989c) *Gene* **75**, 177 - 184

33. Mitraki, A., and King, J. (1989) *Bio/Technology* **7**, 690 - 697

34. O'Brian, M. R., Kirshbom, P. M., and Maier, R. J. (1987) *Proc. Natl. Acad. Sci. USA* **84**, 8390 - 8393

35. Orii, Y., and Webster, D. A. (1986) *J. Biol. Chem.* **261**, 3544 - 3547

36. Privalov, P. L. (1982) *Advan. Prot. Chem.* **35**, 1 - 104

37. Sano, S. (1979) in *The Porphyrins* (Dolphin, D., ed) Vol. 7, pp. 377 - 402, Academic Press

38. Seo, J-H, and Bailey, J. E. (1985) *Biotech. Bioeng.* **27**, 1668 - 1674

39. Schein, C. H., and Noteborn, M. H. (1988) *Bio/Technology* **6**, 291 - 294

40. Schein, C. H. (1989) *Bio/Technology* **7**, 1141 - 1149

41. Stouthamer, A. H. (1973) *Antonie van Leeuwenhoek* **39**, 545 - 565

42. Tsai, L. (1987) *Ind. Microbiol* **2**, 181 - 187

43. Van Hove, B., Staudenmaier, H., and Braun, V. (1990) **172**, 6749 - 6758

44. Wakabayashi, S., Matsubara, H., Webster, D. A. (1986) *Nature* **322**, 481 - 483

45. Wang, L-F., Hum, W. T., Kalyan, N. K., Lee, S. G., Hung, P. P., and Doi, R. H. (1989) *Gene* **84**, 127 - 133

46. Yanisch-Perron, C., Viera, J., and Messing, J. (1985) *Gene* **33**, 103 - 119

47. Zettlmeissl, G., Rudolph, R., and Jaenicke, R. (1979) *Biochemistry* **18**, 5567 - 5575

6.9 Figures

Figure 1: Model of VHb inclusion body formation process.

Figure 2: JM101:pRED2 grown at 37°C in buffered LB medium. (a) Biomass-normalized soluble VHb activity accumulation in 3 ml (open) and 5 ml (filled) cultures. (b) Biomass accumulation in 3 ml (open) and 5 ml (filled) cultures. (c) SDS-PAGE analysis of soluble (lanes 3, 5, 7, 9, 11 and 13) and insoluble (lanes 4, 6, 8, 10, 12 and 14) lysate fractions of 3 ml (lanes 3 - 8) and 5 ml (lanes 9 - 14) cultures collected 3 hours (lanes 3, 4, 9 and 10), 6 hours (lanes 5, 6, 11 and 12) and 12 hours (lanes 7, 8, 13 and 14) post-induction. Molecular weight markers (lane 1; 94, 67, 43, 30, 20.1 and 14.4 kDa) and purified VHb (lane 2) are shown for internal reference.

Figure 3: JM101:pINT2 grown at 37°C in buffered LB medium. See Figure 2 caption for details.

Figure 4: JM101:pRED2 grown at 42°C in buffered LB medium. See Figure 2 caption for details.

Figure 5: JM101:pINT2 grown at 42°C in buffered LB medium. See Figure 2 caption for details.

Figure 6: JM101:pRED2 grown at 37°C for 6 hours in 5 ml buffered LB medium supplemented with 2% (w/w) sugar. (a) Biomass-normalized soluble VHb activity accumulated. (b) Biomass accumulated. (c) SDS-PAGE of soluble (lanes 3, 5, 7, 9 and 11) and insoluble (lanes 4, 6, 8, 10 and 12) lysate fractions of cells grown in buffered LB (lanes 3 and 4)

supplemented with glucose (lanes 5 and 6), lactose (lanes 7 and 8), glycerol (lanes 9 and 10) or sucrose (lanes 11 and 12).

Figure 7: Schematic of *E. coli* heme biosynthetic pathway.

Figure 8: JM101:pRED2 grown at 37°C for 6 hours in 5 ml buffered LB medium containing supplemented glutamate. (a) Biomass-normalized soluble VHb activity accumulated as a function of supplemented glutamate concentration. (b) Biomass accumulated as a function of supplemented glutamate concentration. (c) SDS-PAGE of soluble (lanes 3, 5, 7, 9, 11, 13, 15, 17 and 19) and insoluble (lanes 4, 6, 8, 10, 12, 14, 16, 18 and 20) lysate fractions of cells grown in buffered LB medium (lanes 3 and 4) supplemented with 2 mM (lanes 5 and 6), 4 mM (lanes 7 and 8), 8 mM (lanes 9 and 10), 10 mM (lanes 11 and 12), 20 mM (lanes 13 and 14), 40 mM (lanes 15 and 16), 80 mM (lanes 17 and 18) and 100 mM (lanes 19 and 20) glutamate.

Figure 9: JM101:pRED2 grown at 37°C for 6 hours in 5 ml of buffered LB containing supplemented ferric citrate. Details differ from those in Figure 8 caption only in that 10 fold lower concentrations were used.

Figure 10: JM101:pRED2 grown at 37°C for 6 hours in 5 ml of buffered LB containing supplemented levulinic acid. See Figure 8 caption for details.

Figure 11: JM101:pRED2 grown at 37°C for 6 hours in 5 ml of buffered LB containing supplemented ALA. See Figure 8 caption for details.

Figure 12: JM101:pVSP1 grown at 37°C in buffered LB medium. See Figure 2 caption for details.

Figure 13: JM101:pVDP1 grown at 37°C in buffered LB medium. See Figure 2 caption for details.

Figure 14: JM101:pVDP1 grown at 37°C for 6 hours in 5 ml of buffered LB medium containing supplemented levulinic acid. (a) Biomass-normalized soluble VHb activity accumulated as a function of supplemented levulinic acid concentration. (b) Biomass accumulated as a function of supplemented levulinic acid concentration. (c) SDS-PAGE of soluble (lanes 3, 5, 7, 9 and 11) and insoluble (lanes 4, 6, 8, 10 and 12) lysate fractions of cells grown in buffered LB medium (lanes 3 and 4) supplemented with 20 mM (lanes 5 and 6), 40 mM (lanes 7 and 8), 80 mM (lanes 9 and 10) and 100 mM (lanes 11 and 12) levulinic acid.

Figure 15: JM101:pVDP1 grown at 37°C for 6 hours in 5 ml of buffered LB medium containing supplemented ALA. See Figure 14 caption for details.

Figure 16: JM101:pVHP1 grown at 37°C in buffered LB medium. See Figure 2 caption for details.

Figure 17: JM101:pVHP1 grown at 37°C in buffered LB medium containing 1 mM IPTG. See Figure 2 caption for details.

Figure 1.

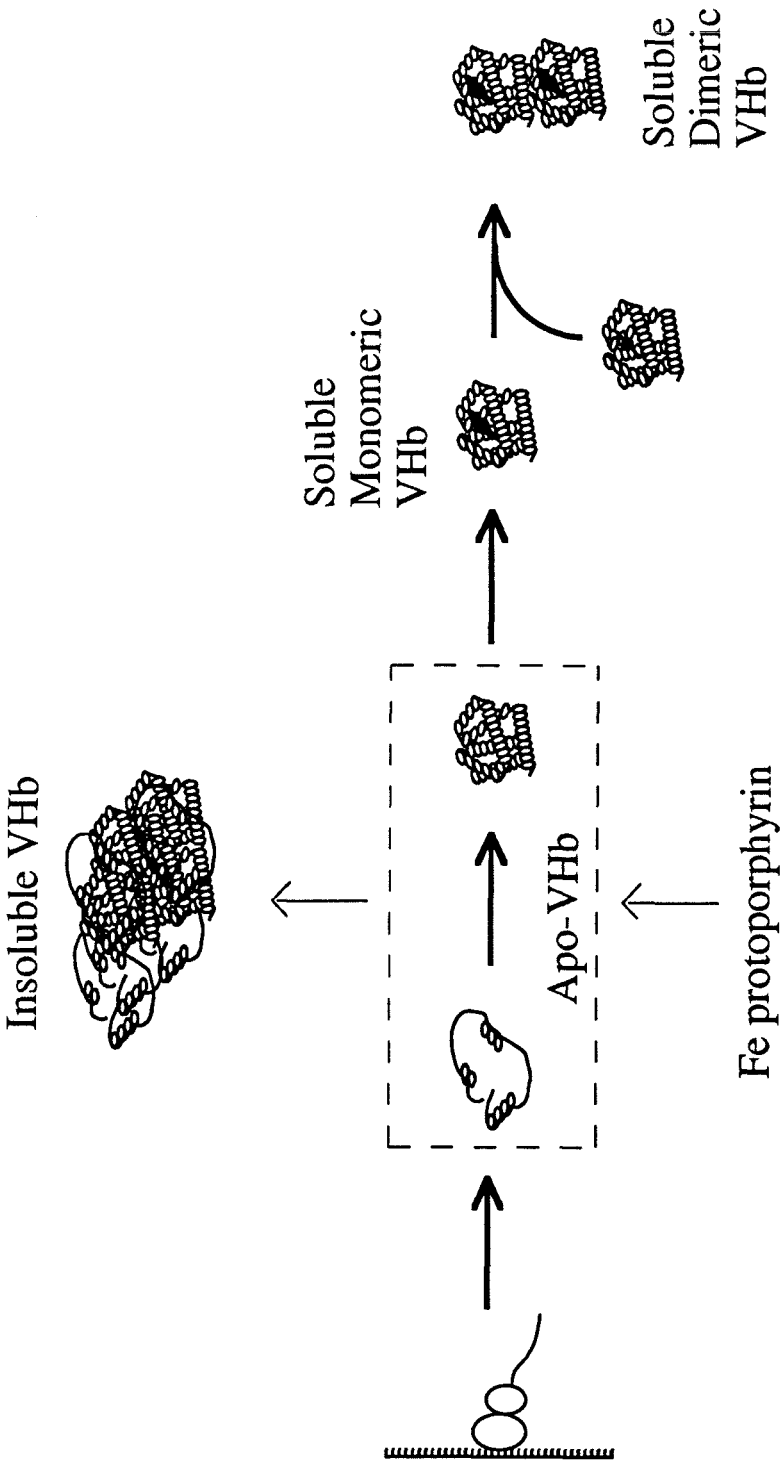
Soluble Dimeric VHb
Soluble Monomeric VHb
Insoluble VHb
Apo-VHb
Fe protoporphyrin

Figure 2.

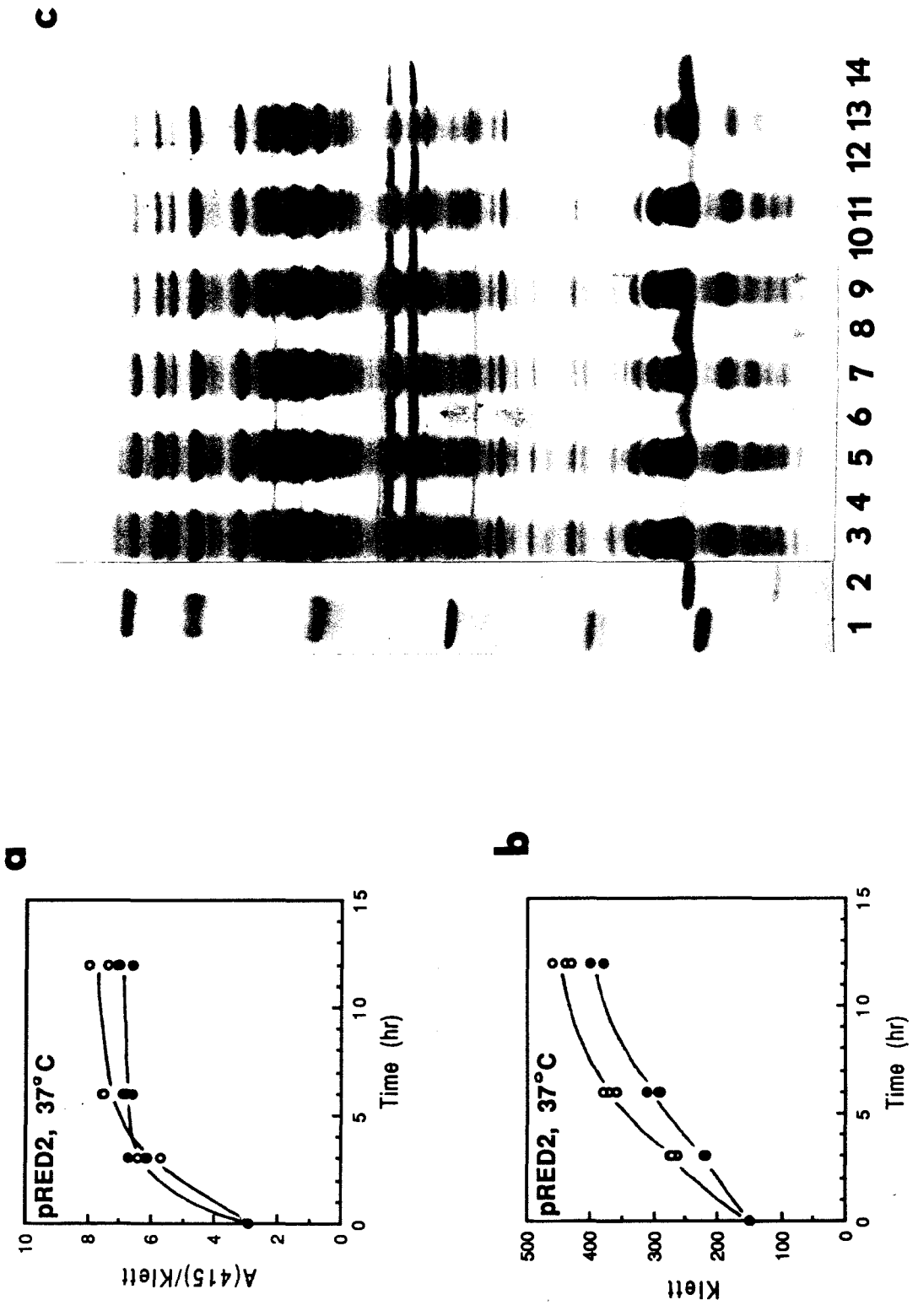
a
pRED2, 37°C
A(415)/Klett
Time (hr)
b
pRED2, 37°C
Klett
Time (hr)
c
1 2 3 4 5 6 7 8 9 10 11 12 13 14

Figure 3.

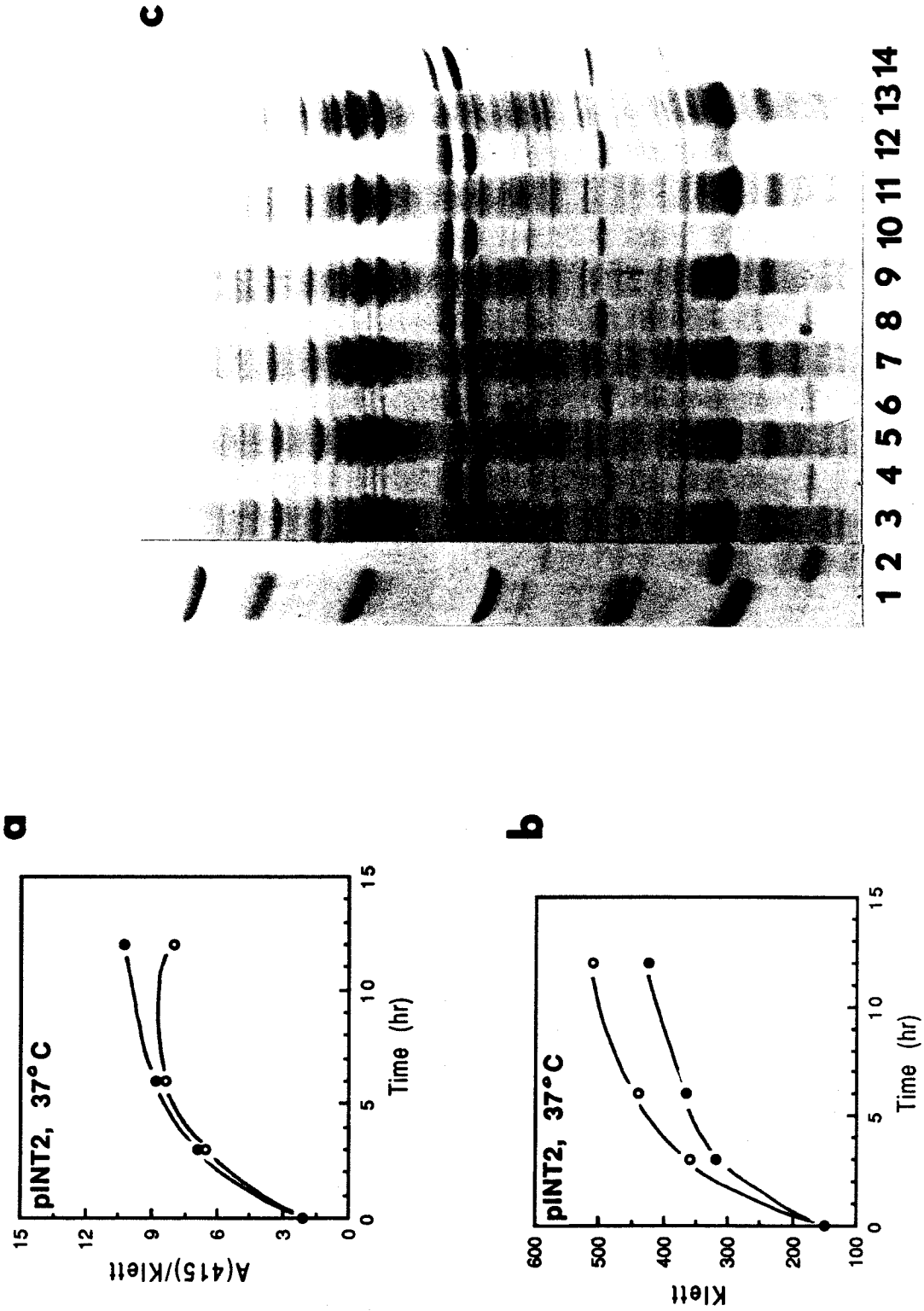
c
1 2 3 4 5 6 7 8 9 10 11 12 13 14
a
pINT2, 37°C
A(415)/Klett
Time (hr)
b
pINT2, 37°C
Klett
Time (hr)

Figure 4.

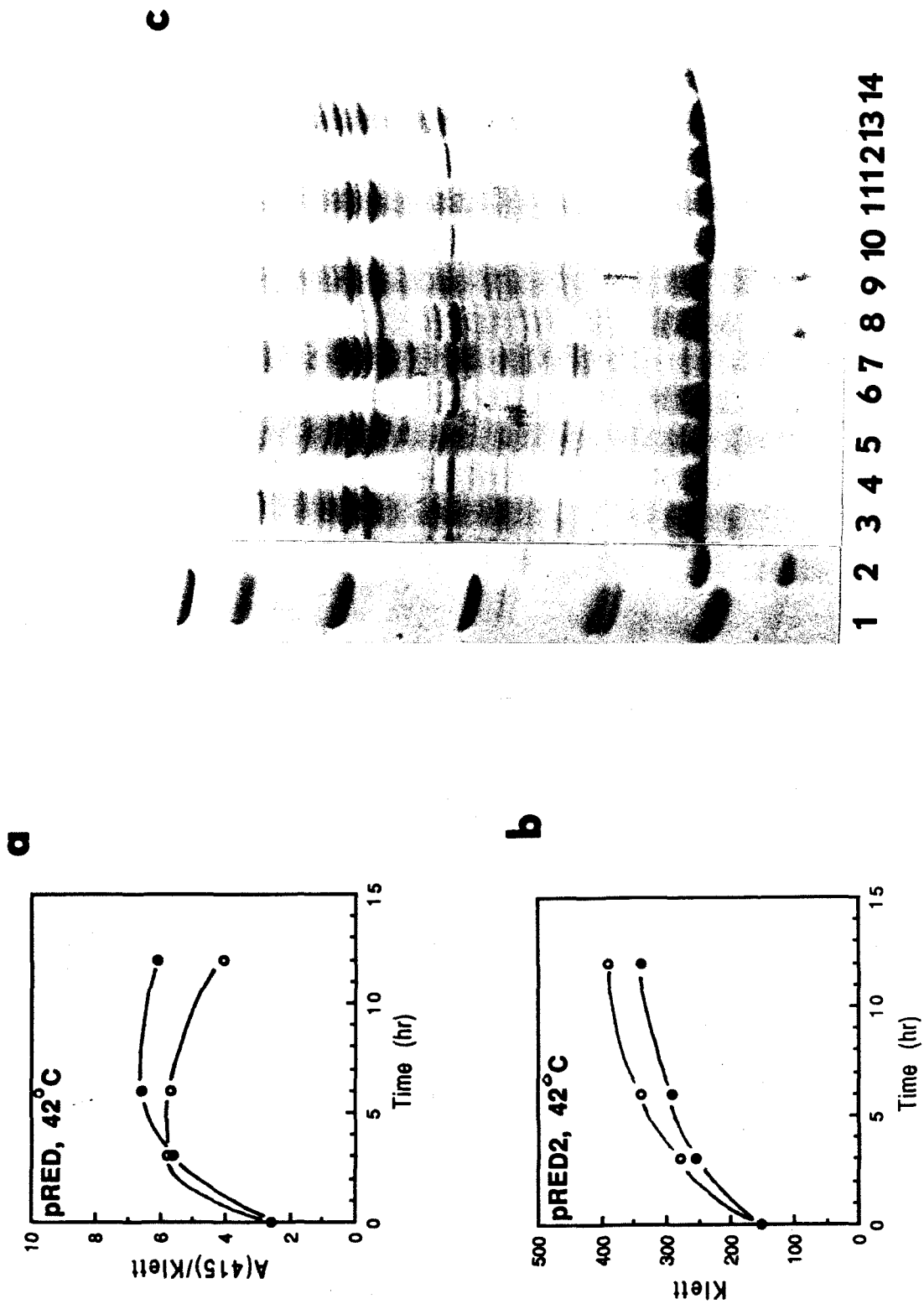
c
1 2 3 4 5 6 7 8 9 10 11 12 13 14
a
pRED, 42°C
A(415)/Klett
Time (hr)
b
pRED2, 42°C
Klett
Time (hr)

Figure 5.

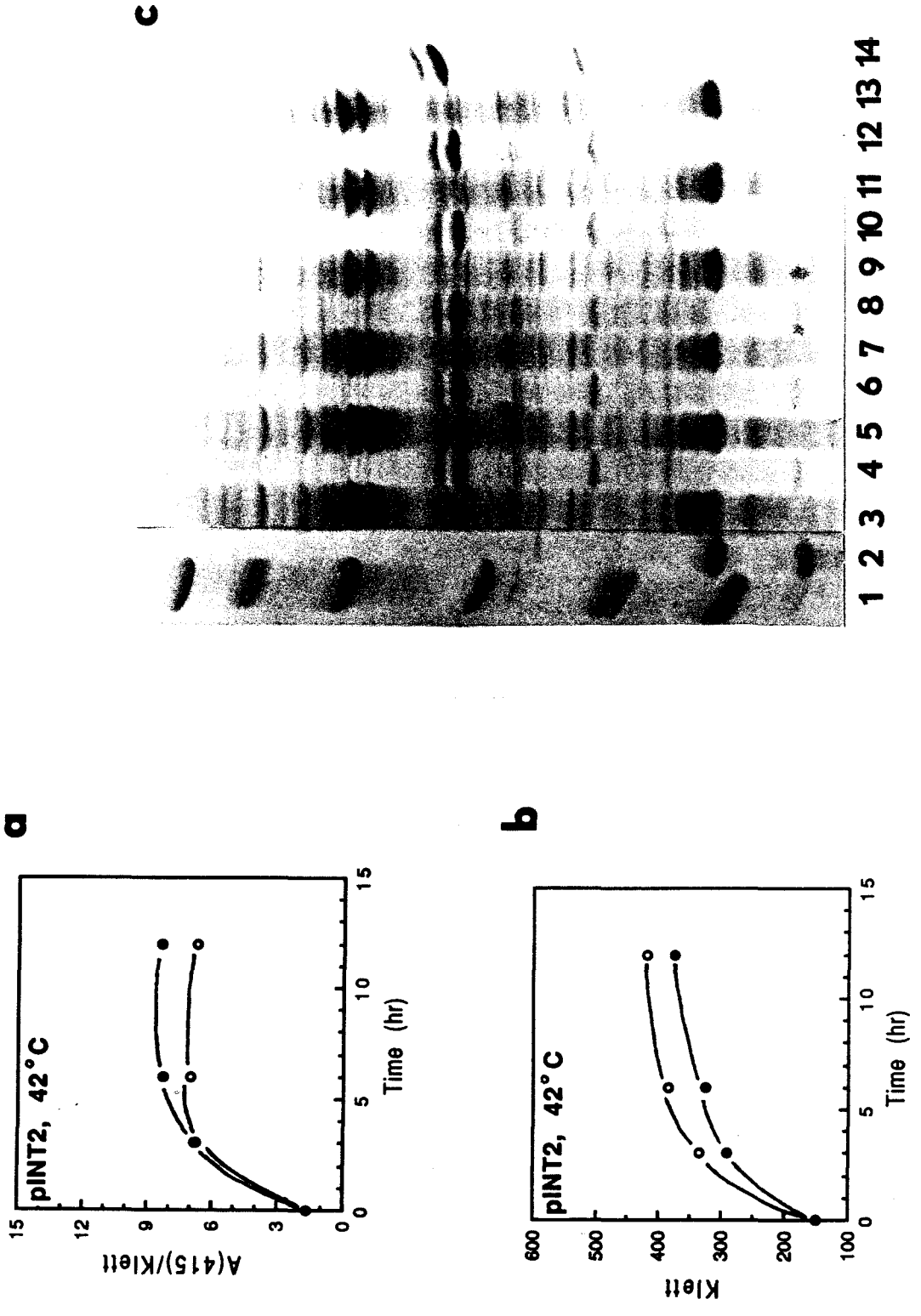
c
1 2 3 4 5 6 7 8 9 10 11 12 13 14
a
pINT2, 42°C
A(415)/Klett
Time (hr)
b
pINT2, 42°C
Klett
Time (hr)

Figure 6.

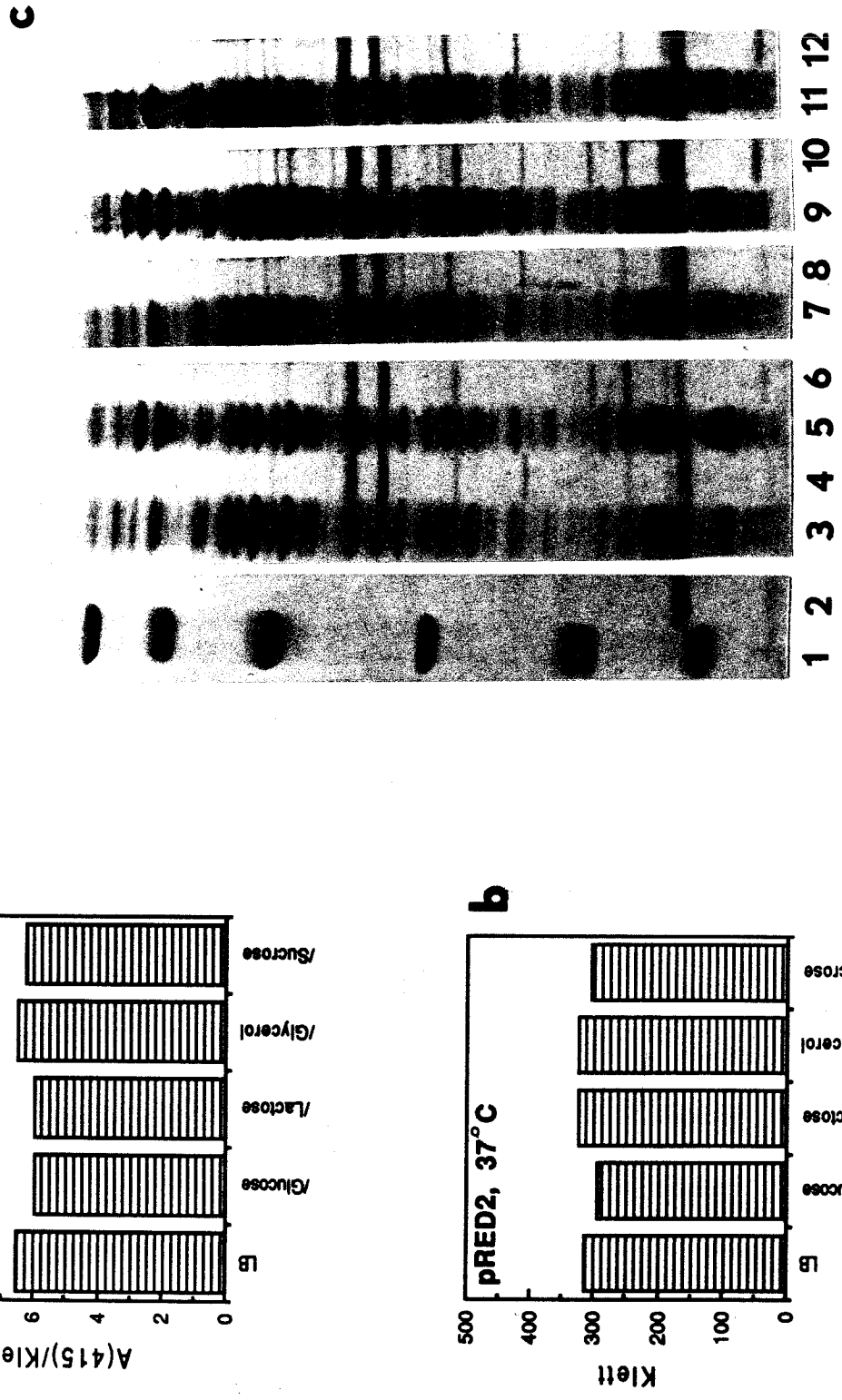
c
1 2 3 4 5 6 7 8 9 10 11 12
a
pRED2, 37°C
A(415)/Klett
0 2 4 6 8 10
LB
/Glucose
/Lactose
/Glycerol
/Sucrose
b
pRED2, 37°C
Klett
0 100 200 300 400 500
LB
/Glucose
/Lactose
/Glycerol
/Sucrose

Figure 7.

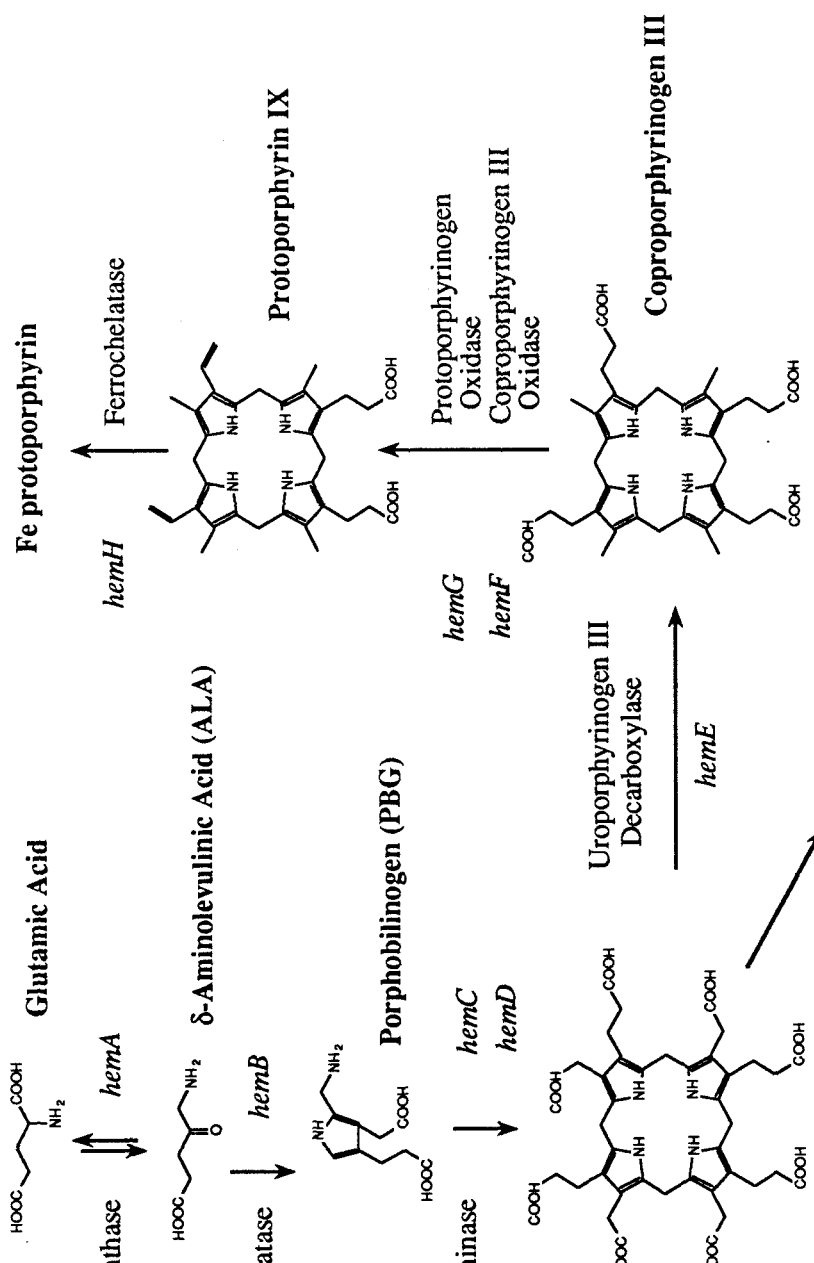
Glutamic Acid
Ala Synthase
hemA
δ-Aminolevulinic Acid (ALA)
ALA Dehydratase
hemB
Porphobilinogen (PBG)
Porphobilinogen Deaminase
Uroporphyrinogen III Cosynthase
hemC
hemD
Uroporphyrinogen III
Uroporphyrinogen III Decarboxylase
hemE
Coproporphyrinogen III
Protoporphyrinogen Oxidase
Coproporphyrinogen III Oxidase
hemG
hemF
Protoporphyrin IX
Ferrochelatase
hemH
Fe protoporphyrin
Vitamin B12

Figure 8.

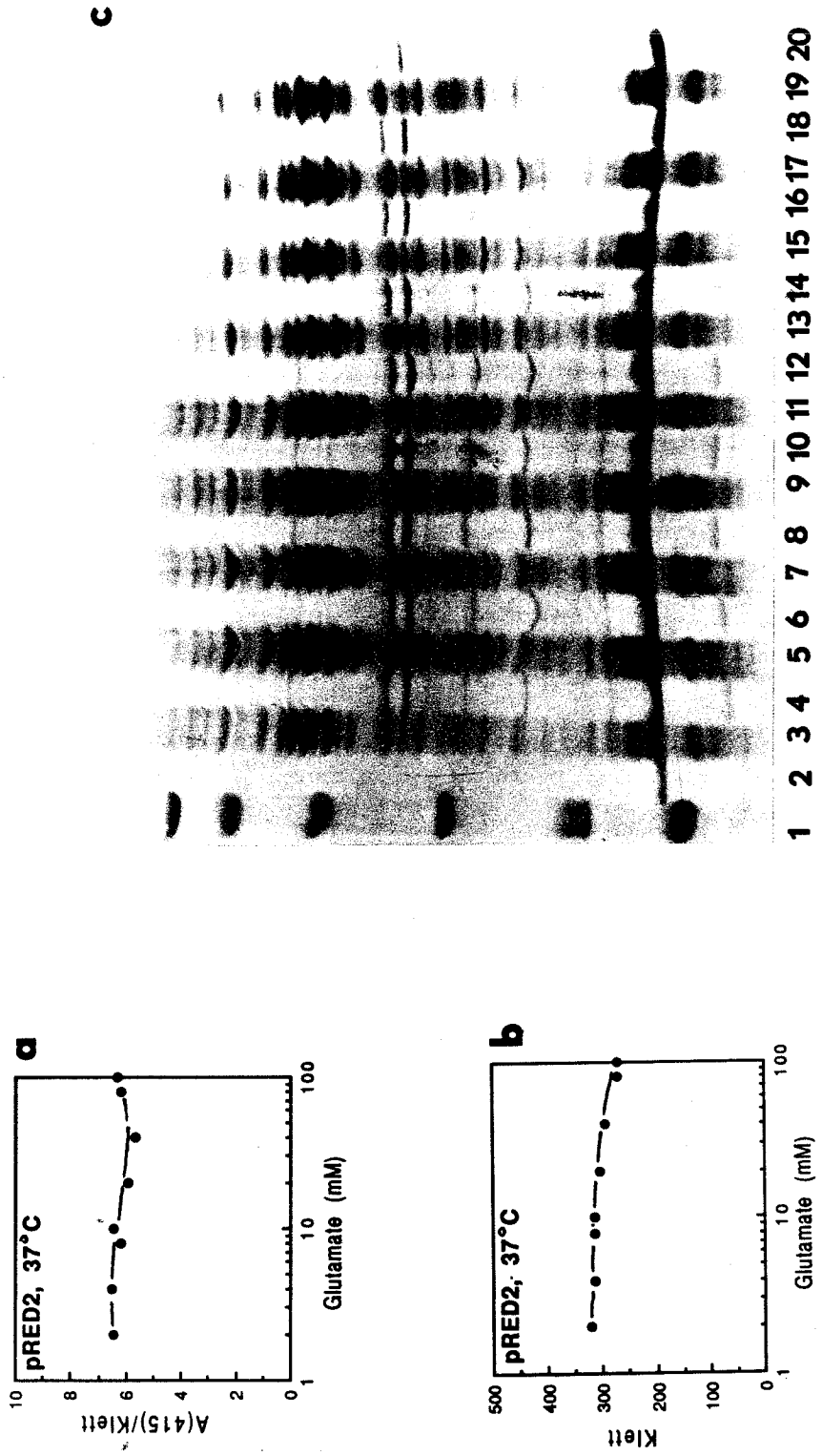
c
1 2 3 4 5 6 7 8 9 10 11 12 13 14 15 16 17 18 19 20
a
pRED2, 37°C
A(415)/Klett
Glutamate (mM)
b
pRED2, 37°C
Klett
Glutamate (mM)

Figure 9.

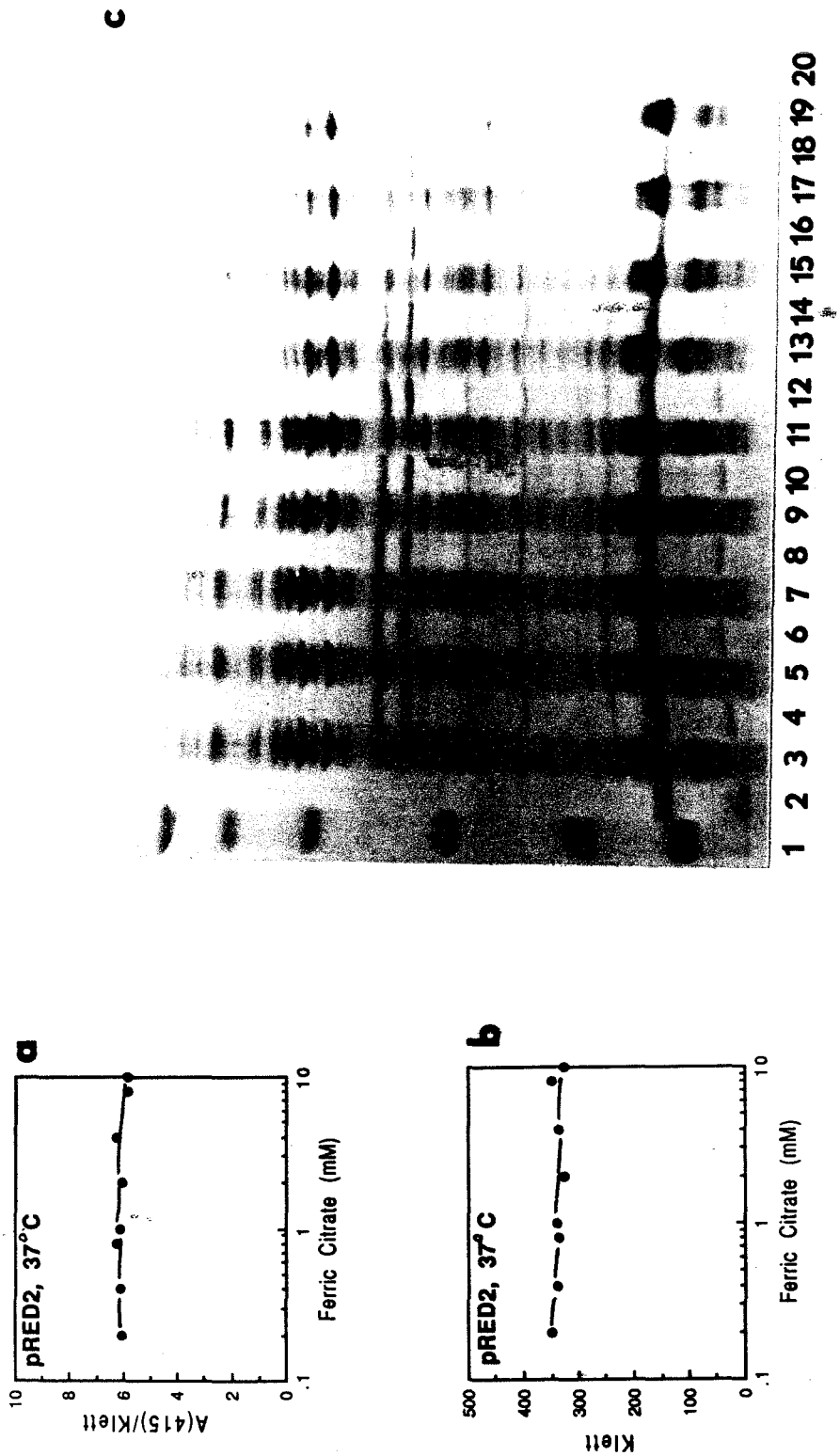
c
1 2 3 4 5 6 7 8 9 10 11 12 13 14 15 16 17 18 19 20
a
pRED2, 37°C
A(415)/Klett
Ferric Citrate (mM)
b
pRED2, 37°C
Klett
Ferric Citrate (mM)

Figure 10.

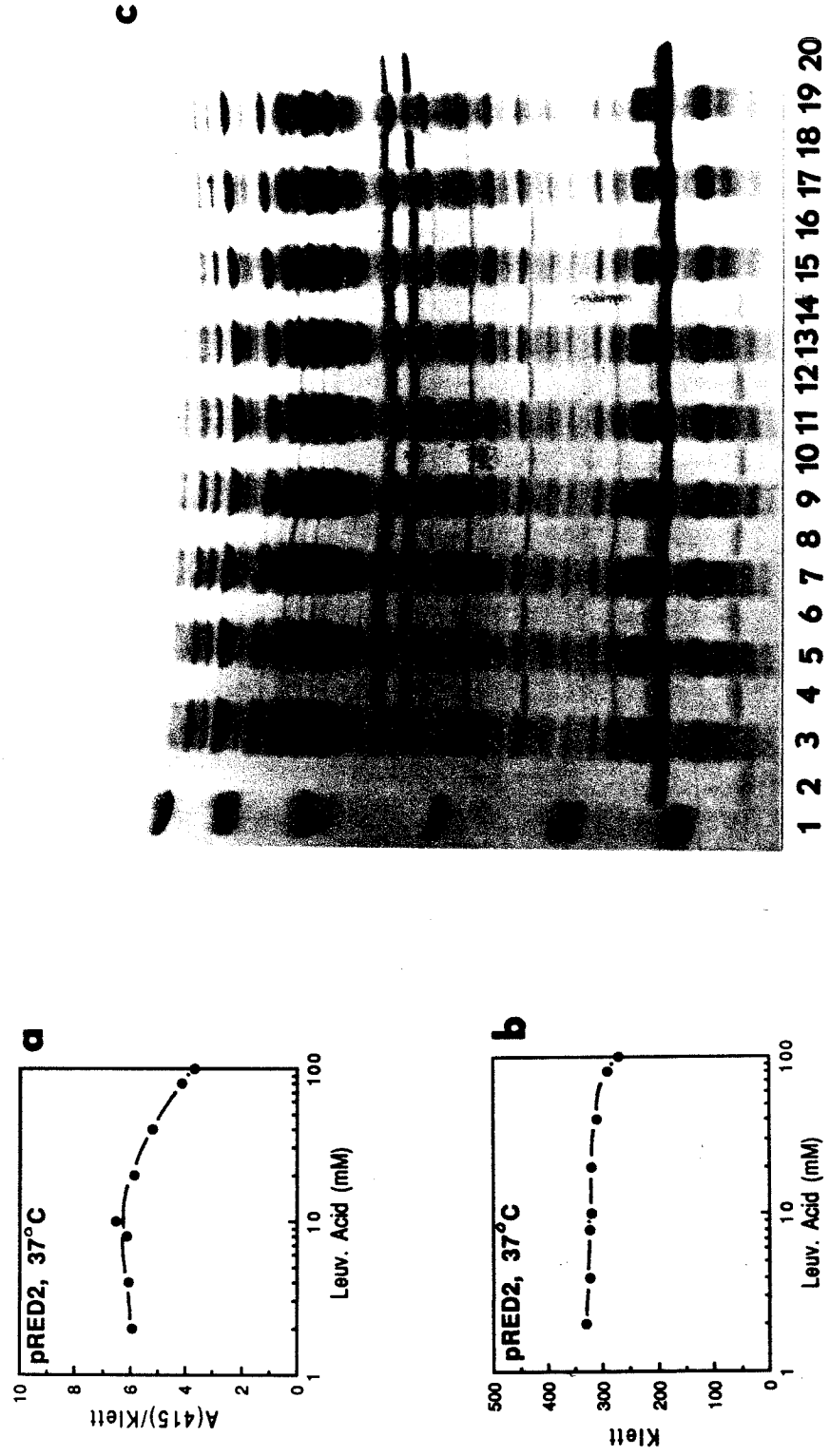
c
1 2 3 4 5 6 7 8 9 10 11 12 13 14 15 16 17 18 19 20
a
pRED2, 37°C
A(415)/Klett
Leuv. Acid (mM)
b
pRED2, 37°C
Klett
Leuv. Acid (mM)

Figure 11.

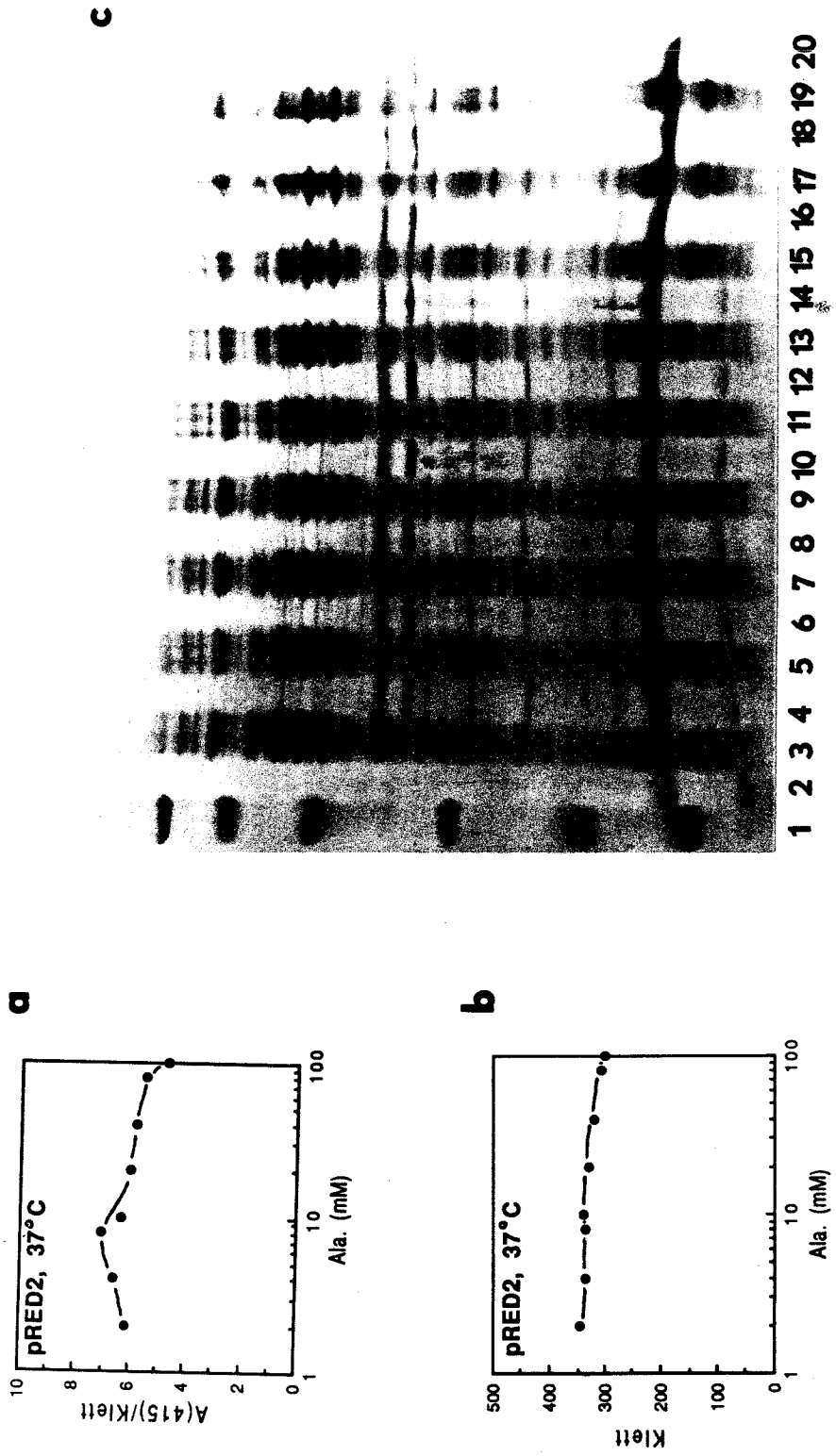
c
1 2 3 4 5 6 7 8 9 10 11 12 13 14 15 16 17 18 19 20
a
pRED2, 37°C
A(415)/Klett
Ala. (mM)
b
pRED2, 37°C
Klett
Ala. (mM)

Figure 12.

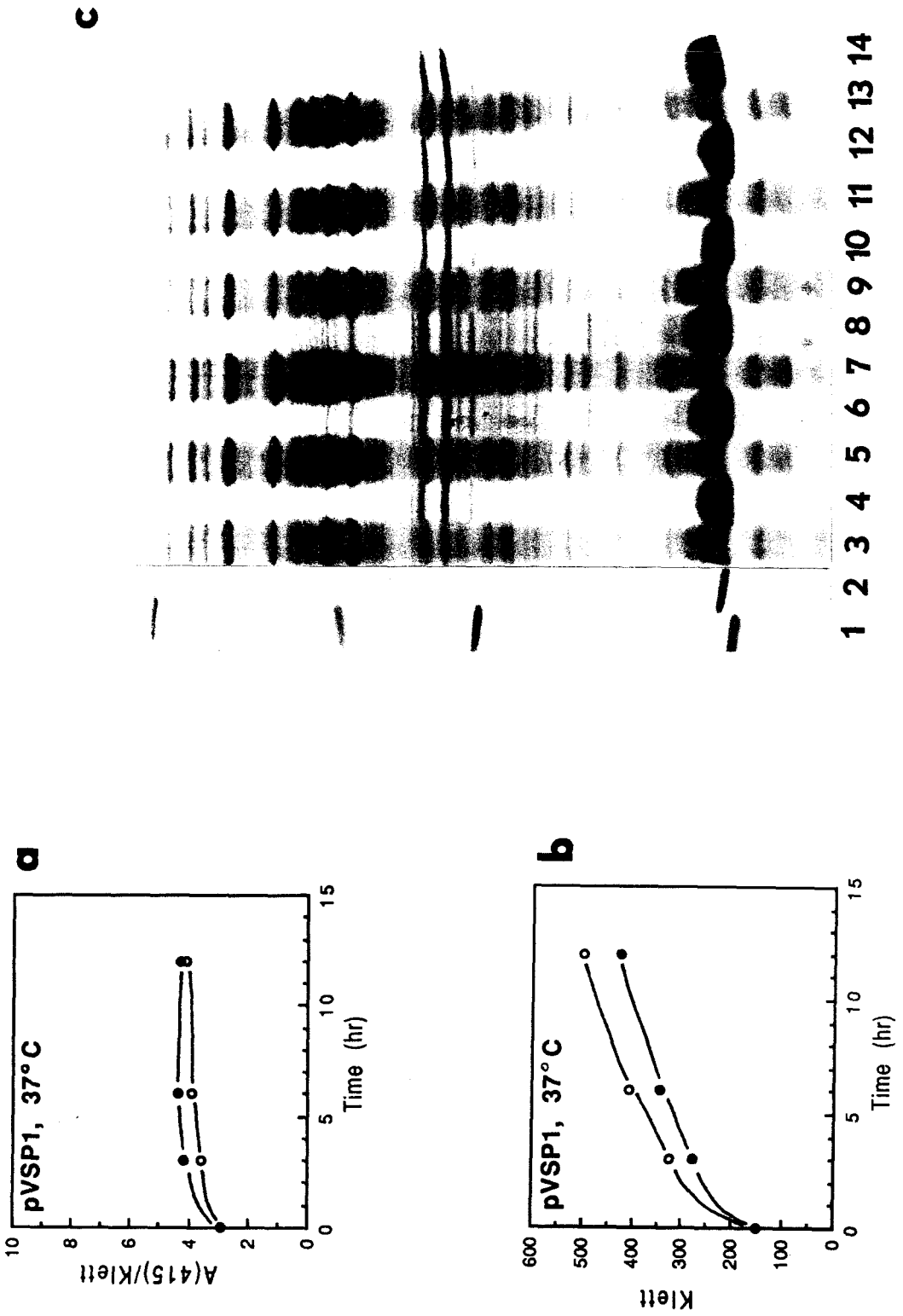
c
1 2 3 4 5 6 7 8 9 10 11 12 13 14
a
pVSP1, 37°C
A(415)/Klett
Time (hr)
b
pVSP1, 37°C
Klett
Time (hr)

Figure 13.

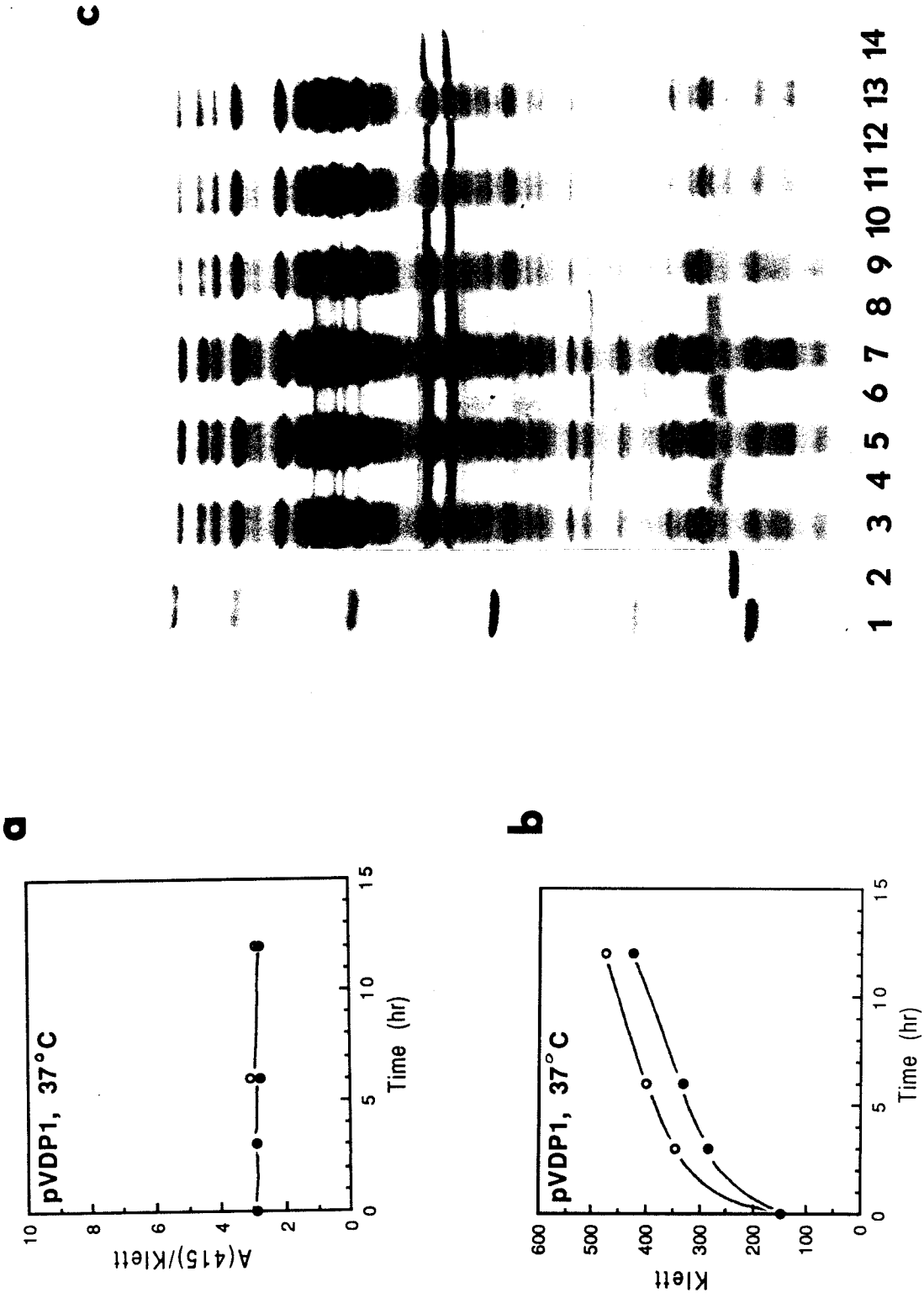
c
1 2 3 4 5 6 7 8 9 10 11 12 13 14
a
pVDP1, 37°C
A(415)/Klett
Time (hr)
b
pVDP1, 37°C
Klett
Time (hr)

Figure 14.

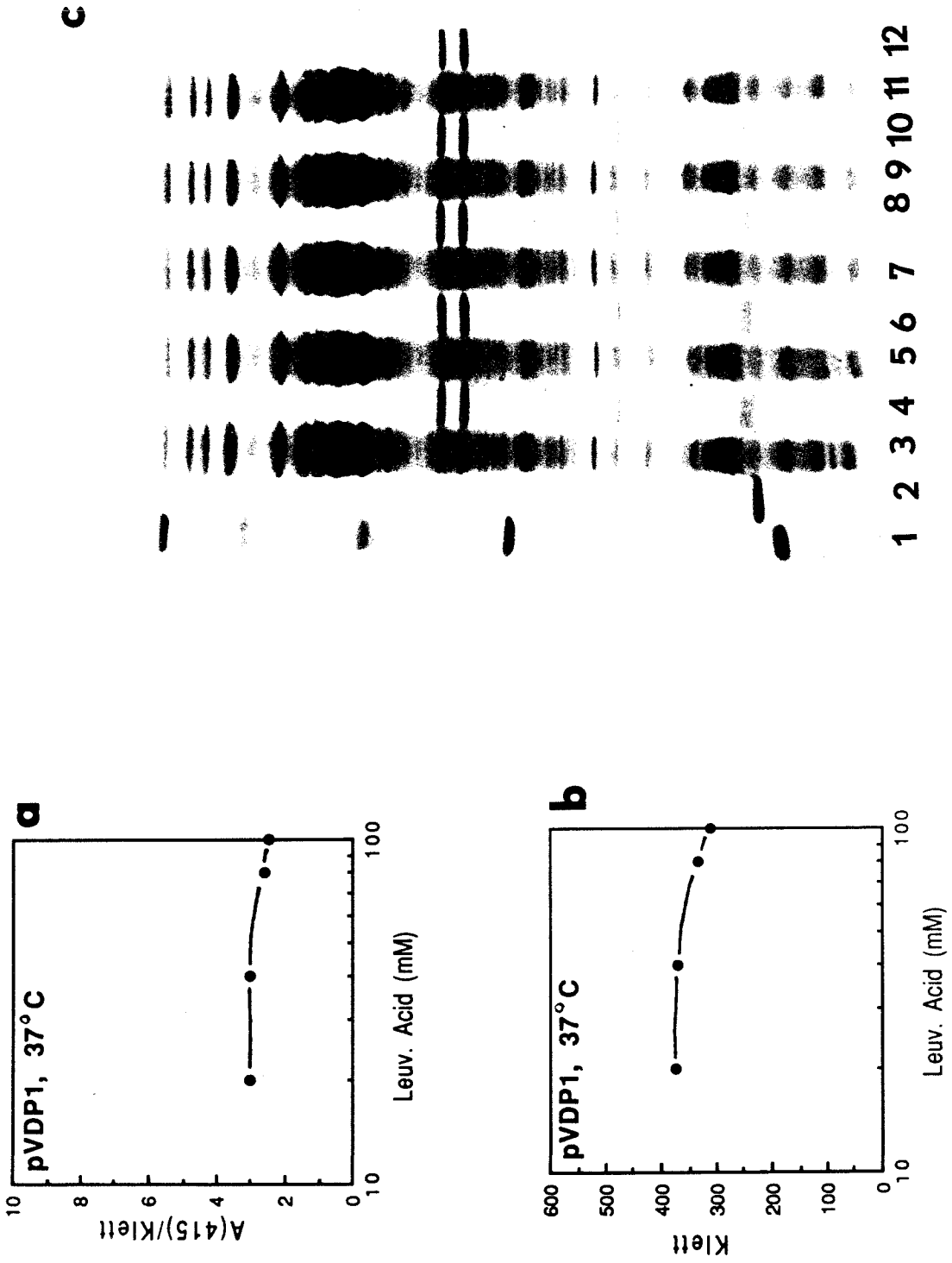
c
1 2 3 4 5 6 7 8 9 10 11 12
a
pVDP1, 37°C
A(415)/Klett
Leuv. Acid (mM)
b
pVDP1, 37°C
Klett
Leuv. Acid (mM)

Figure 15.

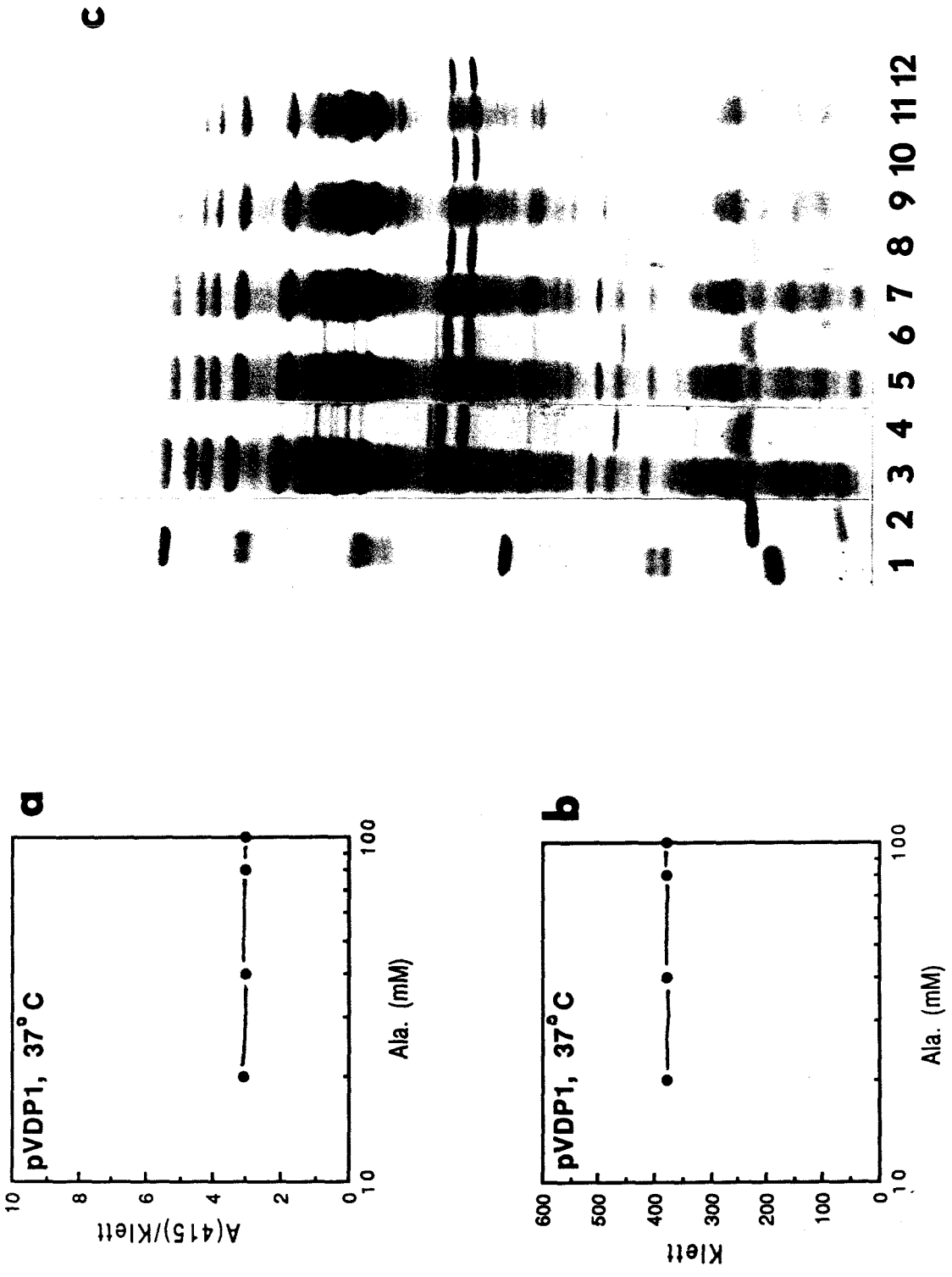
c
1 2 3 4 5 6 7 8 9 10 11 12
a
pVDP1, 37°C
A(415)/Klett
Ala. (mM)
b
pVDP1, 37°C
Klett
Ala. (mM)

Figure 16.

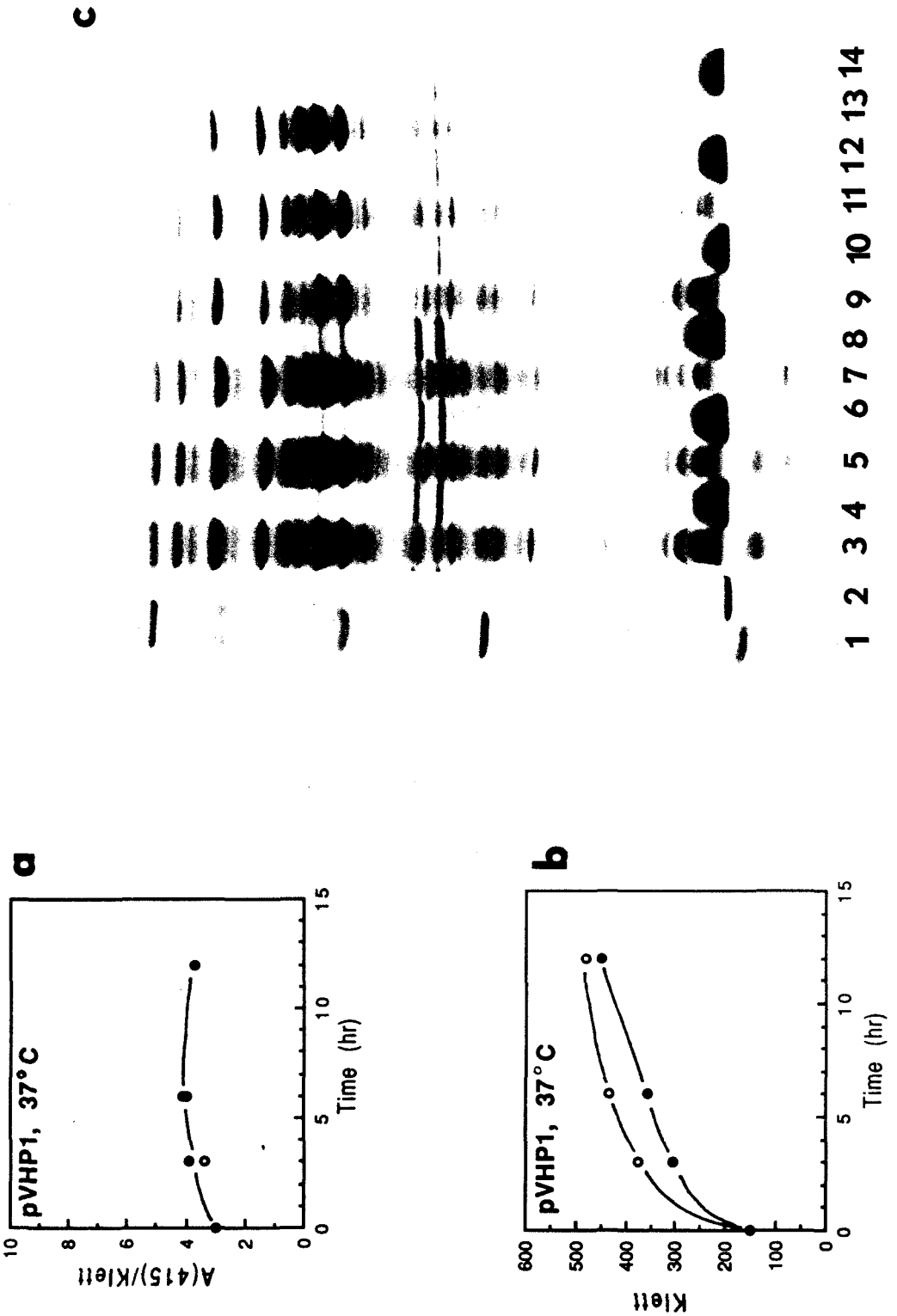
a
pVHP1, 37°C
A(415)/KIeII
Time (hr)
b
pVHP1, 37°C
KIeII
Time (hr)
c
1 2 3 4 5 6 7 8 9 10 11 12 13 14

Figure 17.

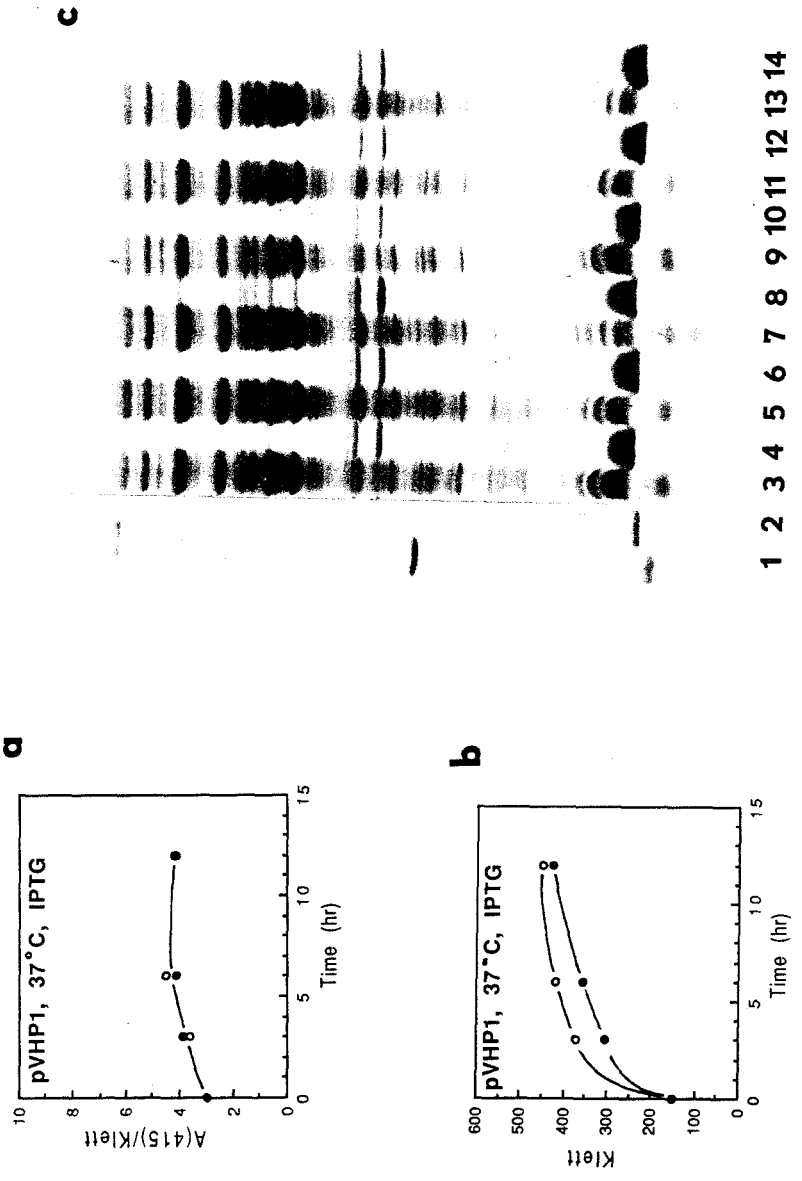
a
pVHP1, 37°C, IPTG
A(415)/Klett
Time (hr)
b
pVHP1, 37°C, IPTG
Klett
Time (hr)
c
1 2 3 4 5 6 7 8 9 10 11 12 13 14

CHAPTER 7

Conclusions

7.1 Summary of Findings

VHb expressed from its native promoter on high copy number plasmids in *E. coli* accumulates in both soluble and insoluble forms. Analysis of the insoluble form demonstrates that VHb is aggregated into inclusion bodies which are relatively devoid of protein contaminants with the exception of pre-β-lactamase and a host-cell protein identified as elongation factor Tu. There is considerable morphological heterogeneity within the aggregate population as determined by electron microscopy. Additionally, two compositionally distinct fractions can be isolated by differential centrifugation.

The soluble form of VHb was purified and characterized. Purified soluble VHb has the correct amino acid content, is dimeric, contains stoichiometric heme, and is spectroscopically indistinguishable from native VHb. The two heme centers in purified VHb are magnetically inequivalent as determined by EPR spectroscopy. The high field rhombicity of one heme center is 5.6% which is similar to the high field rhombicity of leghemoglobin (4.6%). Of known globins, leghemoglobin has the closest amino acid sequence homology to VHb (Wakabayashi, 1986).

The insoluble form of VHb uniformly lacks heme. Some insoluble VHb appears competent for heme binding as determined by spectroscopic titrations. Dissolution analysis with denaturants containing heme suggests heme binding to insoluble VHb makes solubilization of VHb more difficult. Some inclusion body VHb can be solubilized by incubation in buffer lacking denaturant. Of this solubilized protein approximately 25% can be regenerated by heme addition to yield

holoVHb having the same carbon monoxide minus reduced difference absorption spectrum as native VHb. Inclusion body VHb can be partially solubilized by incubation in buffers containing urea at concentrations which are low relative to those usually employed for inclusion body dissolution. The dissolution midpoint of inclusion body apoVHb (3.2 M urea) is similar to the denaturation midpoint of soluble apoVHb (2.9 M urea).

The factors influencing VHb insolubilization *in vivo* were investigated. The extent of VHb insolubilization is dependent on accumulation rate and plasmid vector construction but less so on temperature. Effectors of heme biosynthesis can be used to modulate the extent of VHb insolubilization but these effectors do not eliminate VHb inclusion body formation. Increased levels of the chaperone proteins DnaK and GroEL do not reduce the extent of VHb insolubilized. Attempts to genetically increase heme biosynthesis by cloning ALA synthase and ALA dehydratase did not reduce the extent of VHb insolubilized.

7.2 Properties of Inclusion Bodies

Two different models for inclusion body formation have been proposed. One model states that "aggregation occurs as the nascent polypeptides come off the transcription-translation complex" (Kane and Hartley, 1988). With this mechanism, ribosomal proteins, rRNA, plasmid, and other protein synthetic machinery can be insolubilized with the recombinant protein in inclusion bodies (Kane and Hartley, 1988). This mechanism also implies that recombinant protein is aggregated before it can fold significantly. The other model states that "aggregates

derive from specific partially folded intermediates and not from mature, or fully unfolded proteins" (Mitraki and King, 1989).

Our results suggest that both models are correct to some degree. The presence of pre-β-lactamase and elongation factor TU, a host-cell protein involved in translation, in VHb inclusion bodies supports the first model of inclusion body formation. Results also suggest that some inclusion body VHb bears structural similarity to apoVHb in support of the second model. The correctness of both both models is also indicated by observations from *in vivo* experiments. In particular, amplifying heme biosynthesis with ALA reduces VHb aggregation but does not eliminate inclusion body formation entirely. This suggests that some VHb is insolubilized before it attains a conformation which is competent for heme binding and, hence, cannot be influenced by increased heme availability.

Results in general suggest that VHb inclusion bodies are composed of a population of conformationally heterogeneous VHb molecules. This heterogeneity may provide many possible intermolecular association patterns. With this network of associations, it is possible that some protein remains insoluble primarily from entanglement of unfolded or partially folded molecules. Disruption of this network, however, may generally require treatment with denaturing levels of chaotropic agents.

7.3 References

1. Kane, J. E., and Hartley, D. L. (1988) *TIBTECH*, **6**, 95 - 101

2. Mitraki, A., and King, J. (1989) *Bio/Technology*, **7**, 690 - 697

3. Wakabayashi, S., Matsubara, H., and Webster, D. A. (1986) *Nature*, **322**, 481 - 483